DIGITAL DIAGNOSTICS

A peer-reviewed scientific medical journal

2 Volume   **2** Issue

Digital Diagnostics

EDITOR-IN-CHIEF
Valentin E. Sinitsyn, MD, Dr.Sci. (Med), Professor (Moscow, Russia)
ORCID: 0000-0002-5649-2193

DEPUTY EDITOR-IN-CHIEF
Sergey P. Morozov, MD, Dr.Sci. (Med), Professor (Moscow, Russia)
ORCID: 0000-0001-6545-6170

ECO•VECTOR

Digital Diagnostics

Главный редактор
Синицын Валентин Евгеньевич, д.м.н., профессор (Москва, Россия)
ORCID: 0000-0002-5649-2193

Заместитель главного редактора
Морозов Сергей Павлович, д.м.н., профессор (Москва, Россия)
ORCID: 0000-0001-6545-6170

ЭКО•ВЕКТОР

CONTENTS

СОДЕРЖАНИЕ

Возможности снижения лучевой нагрузки при проведении компьютерной томографии для оценки изменений в лёгких, характерных для COVID-19: использование адаптивной статистической итеративной реконструкции

Д.А. Филатова, В.Е. Синицын, Е.А. Мершина

Московский государственный университет имени М.В. Ломоносова, Москва, Российская Федерация

АННОТАЦИЯ

Обоснование. Большинство пациентов с COVID-19 во время госпитализации проходит многократные визуализационные обследования, кумулятивный эффект которых может значительно увеличивать общую дозу полученного облучения. Эффективная доза облучения может быть снижена за счёт уменьшения тока и напряжения рентгеновской трубки, что, однако, снижает качество изображения. Возможным решением этой проблемы может стать внедрение технологии адаптивной статистической итерационной реконструкции «сырых данных» компьютерной томографии (КТ) — Adaptive Statistical Iterative Reconstruction (ASIR). В последнее время в литературе появились сведения об эффективности низкодозной КТ (НДКТ) в диагностике COVID-19.

Цель — анализ качества и диагностической ценности НДКТ-изображений лёгких после применения итеративного алгоритма обработки; оценка возможности снижения лучевой нагрузки на пациента при диагностике COVID-19.

Материал и методы. В проспективном исследовании приняли участие пациенты, проходившие стационарное лечение в инфекционном отделении МНОЦ МГУ им. М.В. Ломоносова. Исследования КТ выполнялись при поступлении и выписке; в период госпитализации их повторяли по мере клинической необходимости. При первом исследовании использовался стандартный протокол КТ с напряжением тока на трубке 120 кВ и автоматическим модулированием силы тока в диапазоне 200–400 мА, при повторных КТ применяли протокол НДКТ с уменьшенными параметрами напряжения тока на трубке (100 или 110 кВ) и автоматической модуляцией тока в диапазоне 40–120 мА. Для оценки диагностической ценности НДКТ по сравнению со стандартной КТ было проведено анкетирование среди врачей отделения лучевой диагностики МНОЦ МГУ. Анкета включала в себя сравнительную характеристику двух методик при выявлении таких патологических процессов, как уплотнение лёгочной ткани по типу матового стекла, уплотнение по типу матового стекла с ретикулярными изменениями, участки консолидации лёгочной ткани, лимфаденопатия.

Результаты. В исследовании принял участие 151 пациент; средний возраст 58±14,2 года; 53,6% мужчин. При НДКТ в сравнении со стандартной КТ лучевая нагрузка снижалась в среднем в 2,96 раза, компьютерно-томографический индекс дозы (CTDI) — в 2,6 раза, средняя поглощённая доза (DLP) — в 3,1 раза, сила тока на трубке — в 1,83 раза, напряжение на трубке — в 1,2 раза. Полученные анкетные данные свидетельствуют о том, что при проведении НДКТ эффективность выявления основных признаков вирусной пневмонии и оценки динамики состояния пациента существенно не меняется по сравнению с КТ, проведённой по стандартному протоколу.

Заключение. Результаты сравнения стандартной и НДКТ демонстрируют отсутствие значимых потерь диагностической информации и качества при снижении лучевой нагрузки. Таким образом, НДКТ грудной клетки может использоваться в рутинной практике для успешной диагностики COVID-19.

Ключевые слова: COVID-19; НДКТ; лёгкие; лучевая нагрузка; SARS-CoV-2.

Opportunities to reduce the radiation exposure during computed tomography to assess the changes in the lungs in patients with COVID-19: use of adaptive statistical iterative reconstruction

Daria A. Filatova, Valentin E. Sinitsin, Elena A. Mershina

Lomonosov Moscow State University, Moscow, Russian Federation

ABSTRACT

BACKGROUND: Several COVID-19 patients are subjected to multiple imaging examinations during hospitalization, the cumulative effect of which can significantly increase the total dose of radiation received. The effective radiation dose can be reduced by lowering the current and voltage of the X-ray tube, but this reduces image quality. One possible solution is to use adaptive statistical iterative reconstruction technology on the «raw» CT data. Recently, data on the efficacy of low-dose CT (LDCT) in the diagnosis of COVID-19 have appeared in the literature.

AIM: To analyze the quality and diagnostic value of LDCT images of the lungs after applying an iterative processing algorithm and to assess the possibility of reducing the radiation load on the patient when diagnosing COVID-19.

MATERIALS AND METHODS: Patients from the Infectious Diseases Department of the Moscow State University Hospital participated in the prospective study. CT examinations were performed at the time of patient admission and discharge and were repeated as needed during hospitalization. In the first study, a standard CT protocol with a tube voltage of 120 kV and automatic current modulation in the range of 200–400 mA was used; in repeated CT scans, the LDCT protocol was used with reduced tube voltage parameters (100 or 110 kV) and automatic current modulation in the range of 40–120 mA. To assess the diagnostic value of LDCT in comparison with standard CT, a survey was conducted among doctors from the Department of Radiation Diagnostics at Moscow State University Hospital. The questionnaire included a comparison of the two methods for identifying the following pathological processes: «ground-glass» opacities, compaction of the lung tissue with reticular changes, areas of lung tissue consolidation, and lymphadenopathy.

RESULTS: The study included 151 patients. The average age was 58±14.2 years, with men accounting for 53.6% of the population. During LDCT the radiation load was reduced by 2.96 times on average, CTDI by 2.6 times, DLP by 3.1 times, the current on the tube by 1.83 times, and the voltage on the tube by 1.2 times. The results indicate that the effectiveness of detecting the main signs of viral pneumonia and assessing the dynamics of the patient's condition does not differ significantly from CT performed according to the standard protocol.

CONCLUSIONS: The results of a comparison of standard and low-dose CT show that there is no significant loss of diagnostic information and image quality as the radiation load is reduced. Thus, chest LDCT can be used to successfully diagnose COVID-19 in routine practice.

Keywords: COVID-19; X-ray computed tomography; lung; radiation protection; SARS-CoV-2.

在计算机断层扫描期间减少辐射负荷以评估 COVID-19肺特性变化的可能性：使用自适应统计 迭代重建

Daria A. Filatova, Valentin E. Sinitsin, Elena A. Mershina

Lomonosov Moscow State University, Moscow, Russian Federation

简评

论证大多数COVID-19患者在住院期间接受多次成像检查，其累积效应可以显着增加接受的辐射总剂量。有效辐射剂量可以通过降低x射线管的电流和电压来降低，然而，这会降低图像质量。这个问题的一个可能的解决方案是引入自适应统计迭代重建 （Adaptive Statistical Iterative Reconstruction （ASIR））技术，用于计算机断层扫描（CT）的»原始数据»的自适应统计迭代重建。最近，有关低剂量CT（LDCT）有效性的信息已经出现在COVID-19诊断中的文献中。

目的是在应用迭代处理算法后分析肺部LDCT图像的质量和诊断价值，以评估在COVID-19诊断期间减少患者辐射负荷的可能性。

材料与方法。这项前瞻性研究涉及在罗蒙诺索夫莫斯科国立大学医学中心传染病部门接受住院治疗的患者。CT研究在入院和出院时进行； 在住院期间，根据临床需要重复进行。在第一项研究中，使用120kV管电压和200-400mA范围内的自动电流调制的标准CT协议，通过重复CT扫描的时候，LDKT协议使用管电压（100或110kV）和40-120mA范围内的自动电流调。为了评估LDCT与标准CT相比的诊断价值，在莫斯科国立大学医学中心辐射诊断系的医生中进行了问卷调查。调查问卷包括两种方法的比较描述，用于检测这种病理过程，如通过磨砂玻璃类型压实肺组织，通过磨砂玻璃类型压实具有网状变化，肺组织固结区域，淋巴结病。

结果该研究涉及151名患者；平均年龄为58±14.2岁；男性为53.6％。使用LDCT，与标准CT相比，辐射负荷平均下降2.96倍，计算机断层扫描剂量指数（CTDI）－2.6倍，平均吸收剂量（DLP）－3.1倍，管上的电流－1.83倍，管上的电压-1.2倍。获得的问卷数据表明，在LDCT期间，与根据标准协议进行的CT相比，检测病毒性肺炎的主要体征和评估患者病情动态的有效性没有显着变化。

结论比较标准的CT和LDCT的结果表明，在辐射负荷降低的情况下，诊断信息和质量没有显着损失。因此，胸部的LDCT扫描可以在常规实践中用于成功诊断COVID-19。

关键词：COVID-19；LDCT；肺；辐射负荷；SARS-CoV-2。

BACKGROUND

During the coronavirus disease 2019 (COVID-19) pandemic, computed tomography (CT) studies are used to diagnose coronavirus pneumonia in both outpatient and inpatient settings and are recommended to be performed in patients suspected or verified with COVID-19 on the day of hospitalization for an initial examination, then repeatedly after 2–3 days if the required therapeutic effect is not achieved and then after 5–7 days in the absence or improvement of symptoms dynamics [1–5].

A number of patients with COVID-19 undergo multiple imaging studies during hospitalization, whose cumulative effect can significantly increase the total dose of radiation received. The principle "as low as reasonably achievable" (ALARA) states that whenever radiation is required, the impact should be ALARA. Bearing in mind this important principle, it is extremely important to remember that any CT scan must be accompanied by a justification of examination and optimization of radiation dose [6]. CT scans are significant aid in diagnosing COVID-19; however, the potential to increase radiation exposure of large numbers of patients across the country cannot be ignored. Maintaining the balance between the need for efficient imaging for rapid diagnostics and efforts to minimize radiation exposure is important.

Effective dose of radiation during CT studies can be decreased by reducing the current and voltage of X-ray tube; however, this leads to image quality distortion due to an increase in the amount of noise and artifacts. A possible solution to this problem is the introduction of technology adaptive to statistical iterative reconstruction of CT "raw data," for example, using the Adaptive Statistical Iterative Reconstruction (ASIR) technology and numerous similar methods [7–9].

Recently, data on the efficiency of low-dose CT (LDCT) in diagnostics of COVID-19 compared with standard one were presented in literature. It should be noted that CT with a radiation dose of 0.2 mSv or less is considered low dose. In a retrospective study, LDCT with iterative reconstruction in the diagnostics of COVID-19 demonstrated sensitivity, specificity, and predictive value of approximately 90%. Values of these parameters increased to 96% if patients had symptoms for >48 hours. Disease probability increased from 43.2% (before the test) to 91.1% or 91.4% (after the test) in patients with a positive CT scan, whereas the probability of disease decreased from 43.2% (before the test) to 9.6% or 3.7% (after the test) in patients with negative CT result. Additionally, LDCT revealed an additive diagnostic advantage in patients with concomitant bacterial pneumonia or an alternative diagnosis other than COVID-19 [10]. Research in this promising field is actively performed.

This study aimed to analyze the quality and diagnostic value of LDCT images of the lungs after applying the ASIR processing algorithm and to assess the possibility of reducing radiation exposure of patients diagnosed with COVID-19.

METHODS
Study design

Patients undergoing inpatient treatment at the infectious diseases department of the M.V. Lomonosov Moscow State University Medical Research and Education Center took part in a prospective, single-center, uncontrolled study. CT examinations were performed upon patient admission and discharge, then were repeated as clinically required during the period of hospitalization, but at least once every 5 days. Study 1 was conducted in all patients in the standard CT mode, subsequent ones were conducted in LDCT mode.

The primary endpoint of the study was the absence of a significant loss of diagnostic information during LDCT compared to standard CT.

Inclusion criteria

Inclusion criteria included infection with COVID-19 verified by molecular genetic studies (polymerase chain reaction method, PCR), and undergoing inpatient treatment.

Conducting conditions

The study was conducted in the infectious diseases department of the Moscow State University Medical Research and Education Center with the involvement of patients who were hospitalized with COVID-19.

Study duration

The study was conducted from April 21 to May 11, 2020.

Medical intervention description

CT of the lungs and chest organs was performed on a 32-row Somatom Scope CT manufactured by Siemens (Germany). Studies were conducted with a slice thickness of 1 mm. The first study used a standard CT protocol with a tube voltage of 120 kV, with an automatic modulation current of 200–400 mA; with repeated CT, the LDCT protocol was used with reduced parameters of tube voltage (100 or 110 kV) and automatic modulation of tube current of 40–120 mA; the ASIR algorithm was used to reduce radiation exposure. All images obtained in DICOM format were stored in the Radiological Information Network of the Moscow State Scientific and Educational Center of Moscow State University. Syngo.via workstations (Siemens, Germany) were used for CT processing and analysis.

A questionnaire survey was conducted among the doctors of the Department of Radiation Diagnostics of the Medical Research and Education Center of the M.V. Lomonosov Moscow State University to assess the diagnostic value of LDCT in comparison with standard CT. The questionnaire included a comparative description of two methods in identifying pathological processes, namely ground glass opacity induration of the lung tissue, ground glass opacity induration with reticular changes (thickened interlobular septa; "patchwork" presentation, crazy paving), areas of consolidation

of lung tissues, and lymphadenopathy. Medical specialists evaluated each of the two methods on a five-point scale, where the worst detectability of a particular pathological process corresponded to 1 point, the best detectability corresponded to 5 points, and then the arithmetic mean was calculated for each item. In conclusion, it was proposed to assess the efficiency of LDCT diagnostics of COVID-19. Each study was assessed by two medical specialists, and decision was independently made in each case.

Primary study outcome

The primary outcome of the study was comparable diagnostic value of CT performed according to the standard protocol and LDCT.

Ethical considerations

The subject of this article was approved at a meeting of the Local Ethics Committee of the Medical Research and Education Center of the M.V. Lomonosov Moscow State University, dated May 25, 2020 (within the research project on diagnostics and treatment of COVID-19 at the Medical Research and Education Center of the M.V. Lomonosov Moscow State University).

Statistical analysis

Statistical analysis was performed using MS Office Excel software.

RESULTS

Study participants

A total of 151 patients who underwent inpatient treatment at the infectious diseases department of the Medical Research and Education Center of the M.V. Lomonosov Moscow State University participated in the study. The average age of patients was 58 ± 14.2 years; wherein 70 were women (46.4%) and 81 were men (53.6%). COVID-19 diagnosis was confirmed by PCR results.

Main research results

Characteristics of study 1 (standard CT) included average radiation exposure of 3.76 ± 1.28 mSv; average computed tomography dose index (CTDI) of 6.69 ± 2.18 mGy; average dose length product (DLP) of 222.28 ± 76.33 mGy/cm; average tube current of 2165.97 ± 682.83 mA/s; and average tube voltage of 129.43 ± 3.21 mV. Characteristics of subsequent studies (LDCT) included radiation exposure of 1.27 ± 0.47 mSv; CTDI of 1.57 ± 1.40 mGy; DLP of 73.01 ± 19.94 mGy/cm; tube current of 1182.55 ± 366.55 mA/s; and tube voltage of 111.79 ± 5.73 mV. If a patient underwent several LDCT studies, the arithmetic mean between them was considered when calculating statistical indicators.

The following results were obtained from standard and low-dose CT comparison. During LDCT, radiation exposure decreased on average by 2.96 times, CTDI reduced by 2.6 times, DLP reduced by 3.1 times, tube current reduced by 1.83 times, and tube voltage reduced by 1.2 times. These values are presented in Table 1.

Table 2 presents the results of the survey questionnaire of doctors of the Department of Radiation Diagnostics of the Medical Research and Education Center of the M.V. Lomonosov Moscow State University for assessing the diagnostic accuracy of LDCT in comparison with standard CT.

Table 2 demonstrates that with LDCT, the efficiency of detecting the main signs of viral pneumonia, and assessment of the patient's condition dynamics does not significantly change compared to that of standard CT. It should also be noted that, according to survey results, 7 doctors (100% of those surveyed) believe that LDCT is effective for COVID-19 diagnostics.

Here are illustrative examples of clinical cases (Figs. 1–6), demonstrating the similarity of diagnostic value of two aforementioned research methods. Columns on the left (*a*) show images of a standard CT scan performed upon admission of the patient to the hospital, and columns on the right (*b*) present LDCT over time. The top line of images indicates the pulmonary window mode, whereas the bottom line indicates the mediastinal window mode. For comparison, values of radiation exposure in each case are presented. Time intervals between standard CT and LDCT were 2–7 days; thus, the primary endpoint was reached in all patients enrolled in the study.

Adverse events

During the study, no adverse events were recorded because of CT according to the standard protocol and LDCT.

Table 1. Comparative characteristics of standard and low-dose computed tomography

Indicator	Standard CT	Low-dose CT	Difference, times
Average radiation exposure, mSv	3.76±1.28	1.27±0.47	2.96
CTDI, mGy	6.69±2.18	1.57±1.40	2.6
DLP, mGy/cm	222.28±76.33	73.01±19.94	3.1
Average tube current, mA/s	2165.97±682.83	1182.55±366.55	1.83
Tube voltage, mV	129.43±3.21	111.79±5.73	1.2

Note. CT, computed tomography; CTDI (Computed Tomography Dose Index), average computed tomography dose index; DLP, dose length product.

Table 2. Results of the survey questionnaire of doctors of the Department of Radiation Diagnostics of the Medical Research and Education Center of the M.V. Lomonosov Moscow State University

Characteristics	Standard CT	LDCT
Identification of the lung tissue induration by the type of ground glass opacity	5	5
Identification of induration areas by the type of ground glass opacity with reticular changes (thickened interlobular septa)—presentation of patchwork, crazy paving	5	4,43
Identification of lung tissue consolidation areas	5	5
Detection of lymphadenopathy	5	4

Note. The average values of points given for each item are indicated: the minimum point is 1, the maximum is 5. CT, computed tomography; LDCT, low-dose computed tomography.

DISCUSSION

Main research result summary

Study results confirm the absence of significant loss of diagnostic information in chest LDCT in patients with COVID-19; thus, chest LDCT can be routinely used for successful diagnostics of this disease.

Main research result discussion

In the absence of etiotropic treatment of COVID-19, it is especially important to diagnose the disease at an early stage and immediately isolate the infected person. According to clinical guidelines, COVID-19 diagnosis is established based on clinical examination, epidemiological anamnesis data, and laboratory testing results [11]. The task of etiological laboratory diagnostics comprises searching for severe acute respiratory syndrome coronavirus 2 ribonucleic acid using nucleic acid amplification methods (reverse transcription PCR, RT-PCR). Pathogen detection in a nasopharyngeal smear is possible as early as a week before the onset of clinical manifestations of the infection [12]. Nevertheless, evidence that RT-PCR can give false negative results was reported. Therefore, Ch. Long et al. [13] reported that 35 patients had CT signs of characteristic pneumonia among 36 patients diagnosed with COVID-19, whereas a positive RT-PCR result was obtained for the first time in only 30 patients. In the remaining six cases, repeated testing was performed, and the test result was positive in three of them at the second test (after 2 days) and in three more cases at the third test (after 6 days). Thus, CT sensitivity was 97.2%, and RT-PCR in study 1 was 84.6% [13]. In a study by Y. Fang et al. [14], similar results were obtained, when CT sensitivity was 98% and that of RT-PCR was 71% (in study 1, the positive result was obtained in 36 of 51 patients with symptoms of pneumonia on CT and a suitable epidemiological history;
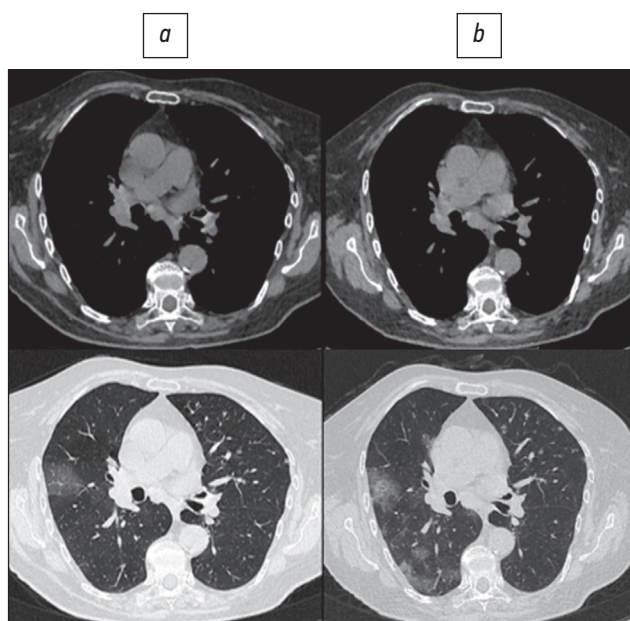
Fig. 1. A 78-year-old patient: standard computed tomography at admission was performed with a radiation exposure of 2.5 mSv (*a*), and low-dose computed tomography was performed with exposure of 1.0 mSv (*b*).
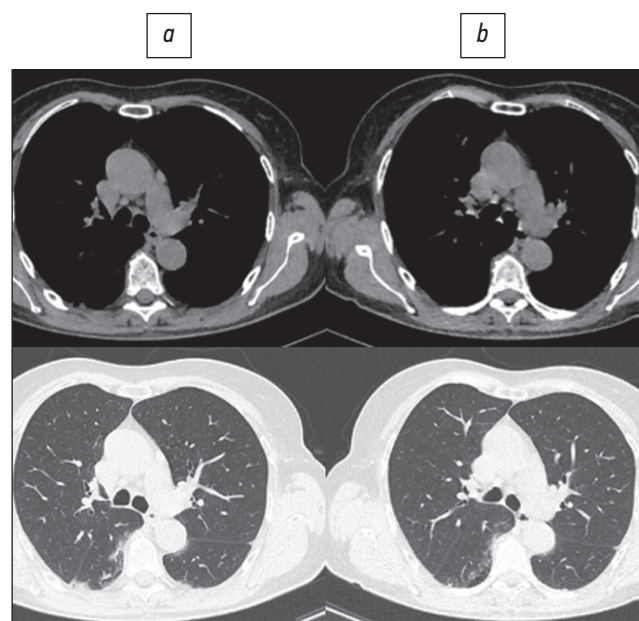
Fig. 2. A 72-year-old patient: standard computed tomography at admission was performed with radiation exposure of 2.1 mSv (*a*), and low-dose computed tomography was performed with exposure of 0.87 mSv (*b*).
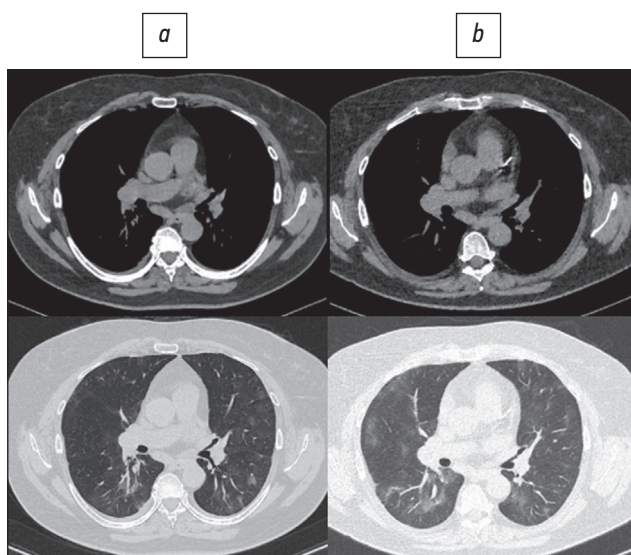
Fig. 3. A 60-year-old patient: standard computed tomography at admission was performed with a radiation exposure of 3.3 mSv (*a*), and low-dose computed tomography was performed with exposure of 1.1 mSv (*b*).
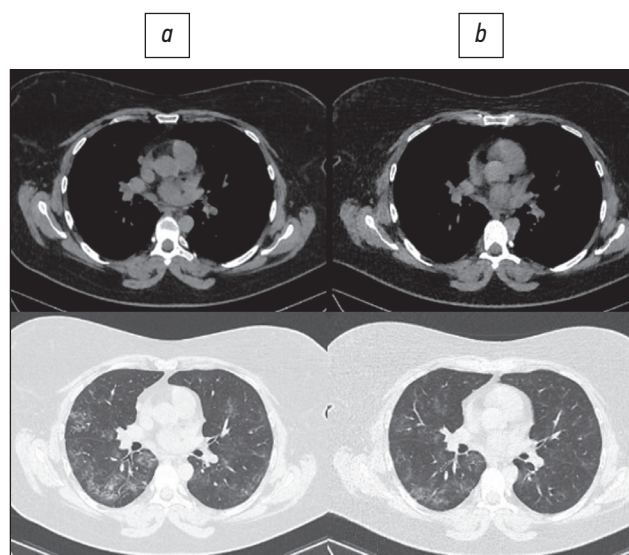
Fig. 4. A 46-year-old patient: standard computed tomography at admission was performed with a radiation exposure of 5.6 mSv (*a*), and low-dose computed tomography was performed with exposure of 1.7 mSv (*b*).
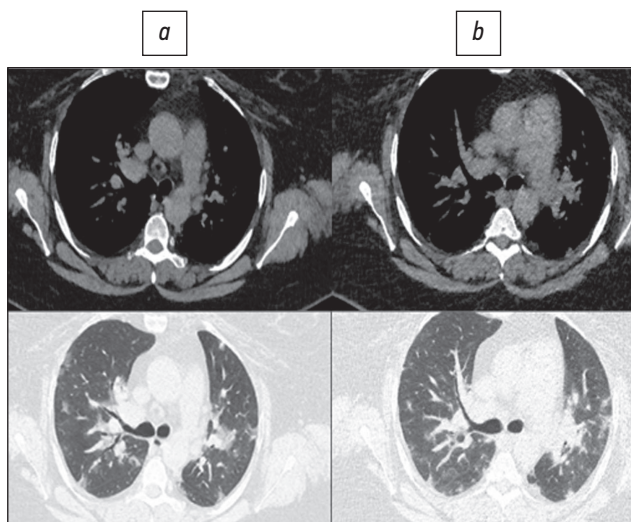
Fig. 5. A 40-year-old patient: standard computed tomography at admission was performed with radiation exposure of 6.8 mSv (*a*), and low-dose computed tomography was performed with exposure of 2.0 mSv (*b*).
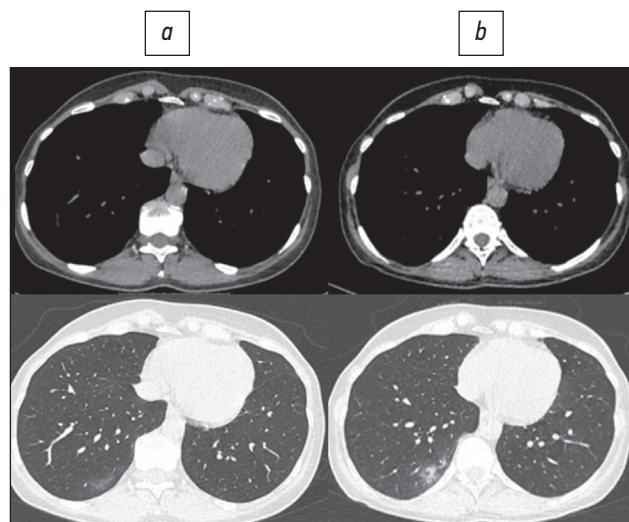
Fig. 6. A 56-year-old patient: standard computed tomography at admission was performed with a radiation exposure of 1.6 mSv (*a*), and low-dose computed tomography was performed with exposure of 0.87 mSv (*b*).

the diagnosis was further confirmed in 12 patients in study 2, 2 patients in study 3, and 1 patient in study 4). Assumed reasons that the RT-PCR sensitivity in COVID-19 diagnosis was lower than that of CT, including the imperfection of nucleic acid amplification technologies, the variability of the sensitivity threshold of tests from different manufacturers, low viral load, and wrong technique of sampling material for analysis. Additionally, the number of viral particles varies depending on the site where the material for analysis is taken, as evidence revealed that it is preferable to examine the sputum first, followed by a nasopharyngeal swab in sensitivity [15]. Thus, despite a negative RT-PCR result, CT is recommended to visualize changes in the lungs if the patient has characteristic symptoms and epidemiological history. In

case of CT signs of pneumonia, it is necessary to take measures for emergency isolation of the patient, after which a repeated laboratory analysis should be performed.

In the context of an increased number of CT examinations, an issue of a significant increase in radiation exposure and associated risk arise, for example, the evidence that approximately 2% of cancers in the USA are associated with radiation doses received as CT result [16]. Despite the absence of major epidemiological studies on this subject, a large amount of data on radiation-induced cancer in survivors of atomic bombs dropped on Japan in 1945 was reported. In the subgroup of people who received radiation doses in the range from 5 to 150 mSv, a significant increase was observed in the overall risk of developing

cancer, the average dose in this subgroup was 40 mSv [17], and the average effective radiation dose for standard chest CT is 5 mSv [18]. As for LDCT of the chest with radiation exposure of 0.4 mSv, no sufficient evidence of efficacy in the context of screening and diagnostics of COVID-19 is currently reported [3].

Radiation dose received by a patient during CT scan depends on tube current strength, voltage, scan time, slice thickness, scan volume, and interval. Scanning time is reduced with the use of modern models of spiral tomographs; however, radiation exposure sometimes even increases due to increased current strength and scan volume. Under these conditions, it is reasonable to resort to radiation dose reduction techniques. The dose is directly proportional to the tube current. Recently, several studies showed that chest LDCT at 10–140 mAs does not significantly reduce the image quality, and nodular structures are still observed [19–21]. In their study, X. Zhu et al. [22] demonstrated a linear correlation between the tube current and the DLP at a constant voltage and scan time, and also assessed the feasibility of optimization of radiation dose by reducing the tube current. By comparing images obtained at different CTDI values, the threshold value of this parameter was determined, which enables to obtain images without a significant loss of information content (25 mAs), and with an increase in the thickness of sections, the loss of image quality occurred more slowly. Statistical analysis revealed no significant difference between images obtained at 115, 40, and 25 mAs. Thus, 25 mAs or more is an acceptable exposure parameter to provide satisfactory image quality for chest CT, whereas CTDI at 25 mAs was reduced by 70% compared to CTDI at 115 mAs. Despite the accuracy of this parameter, clinicians should be aware that its value may vary with different CT systems; additionally, it must be adjusted considering the biological characteristics of patients (for example, the radiation dose should be increased for obese patients and when examining the upper lobe of the lung due to the false shadow caused by the scapula). Threshold values of CDTI parameter obtained in this study are consistent with the results of the study by T. Kubo et al. [23], where standard and low-dose CTs were compared to determine the main characteristics of lung lesions, which enabled us to confirm or rule out malignant nature. Parameters of 20–50 mAs were sufficient to determine the nature of the lesion without additional standard CT. Edge characteristics, calcification, and lobulation, as well as pleural response, standard and low-dose CTs showed the same efficiency to determine parameters of lesions as structure.

For many years, the question of LDCT safety in screening for oncological diseases, for example, lung cancer, has remained controversial [24]. In their study, C. Rampinelli et al. [25] analyzed the possible risks of radiation lung cancer and leukemia in healthy people who had been regularly screened using LDCT for 10 years. It turned out that the total cumulative dose of radiation was approximately 9 mSv for men and 13 mSv for women, which is equivalent to one standard CT scan. Additionally, given that the average dose from background sources in the USA is approximately 30 mSv over 10 years, it can be concluded that LDCT screening accounts for only 1/3 of the exposure to natural background radiation over the same period. Study results revealed that after 10 years of screening with LDCT, in 5203 patients aged over 50 years old who are asymptomatic with smoking experience of more than 20 pack-years, approximately 1.5 cases of lung cancer, and 2.4 cases of other types of cancer were caused by radiation exposure. Compared to the number of cases of lung cancer detected, it can be calculated that approximately 100 cases of cancer are detected by screening per case of radiation-induced cancer. Additionally, results of a study of LDCT screening in the population of smokers aged 55–74 years showed a reduction in mortality from lung cancer by 20% [26]. All these data indicate that the LDCT method is safe and effective for multiple repetitions within screening or monitoring the dynamics of the patient's condition in the hospital despite the possible risks associated with radiation exposure. There is no doubt about the importance of using LDCT to reduce radiation exposure and ensure greater safety of the study for the patient.

CONCLUSION

Comparative analysis of the efficacy and diagnostic value of LDCT and CT performed according to a standard protocol revealed that LDCT is not only a full-fledged alternative, but also a preferable option, since its implementation can significantly reduce the radiation exposure of the patient. Given that during inpatient COVID-19 treatment, patient undergoes several imaging studies, the issue of radiation safety becomes urgent. According to practicing doctors, the amount of information provided by LDCT is not inferior to the standard CT technique in quality and accuracy; therefore, for dynamic studies, it is advisable to prefer LDCT, which is a method that enables the radiation exposure reduction.

ADDITIONAL INFORMATION

REFERENCES

1. Ministry of Health of the Russian Federation. Temporary guidelines: prevention, diagnosis and treatment of new coronavirus infection. Version 8 (03.09.2020). Moscow; 2020. (In Russ). Available from: https://base.garant.ru/74596434/

2. Romanov BK. Coronavirus infection COVID-19. *Safety and Risc of Farmacotherapy*. 2020;8(1):3–8. (In Russ.)

3. Morozov SP, Protsenko DN, Smetanina SV, et al. Radiation diagnostics of coronavirus disease (COVID-19): organization, methodology, interpretation of results: preprint No. CDT-Version 2 of 17.04.2020. Moscow; 2020. 78 p. (In Russ.)

4. Udugama B, Kadhiresan P, Kozlowski HN, et al. Diagnosing COVID-19: the disease and tools for detection. *ACS Nano*. 2020;14(4):3822–3835. doi: 10.1021/acsnano.0c02624

5. Zhao W, Zhong Z, Xie X, et al. Relation between chest ct findings and clinical conditions of coronavirus disease (COVID-19) pneumonia: a multicenter study. *AJR Am J Roentgenol*. 2020;214(5):1072–1077. doi: 10.2214/AJR.20.22976

6. Beregi JP, Greffier J. Low and ultra-low dose radiation in CT: Opportunities and limitations. *Diagn Interv Imaging*. 2019;100(2):63–64. doi: 10.1016/j.diii.2019.01.007

7. Cheng L, Chen Y, Fang T, et al. Fast iterative adaptive reconstruction in low-dose CT imaging. In: 2006 International Conference on Image Processing. Atlanta, GA: IEEE; 2006. P. 889–892. Available from: https://ieeexplore.ieee.org/document/4106673/

8. Hara AK, Paden RG, Silva AC, et al. Iterative reconstruction technique for reducing body radiation dose at CT: feasibility study. *AJR Am J Roentgenol*. 2009;193(3):764–771. doi: 10.2214/AJR.09.2397

9. Prakash P, Kalra M, Kambadakone A, et al. Reducing abdominal CT radiation dose with adaptive statistical iterative reconstruction technique. *Invest Radiol*. 2010;45(4):202–210. doi: 10.1097/RLI.ob013e3181dzfeec

10. Chen LG, Wu PA, Sheu MH, et al. Automatic current selection with iterative reconstruction reduces effective dose to less than 1 mSv in low-dose chest computed tomography in persons with normal BMI. *Medicine (Baltimore)*. 2019;98(28):e16350. doi: 10.1097/MD.0000000000016350

11. Dangis A, Gieraerts C, De Brueker Y, et al. Accuracy and reproducibility of low-dose submillisievert chest CT for the diagnosis of COVID-19. *Radiology Cardiothoracic Imaging*. 2020;2(2):e200196. doi: 10.1148/ryct.2020200196

12. Sethuraman N, Jeremiah SS, Ryo A. Interpreting diagnostic tests for SARS-CoV-2. *JAMA*. 2020;323(22):2249–2251. doi: 10.1001/jama.2020.8259

13. Long C, Xu H, Shen Q, et al. Diagnosis of the Coronavirus disease (COVID-19): rRT-PCR or CT? *Eur J Radiol*. 2020;126:108961. doi: 10.1016/j.ejrad.2020.108961

14. Fang Y, Zhang H, Xie J, et al. Sensitivity of chest CT for COVID-19: comparison to RT-PCR. *Radiology*. 2020;296(2):E115–E117. doi: 10/1148/radiol.2020200432

15. Yang Y, Yang M, Shen C, et al. Evaluating the accuracy of different respiratory specimens in the laboratory diagnosis and monitoring the viral shedding of 2019-nCoV infections. *medRxiv*. 2020. doi: 10.1101/2020.02.11.20021493

16. Brenner DJ, Hall EJ. Computed tomography--an increasing source of radiation exposure. *N Engl J Med*. 2007;357(22):2277–2284. doi: 10.1056/NEJMra072149

17. Pierce DA, Preston DL. Radiation-related cancer risks at low doses among atomic bomb survivors. *Radiat Res*. 2000;154(2):178–186. doi: 10.1667/0033-7587(2000)154[0178:rrcral]2.0.co;2

18. Matkevich E, Sinitsyn V, Mershina E. Comparative analysis of radiation doses of patients with computed tomography in a Federal medical institution. *Journal of Radiology and Nuclear Medicine*. 2016;97(1):33–39. (In Russ). doi: 10.20862/0042-4676-2016-97-1-33-40

19. Naidich DP, Marshall CH, Gribbin C, et al. Low-dose CT of the lungs: preliminary observations. *Radiology*. 1990;175(3):729–731. doi: 10.1148/radiology.175.3.2343122

20. Prasad SR, Wittram C, Shepard JA, et al. Standard-dose and 50%-reduced-dose chest CT: comparing the effect on image quality. *AJR Am J Roentgenol*. 2002;179(2):461–465. doi: 10.2214/ajr.179.2.1790461

21. Zwirewich CV, Mayo JR, Müller NL. Low-dose high-resolution CT of lung parenchyma. *Radiology*. 1991;180(2):413–417. doi: 10.1148/radiology.180.2.2068303

22. Zhu X, Yu J, Huang Z. Low-dose chest CT: optimizing radiation protection for patients. *AJR Am J Roentgenol*. 2004;183(3):809–816. doi: 10.2214/ajr.183.3.1830809

23. Kubo T, Ohno Y, Takenaka D, et al. Standard-dose vs. low-dose CT protocols in the evaluation of localized lung lesions: Capability for lesion characterization – iLEAD study. *Eur J Radiol Open*. 2016;3:67–73. doi: 10.1016/j.ejro.2016.03.002

24. Gombolevsky VA, Chernina VY, Blokhin IA. Main achievements of low-dose computed tomography in lung cancer screening. *Tuberculosis and Lung Diseases*. 2021;99(1):61–70. (In Russ). doi: 10.21292/2075-1230-2021-99-1-61-7025.

25. Rampinelli C, De Marco P, Origgi D, et al. Exposure to low dose computed tomography for lung cancer screening and risk of cancer: secondary analysis of trial data and risk-benefit analysis. *BMJ*. 2017;356:j347. doi: 10.1136/bmj.j347

26. Chiles C. Lung cancer screening with low dose CT. *Radiol Clin North Am*. 2014;52(1):27–46. doi: 10.1016/j.rcl.2013.08.006

СПИСОК ЛИТЕРАТУРЫ

1. Министерство здравоохранения Российской Федерации. Временные методические рекомендации: профилактика, диагностика и лечение новой коронавирусной инфекции. Версия 8 (03.09.2020). Москва, 2020. Режим доступа: https://base.garant.ru/74596434/. Дата обращения: 14.03.2021.

2. Романов Б.К. Коронавирусная инфекция COVID-2019 // Безопасность и риск фармакотерапии. 2020. Т. 8, № 1. С. 3–8. doi: 10.30895/2312-7821-2020-8-1-3-8

3. Морозов С.П., Проценко Д.Н., Сметанина С.В., и др. Лучевая диагностика коронавирусной болезни (COVID-19): организация, методология, интерпретация результатов: препринт № ЦДТ – Версия 2 от 17.04.2020. Москва; 2020. 78 с.

4. Udugama B., Kadhiresan P., Kozlowski H.N., et al. Diagnosing COVID-19: The disease and tools for detection // ACS Nano. 2020. Vol. 14, N 4. P. 3822–3835. doi: 10.1021/acsnano.0c02624

5. Zhao W., Zhong Z., Xie X., et al. Relation between chest ct findings and clinical conditions of coronavirus disease (COVID-19) pneumonia: a multicenter study // AJR Am J Roentgenol. 2020. Vol. 214, N 5. P. 1072–1077. doi: 10.2214/AJR.20.22976

6. Beregi J.P., Greffier J. Low and ultra-low dose radiation in CT: Opportunities and limitations // Diagn Interv Imaging. 2019. Vol. 100, N 2. P. 63–64. doi: 10.1016/j.diii.2019.01.007

7. Cheng L., Fang T., Tyan J. Fast Iterative adaptive reconstruction in low-dose CT imaging // 2006 International Conference on Image Processing. Atlanta: GA: IEEE; 2006. P. 889–892. Режим доступа: https://ieeexplore.ieee.org/document/4106673/. Дата обращения: 14.03.2021.

8. Hara A.K., Paden R.G., Silva A.C., et al. Iterative reconstruction technique for reducing body radiation dose at CT: feasibility study // AJR Am J Roentgenol. 2009. Vol. 193, N 3. P. 764–771. doi: 10.2214/AJR.09.2397

9. Prakash P., Kalra M., Kambadakone A., et al. Reducing abdominal CT radiation dose with adaptive statistical iterative reconstruction technique // Invest Radiol. 2010. Vol. 45, N 4. P. 202–210. doi: 10.1097/RLI.ob013e3181dzfeec

10. Chen L.G., Wu P.A., Sheu M.H., et al. Automatic current selection with iterative reconstruction reduces effective dose to less than 1 mSv in low-dose chest computed tomography in persons with normal BMI // Medicine (Baltimore). 2019. Vol. 98, N 28. P. e16350. doi: 10.1097/MD.0000000000016350

11. Dangis A., Gieraerts C., De Brueker Y., et al. Accuracy and reproducibility of low-dose submillisievert chest CT for the diagnosis of COVID-19 // Radiology Cardiothoracic Imaging. 2020. Vol. 2, N 2. P. e200196. doi: 10.1148/ryct.2020200196

12. Sethuraman N., Jeremiah S.S., Ryo A. Interpreting diagnostic tests for SARS-CoV-2 // JAMA. 2020. Vol. 323, N 22. P. 2249–2251. doi: 10.1001/jama.2020.8259

13. Long C., Xu H., Shen Q., et al. Diagnosis of the Coronavirus disease (COVID-19): rRT-PCR or CT? // Eur J Radiology. 2020. Vol. 126. P. 108961. doi: 10.1016/j.ejrad.2020.108961

14. Fang Y., Zhang H., Xie J., et al. Sensitivity of chest CT for COVID-19: comparison to RT-PCR // Radiology. 2020. Vol. 296, N 2. P. E115–E117. doi: 10/1148/radiol.2020200432

15. Yang Y., Yang M., Shen C., et al. Evaluating the accuracy of different respiratory specimens in the laboratory diagnosis and moni-

toring the viral shedding of 2019-nCoV infections // medRxiv. 2020. doi: 10.1101/2020.02.11.20021493

16. Brenner D.J., Hall E.J. Computed tomography — an increasing source of radiation exposure // N Engl J Med. 2007. Vol. 357, N 22. P. 2277–2284. doi: 10.1056/NEJMra072149

17. Pierce D.A., Preston D.L. Radiation-related cancer risks at low doses among atomic bomb survivors // Radiat Res. 2000. Vol. 154, N 2. P. 178–186. doi: 10.1667/0033-7587(2000)154[0178:rrcral]2.0.co;2

18. Маткевич Е.И., Синицын В.Е., Мершина Е.А. Сравнительный анализ доз облучения пациентов при компьютерной томографии в федеральном лечебном учреждении // Вестник рентгенологии и радиологии. 2016. Т. 97, № 1. С. 33–39. doi: 10.20862/0042-4676-2016-97-1-33-40

19. Naidich D.P., Marshall C., Gribbin C., et al. Low-dose CT of the lungs: preliminary observations // Radiology. 1990. Vol. 175, N 3. P. 729–731. doi: 10.1148/radiology.175.3.2343122

20. Prasad S.R., Wittram C., Sherard J.A., et al. Standard-dose and 50%-reduced-dose chest CT: comparing the effect on image quality // AJR Am J Roentgenol. 2002. Vol. 179, N 2. P. 461–465. doi: 10.2214/ajr.179.2.1790461

21. Zwirewich C.V., Mayo J.R., Müller N.L. Low-dose high-resolution CT of lung parenchyma // Radiology. 1991. Vol. 180, N 2. P. 413–417. doi: 10.1148/radiology.180.2.2068303

22. Zhu X., Yu J., Huang Z. Low-dose chest CT: optimizing radiation protection for patients // AJR Am J Roentgenol. 2004. Vol. 183, N 3. P. 809–816. doi: 10.2214/ajr.183.3.1830809

23. Kubo T., Ohno Y., Takenaka D., et al. Standard-dose vs. low-dose CT protocols in the evaluation of localized lung lesions: Capability for lesion characterization – iLEAD study // Eur J Radiol Open. 2016. Vol. 3. P. 67–73. doi: 10.1016/j.ejro.2016.03.002

24. Гомболевский В.А., Чернина В.Ю., Блохин И.А. Основные достижения низкодозной компьютерной томографии в скрининге рака легкого // Туберкулез и болезни легких. 2021. Т. 99. № 1. С. 61–70. doi: 10.21292/2075-1230-2021-99-1-61-70

25. Rampinelli C., De Marco P., Origgi D., et al. Exposure to low dose computed tomography for lung cancer screening and risk of cancer: secondary analysis of trial data and risk-benefit analysis // BMJ. 2017. Vol. 356. P. j347. doi: 10.1136/bmj.j347

26. Chiles C. Lung cancer screening with low dose CT // Radiol Clin North Am. 2014. Vol. 52, N 1. P. 27–46. doi: 10.1016/j.rcl.2013.08.006

AUTHORS' INFO

* Daria A. Filatova;
address: 1a Shkolnaya street, 143430 Nakhabino, Moscow region, Russia; ORCID: https://orcid.org/0000-0002-0894-1994; eLibrary SPIN: 2665-5973; e-mail: dariafilatova.msu@mail.ru

Valentin E. Sinitsin, MD, Dr. Sci. (Med.), Professor; ORCID: https://orcid.org/0000-0002-5649-2193; eLibrary SPIN: 8449-6590; e-mail: vsini@mail.ru

Elena A. Mershina, MD, Cand. Sci. (Med.), Associate Professor; ORCID: https://orcid.org/0000-0002-1266-4926; eLibrary SPIN: 6897-9641; e-mail: elena_mershina@mail.ru

ОБ АВТОРАХ

* Филатова Дарья Андреевна;
адрес: Россия, 143430, Московская обл., п.г.т. Нахабино, ул. Школьная, д. 1а; ORCID: https://orcid.org/0000-0002-0894-1994; eLibrary SPIN: 2665-5973; e-mail: dariafilatova.msu@mail.ru

Синицын Валентин Евгеньевич, д.м.н., профессор; ORCID: https://orcid.org/0000-0002-5649-2193; eLibrary SPIN: 8449-6590; e-mail: vsini@mail.ru

Мершина Елена Александровна, к.м.н., доцент; ORCID: https://orcid.org/0000-0002-1266-4926; eLibrary SPIN: 6897-9641; e-mail: elena_mershina@mail.ru

* Corresponding author / Автор, ответственный за переписку

Вариабельность заключений при интерпретации КТ-снимков: один за всех и все за одного

Н.С. Кульберг[1, 2], Р.В. Решетников[1, 3], В.П. Новик[1], А.Б. Елизаров[1], М.А. Гусев[1, 4], В.А. Гомболевский[1], А.В. Владзимирский[1], С.П. Морозов[1]

[1] Научно-практический клинический центр диагностики и телемедицинских технологий Департамента здравоохранения г. Москвы, Москва, Российская Федерация

[2] Федеральный исследовательский центр «Информатика и управление» Российской академии наук, Москва, Российская Федерация

[3] Первый Московский государственный медицинский университет имени И.М. Сеченова (Сеченовский Университет), Москва, Российская Федерация

[4] Московский политехнический университет, Москва, Российская Федерация

АННОТАЦИЯ

Обоснование. Разметка наборов медицинских изображений во многом полагается на субъективную интерпретацию наблюдаемых подозрительных структур. На настоящий момент не существует рекомендованного протокола по определению эталонных данных (ground truth), основанных на врачебных описаниях.

Цель — анализ правильности и согласованности оценок рентгенологов, принимавших участие в подготовке общедоступного набора данных CTLungCa-500; определение взаимосвязи этих показателей с количеством специалистов, проводящих независимую интерпретацию изображений, полученных при компьютерно-томографическом (КТ) исследовании.

Материал и методы. Набор данных, в разметке которого принимали участие 34 рентгенолога, включает 536 КТ-исследований пациентов из группы риска развития рака лёгкого. Каждое КТ-исследование было независимо интерпретировано шестью специалистами, после чего обнаруженные ими подозрительные структуры проходили арбитраж другим экспертом. Для каждого эксперта подсчитывали количество истинно положительных, ложноположительных, истинно отрицательных и ложноотрицательных находок, на основании которых проводили оценку диагностической точности рентгенологов. Для анализа согласованности между заключениями рентгенологов использовали метрику процентного показателя.

Результаты. Увеличение количества специалистов, проводящих независимую интерпретацию КТ-исследований, ведёт к росту правильности их оценок при снижении согласованности. Среди факторов, влияющих на согласованность заключений между парами исследователей, выделяется расхождение мнений по поводу наличия лёгочного очага в конкретном участке КТ-снимка.

Заключение. Увеличение числа независимых первичных интерпретаций способно повысить их комбинированную правильность при условии проведения арбитража, причём квалификация рентгенологов не имеет определяющего значения для качества анализа. Проведение первичной разметки силами четырёх рентгенологов является оптимальным с точки зрения сочетания правильности интерпретации и её стоимости.

Ключевые слова: компьютерная томография; набор данных; эталонные данные; согласованность между заключениями.

Inter–observer variability between readers of CT images: all for one and one for all

Nikolas S. Kulberg[1, 2], Roman V. Reshetnikov[1, 3], Vladimir P. Novik[1], Alexey B. Elizarov[1], Maxim A. Gusev[1, 4], Victor A. Gombolevskiy[1], Anton V. Vladzymyrskyy[1], Sergey P. Morozov[1]

[1] Moscow Center for Diagnostics and Telemedicine, Moscow, Russian Federation
[2] Federal Research Center "Computer Science and Control" of Russian Academy of Sciences, Moscow, Russian Federation
[3] Institute of Molecular Medicine, The First Sechenov Moscow State Medical University, Moscow, Russian Federation
[4] Moscow Polytechnic University, Moscow, Russian Federation

ABSTRACT

BACKGROUND: The markup of medical image datasets is based on the subjective interpretation of the observed entities by radiologists. There is currently no widely accepted protocol for determining ground truth based on radiologists' reports.

AIM: To assess the accuracy of radiologist interpretations and their agreement for the publicly available dataset "CTLungCa-500", as well as the relationship between these parameters and the number of independent readers of CT scans.

MATERIALS AND METHODS: Thirty-four radiologists took part in the dataset markup. The dataset included 536 patients who were at high risk of developing lung cancer. For each scan, six radiologists worked independently to create a report. After that, an arbitrator reviewed the lesions discovered by them. The number of true-positive, false-positive, true-negative, and false-negative findings was calculated for each reader to assess diagnostic accuracy. Further, the inter-observer variability was analyzed using the percentage agreement metric.

RESULTS: An increase in the number of independent readers providing CT scan interpretations leads to accuracy increase associated with a decrease in agreement. The majority of disagreements were associated with the presence of a lung nodule in a specific site of the CT scan.

CONCLUSION: If arbitration is provided, an increase in the number of independent initial readers can improve their combined accuracy. The experience and diagnostic accuracy of individual readers have no bearing on the quality of a crowd-tagging annotation. At four independent readings per CT scan, the optimal balance of markup accuracy and cost was achieved.

Keywords: X-ray computed tomography; datasets as topic; ground truth; observer variation.

CT图像解释中结论的可变性：
一个为所有和所有为一

Nikolas S. Kulberg[1, 2], Roman V. Reshetnikov[1, 3], Vladimir P. Novik[1], Alexey B. Elizarov[1],
Maxim A. Gusev [1, 4], Victor A. Gombolevskiy[1], Anton V. Vladzymyrskyy[1], Sergey P. Morozov[1]

[1] Moscow Center for Diagnostics and Telemedicine, Moscow, Russian Federation
[2] Federal Research Center "Computer Science and Control" of Russian Academy of Sciences, Moscow, Russian Federation
[3] Institute of Molecular Medicine, The First Sechenov Moscow State Medical University, Moscow, Russian Federation
[4] Moscow Polytechnic University, Moscow, Russian Federation

结构简评

理由： 医学图像集的标记在很大程度上依赖于观察到的可疑结构的主观解释。目前，没有推荐的协议用于根据医学描述确定参考数据（ground truth）。

目标： 评估参与编制公开数据集»CTLungCa-500»的放射科医生评估的正确性和一致性，以及确定这些指标与对CT研究进行独立解释的专家数量的关系。

方法： 该数据集包括有患肺癌风险的患者的536项CT研究，其中34名放射科医生参加了该研究。每项CT研究都由六位专家独立解释，之后他们发现的可疑结构由另一位专家进行仲裁。对于每位专家计算真阳性，假阳性，真阴性和假阴性结果的数量，在此基础上评估放射科医生的诊断准确性。为了分析放射科医生的结论之间的一致性，使用了百分比度量。

结果： 对CT研究进行独立解释的专家数量的增加在一致性降低的情况下导致其评估的正确性增加。在影响成对研究人员之间结论一致性的因素中，关于CT图像的特定部分中存在肺焦点的观点不一致。

结论： 独立的初级解释数量的增加使它们的组合正确性会升高，但需要仲裁，放射科医生的资格对分析的质量没有决定性的价值。从结合解释的正确性及其成本的角度来看，由四名放射科医生进行主要标记是最佳的。

关键词： 计算机断层扫描，数据集，参考数据，结论之间的一致性.

INTRODUCTION

In 2017, S.P. Morozov et al. prepared a publicly available dataset, "Tagged results of computed tomography of the lungs," later called "CTLung500-Ca" [1, 2]. This set comprises 536 computed tomography (CT) chest X-ray images of lung cancer high risk patients. Each study was independently interpreted by six radiographers, and the findings were subsequently reviewed by an additional expert. The markup used an approach with a weak annotation of findings, i.e., the indication of a limited number of nodules on the CT image, which were localized by specifying the coordinates of the enclosing spheres of maximum diameter with their subsequent clustering [2, 3]. S.P. Morozov et al. developed such a markup and annotation protocol because the interpretations of radiologists tend to be subjective and are not immune to error. Under conditions in which the costs of false positive (FP) and false negative (FN) findings are equally high, the arbitration of primary interpretations can increase the correctness of conclusions [4]. Such arbitration is only effective if radiographers commit different mistakes. According to P.G. Herman and S.J. Hessel, the probability that two or more radiographers can make the same FP finding is low. However, a significant proportion of FN errors, as a rule, is made by two or more specialists [5]. Thus, the number of radiologists who independently interpret CT scans can affect significantly the correctness of markup and annotation.

STUDY AIM

The study primarily aimed to investigate the relationship between the number of independent interpretations located in the CTLungCa-500 CT scan database and the number and type of errors made and to search for a CT scan interpretation protocol that promotes optimal tagging correctness. The secondary aim of the study was the analysis of agreement between the radiographers who participated in the dataset preparation.

METHODS

Study design

In this work, we analyzed the data of a retrospective multicenter observational study focused on the analysis of prospects for the use of computer vision technologies in the healthcare system of Moscow.

Inclusion criteria

The inclusion criteria were patients of polyclinics in Moscow, aged 50–75 years, who underwent a diagnostic CT study referred by an attending physician due to suspected lung cancer.

Conditions in conducting the experiment

In accordance with the inclusion criteria, 3897 CT examinations were downloaded from the Unified Radiological Information Service. A total of 550 CT examinations were selected randomly from this array to create a dataset, "Tagged results of computed tomography of the lungs." Exactly 14 CT scans were excluded from the sample due to non-compliance with the inclusion criteria or the protocol of medical intervention.

Study duration

The dataset included the results of CT examinations conducted from January 01, 2015 to December 31, 2017.

Description of the medical intervention

The recommended scanning parameters for adult patients (height: 170 cm, body weight: 70 kg) included the automatic modulation of the current on the tube at a voltage of 120 kV, field of view of 350 mm, slice thickness of 1.5 mm or less, and the distance between adjacent slices the same as the slice thickness or less. Scanning was performed with the patient in the supine position, with the scanning directed from the diaphragm to the apex of the lungs within a single breath-hold. Reconstruction kernels were specific for a particular tomographic scanner manufacturer, namely, FC50, FC51, FC52, FC53, and FC07 for lungs and FC07, FC08, FC09, FC17, and FC18 for soft tissues for Toshiba machines; B70, B75, and B80 for Siemens devices; Y-Sharp and LUNG for lungs and SOFT for soft tissues for Philips devices; LUNG for lungs and SOFT for soft tissues for GE (General Electrics) devices.

Primary study outcome

Two groups of volunteer radiographers participated in the tagging and annotation of the studies. Representatives of Group 1 (primary experts), consisting of 15 specialists with working experience of 2–10 years or more, performed the primary interpretation of CT scans. In accordance with the developed methodology, doctors searched for pulmonary nodules with sizes from 4 mm to 30 mm on CT images and retained the information about the findings, such as localization of pulmonary nodules (position of the center of the finding by defined by two dimensions in the image and the slice number); diameter of the finding; type of pulmonary nodule (solid, part solid, or ground glass opacity nodule). Medical specialists were advised not to mark calcified and peri-fissural lesions in the lungs and not to mark more than five of the largest pulmonary nodules on a single CT scan. Each study was reviewed independently by six radiographers to reduce the probability of missing potential pulmonary lesions. Then, one of the participants in Group 2 (arbitrators), consisting of three radiologists with 10 or more years of working experience, reviewed the tagging made by the radiologists of Group 1 to assess the significance of each mark. The arbitrators also assessed the malignancy of the lesions detected, referring them to the category of "malignant" or "benign," guided by the Fleischner Society recommendations [6].

Ethical considerations

The study, whose data were used for the analysis in this work, was approved by the Independent Ethics Committee of the Moscow Regional Branch of the Russian Society of Roentgenologists and Radiologists (Protocol No. 2 1-II-2020 dated February 20, 2020). All procedures performed on patients during the study were in accordance with the standards of the regional and national research committee and the Declaration of Helsinki and the Taipei Declaration of the World Medical Association.

Statistical analysis

The numbers of true positive (TP), FP, true negative (TN), and FN findings were counted for each radiologist who performed the initial interpretation to determine the specificity (Sp) and sensitivity (Se) of individual specialists. The cases were considered TP if the opinions of the radiologist and the arbitrator coincided about the presence and type of a pulmonary nodule (solid, part solid, or ground glass) in a particular area. The cases were FP if the arbitrator recognized the primary expert's assessment as erroneous regarding the presence or type of a pulmonary nodule in a given area. The cases were considered TN when the radiologist did not mark the entity, which in the opinion of the arbitrator, was mistaken for a lung nodule by one or more of the other five primary experts. Finally, for FN cases, the radiologist did not recognize a pulmonary nodule that was correctly identified by one or more of the five other participants, in the opinion of the arbitrator. When analyzing the data, we assumed that the arbitrator's opinion is always correct.

Se was calculated by the following equation:

$$Se = \frac{TP}{(TP + FN)}. \tag{1}$$

Sp was calculated as follows:

$$Sp = \frac{TN}{TN + FP}. \tag{2}$$

For each participant, Youden's index (J) was determined:

$$J = Se + Sp - 1. \tag{3}$$

To calculate the accuracy indicator (*Acc*) of different samples of primary experts, we defined the TP as the cases when at least one specialist from the sample identified correctly, in the opinion of the arbitrator, a pulmonary nodule in a specific area of the CT scan. The TN results included cases in which at least one specialist from the sample did not notice a lesion, which was mistaken, in the opinion of the arbitrator, for a pulmonary nodule by any other participant in the study. The accuracy was calculated as follows

$$Acc = \frac{(TP + TN)}{(P + N)} \times 100, \tag{4}$$

where P is the number of correct findings, and N is the number of incorrect findings.

A number of metrics are available for the assessment of agreement among one or more researchers. O. Gerke et al., in their recommendations for the systematization of agreement studies, suggested using the Bland–Altman analysis [7]. Other common metrics are Cohen's [8] and Fleiss' [9] kappa. However, with all the advantages of these methods, they are difficult to interpret. Thus, the authors of this work settled on the simplest option, that is, the percentage agreement between researchers, which disregards the factor of random coincidences of radiologists' conclusions but at the same time is intuitively comprehensible and reflects reliably the main regularities, provided that repeated experiments are performed. The percentage was calculated as the proportion of nodules for which expert opinions (presence, type) coincided in relation to the total number of jointly tagged nodules:

$$Consistency = \frac{Matches}{Matches + Mismatches} \times 100. \tag{5}$$

Statistical analysis was performed using the dplyr [10], irr [11], and ggplot2 [12] packages for R 3.6.3 [13]. When preparing the data, we used self-written scripts in the Python 3.8.2 language [14].

RESULTS

Research objects

A total of 31 radiologists took part in the primary interpretation of CT images. Each radiologist from the initial cohort of 15 specialists was replaced by another specialist during the study due to refusal or inability to continue the study; one participant was replaced twice. The radiographers' workload was distributed unevenly. Each specialist from the initial cohort participated in labeling and annotating an average of 1050 ± 140 lesions. The radiologists who replaced them tagged an average of 110 ± 42 lesions.

Based on the tagging results, the dataset included 72 CT scans, in which radiologists did not find pulmonary nodules from 4 mm to 30 mm, and 464 CT scans with pulmonary nodules, comprising 3151 findings confirmed by the arbitrator. A total of 1761 lesions were classified by experts as presumable malignant, 445 lesions as benign, and 945 entities of a different nature (they contained calcifications, adipose tissue, fibrous tissue, or fluid).

Key research findings

Se and Sp of radiographers involved in the tagging

During the work on the dataset, a three-digit identification number (ID) was assigned to each radiologist. In the case of replacement of a specialist, the new participant inherited his ID with an additional "+" symbol. The average value of Se was 34.9% (95% confidence interval [CI]: 30.4–39.4), and that of Sp was 78.4% (95% CI: 74.9–81.9),

which was noticeably inferior to the minimum indicators demonstrated by radiologists in a similar study of D. Ardila et al., namely, 62.5% (95% CI: 54.4–70.7) and 95.3% (95% CI: 94.0–96.6), respectively [15].

The difference noted was possibly caused by the tagging recommendations, guided by which the primary experts tagged a maximum of five nodules in the image. This recommendation is based on the results of the NELSON study, according to which the risk of primary cancer increases with increase in the number of lesions to four but decreases for patients with five or more lesions [16]. In cases of multiple lesions (>5), this approach can artificially underestimate the diagnostic accuracy of primary experts because it introduces an additional degree of freedom associated with a specific set of lesions that each radiologist

has tagged. This uncertainty can be corrected by introducing an alternative classification of findings, recognizing the cases as TP when the primary expert tagged at least one confirmed nodule on the CT scan. With this assessment scheme, the average Se of primary experts was 66.2% (95% CI: 62.1–69.9), and the Sp was 78.5% (95% CI: 72.3–84.8). However, the markup was aimed at creating a dataset designed to train artificial intelligence algorithms, and every suspicious structure on a CT image was of interest. For this reason, in this work, the criteria set out in the Methods section were used to assess the diagnostic accuracy. In accordance with these criteria and based on Youden's index, the radiologist with ID 012+ showed the highest accuracy (J = 0.472), and the specialist with ID 008+ had the owest (J = −0.188) (Table 1).

Table 1. Diagnostic correctness of study participants.

Expert ID	Indicators for individual nodules			
	Se, %	Sp, %	Youden's Index	Number of tagged nodules*
000	39,52	73,17	0,127	1079
001	32,63	79,04	0,117	1068
002	28,25	80,19	0,084	1045
003	44,05	67,75	0,118	1094
004	31,37	68,75	0,001	844
005	33,08	72,76	0,058	1222
006	36,91	71,32	0,082	1085
007	37,31	73,43	0,107	884
008	42,01	68,00	0,100	1227
009	36,79	79,50	0,163	1265
010	38,62	71,16	0,098	1166
011	26,05	79,51	0,056	853
012	33,97	71,88	0,058	1045
013	38,52	77,40	0,159	1028
014	37,16	82,32	0,195	850
000+	31,63	79,17	0,108	194
001+	52,94	82,46	0,354	108
002+	62,50	57,14	0,196	46
003+	60,71	86,21	0,469	86
004+	27,78	86,49	0,143	110
005+	41,49	75,86	0,173	152
006+	31,34	74,14	0,055	125
007+	29,73	85,71	0,154	86
008+	18,99	62,16	−0,188	176
009+	25,76	85,11	0,109	113
010+	25,00	75,36	0,004	145
011+	31,58	93,33	0,249	68
012+	53,85	93,33	0,472	97
013+	34,29	85,71	0,170	77
014+	17,95	100,0	0,179	63
000++	0,00	94,87	−0,051	48

Note. *All lesions revealed in CT examinations were considered in the tagging in which the expert participated, regardless of whether he recognized them or not.

Influence of the number of researchers on the interpretation accuracy

Interpretation by two primary experts. In this analysis, a sample of 97 CT studies was considered and interpreted by the radiologist (ID 012+) who showed the highest Youden's index score among all participants (Table 1). With this sample size, all estimates obtained may differ from the average for the full data set by no more than 10% [17]. The sample tagged by this specialist contained 53 solid pulmonary lesions, 6 part solid, and 5 ground glass lesions. In addition, 33 entities discovered by radiologists were not confirmed in the course of arbitration. The accuracy of assessments by Radiologist 012+ was 65.98%, that is, he correctly identified 28 solid nodules and avoided 32 out of 33 FP errors made by other specialists in the same studies while recognizing incorrectly 2 solid and 1 part solid nodules and committing 34 FN errors. In addition, the radiologist with ID 012, who had one of the lowest Youden's index scores (0.058, place 24; Table 1), also participated in tagging all 97 CT studies in the sample. This specialist correctly recognized 32 solid lesions, 1 part solid, and 1 ground glass lesion and avoided 18 FP errors. With the agreement between researchers equaling 59.8%, the joint accuracy of their estimates was 81.44%. The sources of disagreement were the discrepancy between the opinions within the pair regarding the presence of a lesion in a particular area (92.3% of cases) and the type of pulmonary nodule (7.7% of cases).

The distribution of CT studies among specialists was performed in a random manner. For this reason, all 97 CT studies in the studied sample were interpreted only by primary Experts 012 and 012+. In addition, 17 radiographers participated in sample tagging (the number of tagged nodules is indicated in the brackets for each ID), namely, 000(11), 002(54), 003(30), 004(27), 005(18), 006(40), 007(10), 008(16), 009(17), 010(32), 011(24), 013(30), 014(52), 004+(7), 005+(10), 011+(1), and 014+(9). They enabled the comparison of the situation in which the second opinion on all studies in the sample was expressed by one specialist, with the crowd-tagging model, in which an opinion is provided by a participant selected randomly from a certain expert group with variable Sp and Se indices.

Group 1 included six researchers (Table 2). The average Youden's index in this group was 0.078 ± 0.045 (maximum value: 0.127; minimum value: 0.001), which exceeded the indicator of Radiologist ID 012 (0.058). Nevertheless, the agreement of estimates with Radiologist 012+ was 40.2%, and the joint accuracy of the estimates was 74.23%. The source of most of disagreements in the pair (97.4%) was the divergence of opinions about the presence of pulmonary nodules.

In a repeated similar experiment, a group with a different composition of participants was analyzed (Table 3). The number and composition of participants differed between Groups 1 (Table 2) and 2 (Table 3). Moreover, the distribution of the number of nodules tagged by each expert was uneven.

The mean Youden's index in Group 2 was 0.099 ± 0.055 (maximum: 0.173, minimum: 0.01) and was higher than that by Radiologist 012 and in Group 1. The agreement and joint accuracy of the assessments of participants in Group 2 and Radiologist 012+ were the highest of the three considered options for the interpretation of CT studies by two experts, accounting for 71.1% and 83.50%, respectively. The disagreement between researchers in 89.3% of cases was associated with the presence of a pulmonary nodule in this area and with its type in 10.7%. The average accuracy of interpretations during the primary tagging by two specialists in any combination was 79.72% ± 4.87%.

Interpretation by three or more researchers. When analyzing the interpretation by three or more researchers, all groups included Radiologists 012 and 012+. With the primary tagging and annotation by three radiologists, the agreement of their estimates ranged from 32.0% to 42.3%, and the average joint accuracy was 89.18% ± 5.10%. The inter-observer agreement between the assessments of four independent specialists decreased to 16.5% ± 5.7%, whereas the average joint accuracy increased to 93.82% ± 3.57%. For five radiographers, the inter-observer agreement continually declined to 9.8% ± 8.1%, and the accuracy continually increased to 97.94% ± 0.14%. Finally, the joint accuracy of the six experts was 100% under our experimental conditions, with the agreement of 3.1% (Fig. 1). Thus, a significant inverse correlation existed between the accuracy and agreement of expert assessments ($r = -0.78$, $p < 0.05$).

In support of the conclusions by P.G. Herman and S.J. Hessel [5], in a sample of 97 studies, when interpreted by six specialists, 85.7% of FP errors were made by one expert, 11.4% by two experts, and 2.9% by three experts at the same time. All six experts identified correctly 8.1% of positive findings in the sample. Meanwhile, 25.8% of FN errors

Table 2. Distribution of tagged suspicious structures in Group 1.

Researcher ID	000	002	003	004	005	006
Number of tagged nodules	11	54	9	3	11	9

Table 3. Distribution of tagged suspicious structures in Group 2.

Researcher ID	005+	010	003	004	005	006	008	009
Number of tagged nodules	10	10	21	9	7	31	8	1
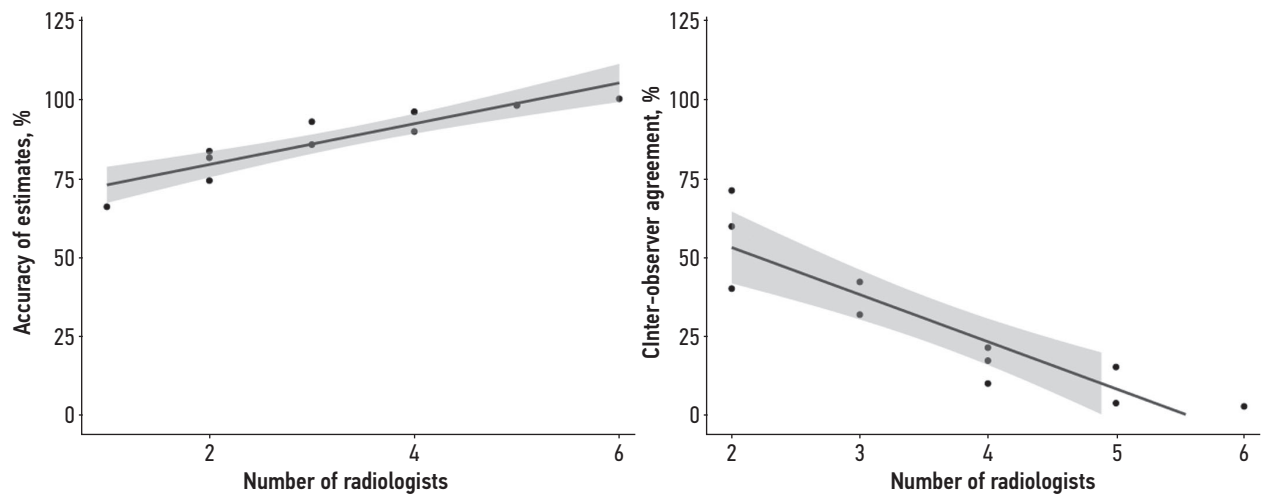
Fig. 1. Accuracy and agreement of estimates as a function of the number of radiologists participating in the primary tagging. The 95% CI is presented in gray. The points correspond to different samples of primary experts. For experiments with two, three, and four experts, three different samples were selected from the initial six radiologists; two various samples were used for five experts.

were made by one expert out of six, 8.1% by two experts, 8.1% by three experts, 19.3% by four experts, and 30.6% by five experts (Fig. 2).

Markup cost

To assess the optimal efficiency of tagging from the standpoint of the rational use of resources, we considered the cost of involving additional experts in the interpretation of CT images. Thus, the improvement in accuracy can be balanced against the increased cost of annotating the studies.

Given that volunteer radiologists participated in tagging the dataset, their work was not paid. Thus, we calculated the cost of tagging in terms of the time spent by the experts. On the average, the primary expert spent 12 min on
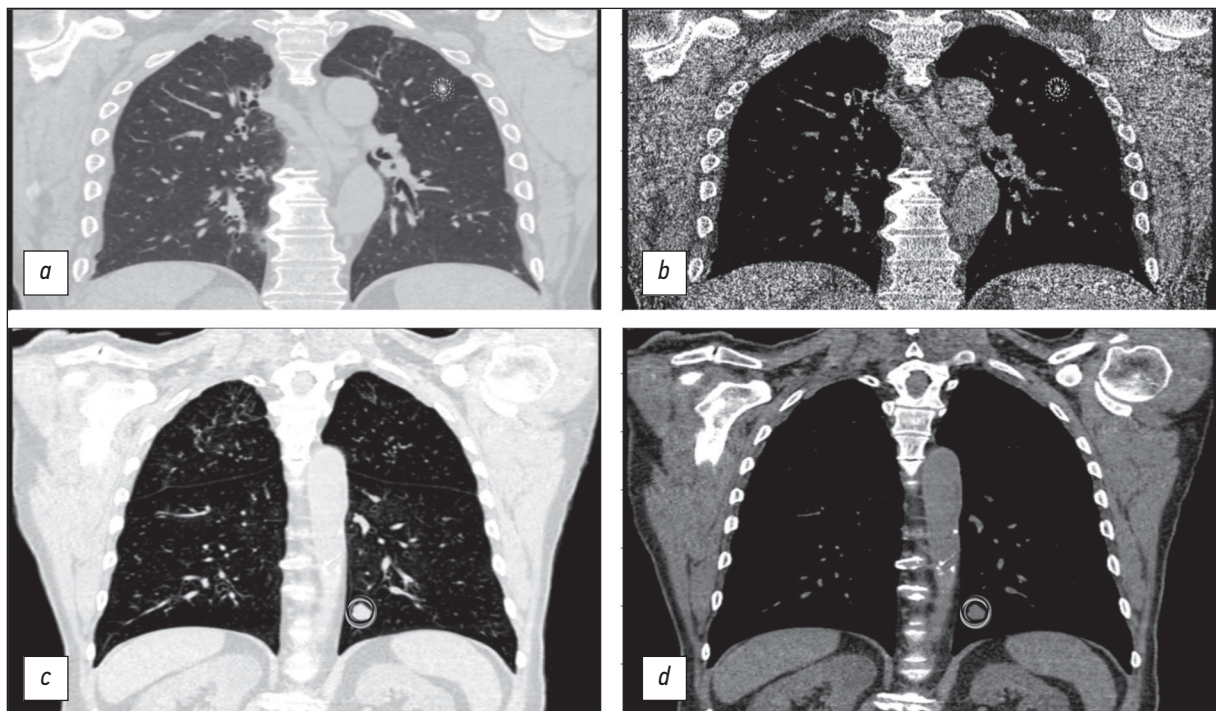
Fig. 2. Examples of CT studies with significant disagreement (*a* and *b*; CTLungCa-500 AN RLADD02000018919, ID RLSDD02000018855) and full consistency (*c* and *d*; CTLungCa-500 AN RLAD42D007-25151, ID RLSD42D007-25151) between experts. The studies are presented in frontal projection in pulmonary (*a* and *c*) and soft tissue (*b* and *d*) modes. The vertical division is 50 mm, and the horizontal division is 100 pixels. The radiologists' marks are presented with different colors: *a* and *b*: the nodule was tagged by five primary experts out of six; four experts classified it as a solid type, and one expert classified it as a semi-solid one. The arbitrator disagreed with their opinion, recognizing the finding as benign calcification; *c* and *d*: all six primary experts and the arbitrator classified the lesion as a potentially malignant solid.

Table 4. Estimated cost of error elimination

Number of primary experts	Number of errors eliminated	Cost, min/error
2	15	129,3
3	19	183,8
4	29	173,9
5	31	212,8
6	33	246,9

the interpretation of one CT image, and the arbitrator spent 4 min. In the present study, the cost of eliminating error C in the studied sample of 97 CT images was calculated as the difference in the average cost of tagging by a given number of primary experts with the involvement of an arbitrator and the cost of tagging by one radiologist without the involvement of an arbitrator divided by the number of errors eliminated (N_{err}):

$$C = \frac{(n \times 12 \times 97 + n \times 4 \times 97) - 12 \times 97}{N_{err}} \ , \qquad (6)$$

where n is the number of primary experts.

Expert 012+ committed 33 FP and FN errors. Table 4 presents the number of errors eliminated due to attracting additional experts and conducting arbitration and the corresponding cost of eliminating the error. We observed a dependence according to which each new primary expert increased the cost of error elimination by 42.5 ± 10.7 min, excluding one point. The tagging of the dataset by four primary experts with subsequent arbitration was accompanied by a rapid increase in the number of eliminated errors and a decrease in cost (Table 4).

Additional research findings

Given the aspects of the study design, in which each expert interpreted an individual CT scan only once, this study did not assess the intra-observer agreement among individual radiologists. The average value of inter-observer agreement between pairs of specialists was 60.5% ± 5.3%, with a minimum value of 53.1% and a maximum value of 73.0%.

Another way to assess the agreement between primary experts was the analysis of positive findings of each radiologist (Fig. 3). For each representative of the initial cohort, the maximum proportion of detected nodules (37.6% ± 5.4%) corresponded to unique findings that were not recognized by other experts (Fig. 3a). Then, in descending order, the findings were approved by one (21.4% ± 2.8%), two (14.0% ± 2.0%), four (9.5% ± 2.3%), three (9.2% ± 1.8%), and five (8.1% ± 3.1%) primary experts. The proportion of
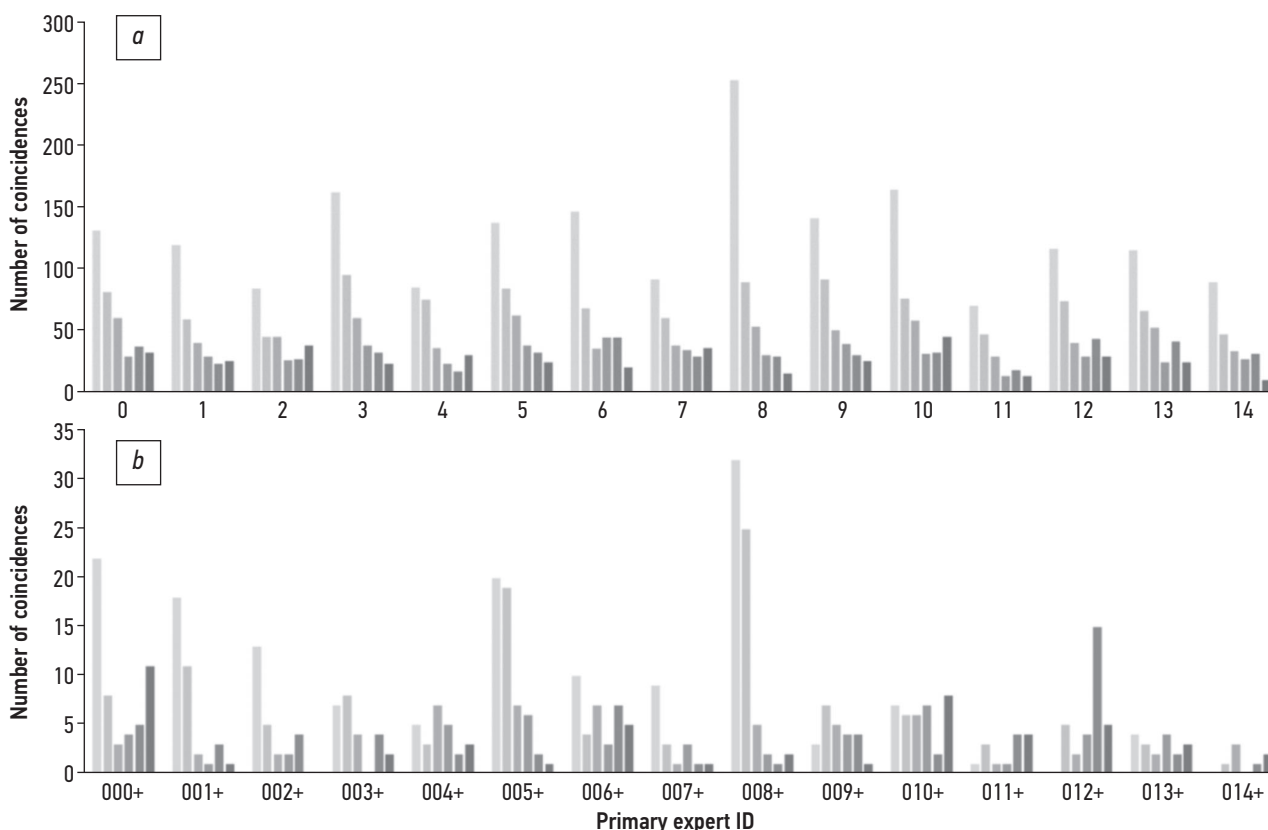
Fig. 3. Agreement between primary experts: *a*. representatives of the initial cohort of 15 radiographers; *b*. replacement radiographers. The data for the expert with ID 000++ are not given due to the small number of lesions annotated. For each radiologist, Column 1 corresponds to the number of lesions tagged uniquely by that specialist (none of the other five experts recognized this finding). The following are columns corresponding to cases where the lesion identified by the radiologist was noted by one, two, three, four, and five other primary experts. The graph disregards the approval of the arbitrator and the differences in the opinion between radiologists about the type of lesion.

unanimously approved findings exceeded 10% for four radiologists from the initial cohort (ID 002, 004, 007, and 010). None of these experts was included in the leading group in terms of Youden's index, which was calculated in accordance with the methodology proposed in this work. Moreover, Radiologist 004 showed the poorest performance in the cohort for this indicator (Table 1). Meanwhile, Radiologist 014, which showed the highest Youden's score in the cohort (0.195), did not stand out among his colleagues in terms of the consistency of positive findings (Fig. 3*a*).

The cohort of radiographers who replaced the initial primary experts had a different distribution of finding agreement (Fig. 3*b*). The maximum proportion of identified nodules (28.9% ± 18.2%) was still represented by unique findings. This result was followed by findings identified simultaneously by two (23.3% ± 11.0%), three (13.3% ± 10.7%), five (13.2% ± 11.9%), six (11.5% ± 9.8%), and four (9.7% ± 7.6%) experts. This cohort had eight radiographers (ID 000+, 004+, 006+, 010+, 011+, 012+, 013+, and 014+), for which the proportion of unanimously approved positive findings exceeded 10%, and the value was above 20% for four of them (ID 000+, 010+, 011+, and 014+). Nevertheless, these indicators may be due to the small number of positive findings in this cohort, which is indirectly evidenced by the high variation in their consistency, expressed in terms of mean values and standard deviations. For example, Expert 014+ participated in the interpretation of CT studies, where other experts identified 63 entities (Table 1). This expert tagged seven nodules, one of which was identified by another expert, three by two experts, one by five experts, and two nodules by six experts (Fig. 3*b*). Furthermore, the expert committed 32 FN errors, thus ignoring approximately 50% of true positive findings. For this cohort, no correlation was registered between the consistency of the positive findings and the expert's Youden's score.

DISCUSSION

Summary of the main research findings

Our results demonstrated that an increase in the number of specialists conducting an independent interpretation of CT studies led to an increase in the accuracy of their estimates, and the level of qualification showed no significant effect on either the consistency of opinions of radiologists or their joint accuracy. Among the factors affecting the inter-observer agreement between the pairs of researchers, a discordance of opinions was observed concerning the presence of lesions in a particular area of the CT scan.

Main research results

No consensus is currently available regarding the recommended number of radiologists to participate in the primary markup and annotation of medical imaging datasets. In general, this number ranges from one [18, 19] to four [20].

Only the work by P.G. Herman and S.J. Hessel addressed this issue; according to their research, the number of error-free descriptions gradually decreases with the increase in the number of specialists providing independent interpretations of studies [5]. Although this finding piques interest, it is of little practical value because the arbitrage model is, in principle, based on the assumption that primary interpretations comprise errors. Moreover, its efficiency increases provided that these errors are different.

The last statement is not always true. In particular, the results of this work indicate that radiologists committing different mistakes does not lead automatically to an increase in the joint accuracy of their conclusions. In an experiment with two specialists who performed the primary interpretation of CT images, the highest level of disagreement was registered in pair 2 (agreement 40.2%), which had also the lowest accuracy of the three considered pairs (74.2% versus 81.4% and 83.5%). In addition, pair 3 showed the highest accuracy value with the maximum agreement (71.1%). Nevertheless, according to the data obtained in this work, a significant negative correlation existed between the agreement of expert assessments and their accuracy ($r = -0.78$). Thus, at the initial interpretation by two radiographers, the agreement of 57.0% ± 15.6% was noted, with the accuracy of 79.7% ± 4.9%. For five radiographers, these indicators were equal to 9.8% ± 8.1% and 97.9% ± 0.1%, respectively, and this dependence was retained in all the considered variants of dataset tagging (Fig. 1).

According to the results of this study, the optimal combination of accuracy and markup cost can be achieved by an approach involving four primary experts and subsequent arbitration (Table 4). In that case, a rapid increase in the number of eliminated errors was observed in comparison with the tagging by three radiologists, accompanied by a decrease in the time spent on eliminating one error (−9.9 min). The involvement of additional primary experts led to a further increase in the accuracy of interpretations. However, this finding was due to an increase in the cost of eliminating errors by an average of 42.5 ± 10.7 min.

In the present work, when classifying the assessments of primary experts to the categories of FN, TN, FP, and TP, we relied on the assumption that all pulmonary nodules will be tagged on each CT scan. However, the study results indicated that the study participants limited themselves to the five largest pulmonary lesions on CT scans, following the recommendations given to them. Thus, some pulmonary nodules were ignored by individual radiographers, which affected their diagnostic accuracy and the inter-agreement values in expert pairs. Nevertheless, differences in the opinions between primary experts are a desirable outcome when using arbitration because they expand the range of tagged lesions. This condition reduces the proportion of FN findings, even under artificial restrictions on the number of nodules to be tagged. One of the main outcomes of this work is that consensus among several radiographers

is not a prerequisite for proper tagging of datasets. The arbitrators bear the main responsibility because they must correctly interpret all entities noted by the primary experts (Figs. 2*a* and 2*b*).

Research Limitations

The main limitation of this work was the model for determining the ground truth, that is, the findings that should be considered pulmonary nodules. When interpreting CT scans, radiologists lacked access to the clinical, biological, and genomic data of patients. Moreover, the set did not contain two studies that spread out over a period of time, which would have enabled the assessment of the dynamics of development of lesions, for any of the patients. We also proceeded from the assumption that the opinion of the arbitrator is always correct, and we interpreted the disagreements between the primary experts and the arbitrator always in favor of the latter. However, the set presented a number of examples that raised doubts about the reliability of this approach. In particular, 19 pulmonary lesions were tagged by the arbitrator as both benign and malignant. This result is consistent with the results of S.J. Hessel et al., who demonstrated that arbitrators can resolve correctly about 80% of disagreements between primary experts [4].

Another limitation of the work was the inability to assess the reproducibility of the conclusions of individual radiographers. A limited sample was used to achieve the main objectives of the study. For more reliable statistics, the optimal approach would be the bootstrap method. Finally, the assessment of the diagnostic accuracy of the primary experts in the present study relied on the assumption that they would mark all pulmonary nodules. If more than five lesions were observed on the CT scan, this assumption was in conflict with the recommendations for tagging, which can affect the final individual indicators of Se and Sp. To compensate for this methodological limitation, the study authors attempted to assess the consistency in the number of positive findings for each primary examiner approved by two, three, four, and five other radiographers (Fig. 3). However, such an analysis neglected the FN errors, and therefore, its results showed no correlation with the obtained values of Youden's index for each expert. In addition, this study analyzed the results of interpretation of standard dose CT scans. Thus, its findings may not apply to the data obtained from screening studies characterized by the use of low-dose and ultra-low-dose CT protocols.

CONCLUSION

Despite its limitations, this work demonstrated convincingly that an increase in the number of independent primary interpretations can increase their accuracy, if the arbitration is performed. In addition, the qualifications of radiologists are not the decisive factor of the quality of their analysis because according to the results obtained, the joint accuracy of their assessments was independent of individual Youden's indices. The optimal combination of accuracy and cost of tagging was achieved during the initial independent interpretation of CT examinations by four experts. This statement created a theoretical basis for the development of requirements for artificial intelligence algorithms intended for use in the diagnosis of diseases by tagging suspicious structures on CT scans, guiding and attention of radiologists. In addition, the results obtained in this work enable the substantiation of the project model for crowd-tagging of datasets, in which an increase in the number of taggers will lead to a decrease in agreement and a simultaneous increase in the quality of the final product, given arbitration.

ADDITIONAL INFORMATION

REFERENCES

1. Morozov SP, Kulberg NS, Gombolevsky VA, et al. Moscow Radiology Dataset CTLungCa-500. 2018. (In Russ). Available from: https://mosmed.ai/datasets/ct_lungcancer_500/
2. Morozov SP, Gombolevskiy VA, Elizarov AB, et al. A simplified cluster model and a tool adapted for collaborative labeling

of lung cancer CT Scans. *Comput Methods Programs Biomed.* 2021;206:106111. doi: 10.1016/j.cmpb.2021.106111
3. Kulberg NS, Gusev MA, Reshetnikov RV, et al. Methodology and tools for creating training samples for artificial intelligence systems for recognizing lung cancer on CT images. *Heal Care Russ Fed.*

2020;64(6):343–350. doi: 10.46563/0044-197X-2020-64-6-343-350

4. Hessel SJ, Herman PG, Swensson RG. Improving performance by multiple interpretations of chest radiographs: effectiveness and cost. *Radiology.* 1978;127(3):589–594. doi: 10.1148/127.3.589

5. Herman PG, Hessel SJ. Accuracy and its relationship to experience in the interpretation of chest radiographs. *Invest Radiol.* 1975;10(1):62–67. doi: 10.1097/00004424-197501000-00008

6. MacMahon H, Naidich DP, Goo JM, et al. Guidelines for management of incidental pulmonary nodules detected on ct images: from the fleischner society 2017. *Radiology.* 2017;284:228–243. doi: 10.1148/radiol.2017161659

7. Gerke O, Vilstrup MH, Segtnan EA, et al. How to assess intra- and inter-observer agreement with quantitative PET using variance component analysis: a proposal for standardisation. *BMC Med Imaging.* 2016;16(1):54. doi: 10.1186/s12880-016-0159-3

8. Rasheed K, Rabinowitz YS, Remba D, Remba MJ. Interobserver and intraobserver reliability of a classification scheme for corneal topographic patterns. *Br J Ophthalmol.* 1998;82(12):1401–1406. doi: 10.1136/bjo.82.12.1401

9. Van Riel SJ, Sánchez CI, Bankier AA, et al. Observer variability for classification of pulmonary nodules on low-dose ct images and its effect on nodule management. *Radiology.* 2015;277(3):863–871. doi: 10.1148/radiol.2015142700

10. Wickham H, François R, Henry L, Müller K. dplyr: A Grammar of Data Manipulation. R package version 1.0.4. 2021.

11. Gamer M, Lemon J, Fellows I, Singh P. irr: Various Coefficients of Interrater Reliability and Agreement. 2019.

12. Wickham H. ggplot2: elegant Graphics for Data Analysis. Springer-Verlag New York; 2016. 260 p.

13. R Core Team. R: A Language and Environment for Statistical Computing. R Foundation for Statistical Computing, Vienna, Austria; 2020. Available from: http://www.r-project.org/index.html

14. Van Rossum G, Drake FL. Python 3 Reference Manual. CreateSpace, Scotts Valley, CA; 2009.

15. Ardila D, Kiraly AP, Bharadwaj S, et al. End-to-end lung cancer screening with three-dimensional deep learning on low-dose chest computed tomography. *Nat Med.* 2019;25(6):954–961. doi: 10.1038/s41591-019-0447-x

16. Peters R, Heuvelmans M, Brinkhof S, et al. Prevalence of pulmonary multi-nodularity in CT lung cancer screening. 2015.

17. Creative Research Systems. The survey systems: Sample size calculator. 2012.

18. Hugo GD, Weiss E, Sleeman WC, et al. A longitudinal four-dimensional computed tomography and cone beam computed tomography dataset for image-guided radiation therapy research in lung cancer. *Med Phys.* 2017;44(2):762–771. doi: 10.1002/mp.12059

19. Bakr S, Gevaert O, Echegaray S, et al. A radiogenomic dataset of non-small cell lung cancer. *Sci Data.* 2018;5:180202. doi: 10.1038/sdata.2018.202

20. Armato SG, McLennan G, Bidaut L, et al. The lung image database consortium (LIDC) and image database resource initiative (IDRI): a completed reference database of lung nodules on ct scans. *Med Phys.* 2011;38(2):915–931. doi: 10.1118/1.3528204

СПИСОК ЛИТЕРАТУРЫ

1. Морозов С.П., Кульберг Н.С., Гомболевский В.А., и др. Датасет радиологии Москвы CTLungCa-500. 2018. Режим доступа: https://mosmed.ai/datasets/ct_lungcancer_500/. Дата обращения: 11.02.2021.

2. Morozov S.P., Gombolevskiy V.A., Elizarov A.B., et al. A simplified cluster model and a tool adapted for collaborative labeling of lung cancer CT Scans // Comput Methods Programs Biomed. 2021. Vol. 206. P. 106111. doi: 10.1016/j.cmpb.2021.106111

3. Kulberg N.S., Gusev M.A., Reshetnikov R.V., et al. Methodology and tools for creating training samples for artificial intelligence systems for recognizing lung cancer on CT images // Heal Care Russ Fed. 2020. Vol. 64, N 6. P. 343–350. doi: 10.46563/0044-197X-2020-64-6-343-350

4. Hessel S.J., Herman P.G., Swensson R.G. Improving performance by multiple interpretations of chest radiographs: effectiveness and cost // Radiology. 1978. Vol. 127, N 3. P. 589–594. doi: 10.1148/127.3.589

5. Herman P.G., Hessel S.J. Accuracy and its relationship to experience in the interpretation of chest radiographs // Invest Radiol. 1975. Vol. 10, N 1. P. 62–67. doi: 10.1097/00004424-197501000-00008

6. MacMahon H., Naidich D.P., Goo J.M., et al. Guidelines for management of incidental pulmonary nodules detected on ct images: from the fleischner society 2017 // Radiology. 2017. Vol. 284, N 1. P. 228–243. doi: 10.1148/radiol.2017161659

7. Gerke O., Vilstrup M.H., Segtnan E.A., et al. How to assess intra- and inter-observer agreement with quantitative PET using variance component analysis: a proposal for standardisation // BMC Med Imaging. 2016. Vol. 16, N 1. P. 54. doi: 10.1186/s12880-016-0159-3

8. Rasheed K., Rabinowitz Y.S., Remba D., Remba M.J. Interobserver and intraobserver reliability of a classification scheme for corneal topographic patterns // Br J Ophthalmol. 1998. Vol. 82, N 12. P. 1401–1406. doi: 10.1136/bjo.82.12.1401

9. Van Riel S.J., Sánchez C.I., Bankier A.A., et al. Observer variability for classification of pulmonary nodules on low-dose ct images and its effect on nodule management // Radiology. 2015. Vol. 277, N 3. P. 863–871. doi: 10.1148/radiol.2015142700

10. Wickham H., François R., Henry L., Müller K. dplyr: A Grammar of Data Manipulation. R package version 1.0.4. 2021.

11. Gamer M, Lemon J, Fellows I, Singh P. irr: Various Coefficients of Interrater Reliability and Agreement. 2019.

12. Wickham H. ggplot2: elegant Graphics for Data Analysis. Springer-Verlag New York; 2016. 260 p.

13. R Core Team. R: A Language and Environment for Statistical Computing. R Foundation for Statistical Computing, Vienna, Austria. 2020. Режим доступа: http://www.r-project.org/index.html. Дата обращения: 11.02.2021.

14. Van Rossum G., Drake F.L. Python 3 Reference Manual. CreateSpace, Scotts Valley, CA; 2009.

15. Ardila D., Kiraly A.P., Bharadwaj S., et al. End-to-end lung cancer screening with three-dimensional deep learning on low-dose chest computed tomography // Nat Med. 2019. Vol. 25, N 6. P. 954–961. doi: 10.1038/s41591-019-0447-x

16. Peters R., Heuvelmans M., Brinkhof S., et al. Prevalence of pulmonary multi-nodularity in CT lung cancer screening. 2015.

17. Creative Research Systems. The survey systems: Sample size calculator. 2012.

18. Hugo G.D., Weiss E., Sleeman W.C., et al. A longitudinal four-dimensional computed tomography and cone beam computed tomography dataset for image-guided radiation therapy research in lung cancer // Med Phys. 2017. Vol. 44, N 2. P. 762–771. doi: 10.1002/mp.12059

19. Bakr S., Gevaert O., Echegaray S., et al. A radiogenomic dataset of non-small cell lung cancer // Sci Data. 2018. Vol. 5. P. 180202. doi: 10.1038/sdata.2018.202

20. Armato S.G., McLennan G., Bidaut L., et al. The lung image database consortium (LIDC) and image database resource initiative (IDRI): a completed reference database of lung nodules on ct scans // Med Phys. 2011. Vol. 38, N 2. P. 915–931. doi: 10.1118/1.3528204

AUTHORS' INFO

* Nikolas S. Kulberg, Cand. Sci. (Phys.-Math.);
address: 24 Petrovka str., 109029, Moscow, Russia;
ORCID: https://orcid.org/0000-0001-7046-7157;
eLibrary SPIN: 2135-9543; e-mail: kulberg@npcmr.ru

Roman V. Reshetnikov, Cand. Sci. (Phys.-Math.);
ORCID: https://orcid.org/0000-0002-9661-0254;
eLibrary SPIN: 8592-0558; e-mail: reshetnikov@fbb.msu.ru

Vladimir P. Novik;
ORCID: https://orcid.org/0000-0002-6752-1375;
eLibrary SPIN: 2251-1016; e-mail: v.novik@npcmr.ru

Alexey B. Elizarov, Cand. Sci. (Phys.-Math.);
ORCID: https://orcid.org/0000-0003-3786-4171;
eLibrary SPIN: 7025-1257; e-mail: a.elizarov@npcmr.ru

Maxim A. Gusev;
ORCID: https://orcid.org/0000-0001-8864-8722;
eLibrary SPIN: 1526-1140; e-mail: m.gusev@npcmr.ru

Victor A. Gombolevskiy, MD, Cand. Sci. (Med.);
ORCID: https://orcid.org/0000-0003-1816-1315;
eLibrary SPIN: 6810-3279; e-mail: g_victor@mail.ru

Anton V. Vladzymyrskyy, MD, Dr. Sci. (Med.), Professor;
ORCID: https://orcid.org/0000-0002-2990-7736;
eLibrary SPIN: 3602-7120; e-mail: a.vladzimirsky@npcmr.ru

Sergey P. Morozov, MD, Dr. Sci. (Med.), Professor;
ORCID: https://orcid.org/0000-0001-6545-6170;
eLibrary SPIN: 8542-1720; e-mail: morozov@npcmr.ru

ОБ АВТОРАХ

* Кульберг Николай Сергеевич, к.ф.-м.н.;
адрес: Россия, 127051, Москва, ул. Петровка, д. 24;
ORCID: https://orcid.org/0000-0001-7046-7157;
eLibrary SPIN: 2135-9543; e-mail: kulberg@npcmr.ru

Решетников Роман Владимирович, к.ф.-м.н.;
ORCID: https://orcid.org/0000-0002-9661-0254;
eLibrary SPIN: 8592-0558; e-mail: reshetnikov@fbb.msu.ru

Новик Владимир Петрович;
ORCID: https://orcid.org/0000-0002-6752-1375;
eLibrary SPIN: 2251-1016; e-mail: v.novik@npcmr.ru

Елизаров Алексей Борисович, к.ф.-м.н.;
ORCID: https://orcid.org/0000-0003-3786-4171;
eLibrary SPIN: 7025-1257; e-mail: a.elizarov@npcmr.ru

Гусев Максим Александрович;
ORCID: https://orcid.org/0000-0001-8864-8722;
eLibrary SPIN: 1526-1140; e-mail: m.gusev@npcmr.ru

Гомболевский Виктор Александрович, к.м.н.;
ORCID: https://orcid.org/0000-0003-1816-1315;
eLibrary SPIN: 6810-3279; e-mail: g_victor@mail.ru

Владзимирский Антон Вячеславович, д.м.н., профессор;
ORCID: https://orcid.org/0000-0002-2990-7736;
eLibrary SPIN: 3602-7120; e-mail: a.vladzimirsky@npcmr.ru

Морозов Сергей Павлович, д.м.н., профессор;
ORCID: https://orcid.org/0000-0001-6545-6170;
eLibrary SPIN: 8542-1720; e-mail: morozov@npcmr.ru

* Corresponding author / Автор, ответственный за переписку

Роль системы контроля качества лучевой диагностики онкологических заболеваний в радиомике

А.Н. Хоружая, Е.С. Ахмад, Д.С. Семенов

Научно-практический клинический центр диагностики и телемедицинских технологий Департамента здравоохранения города Москвы, Москва, Российская Федерация

АННОТАЦИЯ

Современные методы медицинской визуализации дают возможность качественно и количественно оценить как ткани опухоли, так и пространство вокруг неё. Прогресс в информатике, особенно с участием методов машинного обучения в анализе медицинских изображений, позволяет преобразовывать любые радиологические исследования в поддающиеся анализу наборы данных. Среди этих наборов данных затем можно искать статистически значимые корреляции с клиническими событиями, чтобы впоследствии оценивать их прогностическую значимость и способность предсказывать тот или иной клинический исход. Эта концепция впервые была описана в 2012 г. и получила название «радиомика». Особую значимость она представляет для онкологии, поскольку известно, что каждый тип опухоли может подразделяться на множество различных молекулярно-генетических подтипов, и просто визуальной характеристики сейчас уже недостаточно. А радиомика при абсолютной неинвазивности способна обеспечить врача-радиолога информацией, которую порой может дать только гистологическое исследование биопсийного материала. Однако, как и в любой методике, основанной на использовании больших данных, здесь остро встаёт вопрос о качестве исходной информации данных, потому как это прямым образом может повлиять на исход анализа и дать неверную диагностическую информацию.

В литературном обзоре мы анализируем возможные подходы к обеспечению качества исследований на всех этапах — от технического контроля за состоянием диагностического оборудования до извлечения маркеров визуализации в онкологии и вычисления их корреляции с клиническими данными.

Ключевые слова: радиомика; лучевая диагностика; контроль качества; стандартизация; опухоли; онкологические заболевания.

The role of the quality control system for diagnostics of oncological diseases in radiomics

Anna N. Khoruzhaya, Ekaterina S. Akhmad, Dmitry S. Semenov

Moscow Center for Diagnostics and Telemedicine, Moscow, Russian Federation

ABSTRACT

Modern medical imaging methods allow for both qualitative and quantitative evaluations of tumors and issues surrounding them. Advances in computer science and big data processing are transforming any radiological study into analytic datasets, especially with the use of machine learning in medical image analysis. Among these datasets, statistically significant correlations with clinical events can then be searched for to subsequently assess their predictive value and ability to predict a particular clinical outcome. This concept, known as "radiomics," was first described in 2012. It is particularly important in oncology because each type of tumor can be subdivided into many different molecular genetic subtypes, and simple visual characteristics are no longer sufficient. Moreover, as an absolutely noninvasive method, radiomics can provide a radiologist with additional information that would otherwise be unavailable without a histological examination of biopsy material. However, as with any methodology based on the use of big data, the question of the quality of the initial data becomes critical, because this can directly affect the outcome of the analysis and provide incorrect diagnostic information.

In this literature review, we examine potential approaches to ensuring the quality of research at all stages, from technical control of the state of diagnostic equipment to the extraction of imaging markers in oncology and the calculation of their correlation with clinical data.

Keywords: radiomics; radiology; quality assurance; quality control; tumors; cancer; standardization.

肿瘤疾病放射诊断质量控制系统在放射组学中的作用

Anna N. Khoruzhaya, Ekaterina S. Akhmad, Dmitry S. Semenov

Moscow Center for Diagnostics and Telemedicine, Moscow, Russian Federation

简评

现代医学成像方法可以定性和定量地评估肿瘤组织及其周围的空间。计算机科学的进步，特别是机器学习方法在医学图像分析中的参与，允许将任何放射学研究转变为可分析的数据集。在这些数据集中，可以寻找有统计学意义夫人相关性与临床事件，以便随后评估其预后意义和预测不同临床结果的能力。 这个概念在2012年首次被描述并称为»放射组学»。这对于肿瘤学特别重要，因为已知每种类型的肿瘤可以分为许多不同的分子遗传亚型，而仅仅是视觉特征已经不够了。在绝对非侵入性的情况下，放射组学能够为放射科医生提供有时只有活检材料的组织学检查才能提供的信息。然而，正如在任何基于使用大数据的方法中一样，存在关于初始数据信息的质量的尖锐问题，因为这可能直接影响分析的结果并给出不正确的诊断信息。

在文献综述中，我们分析了确保各个阶段研究质量的可能方法 – 从诊断设备状态的技术控制到提取肿瘤学中的成像标记并计算其与临床数据的相关性。

关键词： 放射学；放射诊断；质量控制；标准化；肿瘤；肿瘤疾病。

INTRODUCTION

Advances in the field of radiation imaging significantly expanded their role in the entire range of methods for tumor processes management, from diagnosing primary foci and detecting metastases to monitoring treatment response and predicting individual patient outcomes. However, a simple visual analysis of tumor using radiation diagnostics is no longer sufficient, since each type of tumor is known to subdivide into many different molecular genetic subtypes. Accordingly, each tumor requires its own therapeutic and diagnostic approach. Here from the side of diagnostics, radiomics can be of great help.

Radiomics represents a method not just for visual analysis of medical images, but for large number extraction of quantitative signs, which allow deeper analysis and comprehensive assessment, such as tumor phenotypes and other pathological properties of affected tissues, as well as tumor biological characteristic assessment and treatment response prediction [1, 2]. For example, solid cancer is heterogeneous in time and space, which limits the use of molecular analysis based on invasive biopsy but offers great potential for medical imaging and enables non-invasive detection of intratumoral heterogeneity [3–5].

Quantitative analysis transition requires the development of automated and reproducible analysis methodologies to extract additional information from images [6]. Hence, a question in initial data quality arises, since this can affect the analysis outcome and provide incorrect diagnostic information, which will affect the clinical significance of detected indicators and patient health [7, 8].

Therefore, this literature review aimed to analyze possible approaches to ensure the quality of radiation diagnostics studies at all stages, from technical control over the state of diagnostic equipment to extracting imaging markers in oncology and calculating their correlation with clinical data.

Literature search was performed in the PubMed, GoogleScholar, and eLibrary databases in English and Russian languages. Requests such as "radiomics," "cancer and tumors," "standardization," and "quality assurance or quality control" were used for PubMed and GoogleScholar.

METHODOLOGY OF RADIOMICS

Image acquisition

The step 1 in radiomics consists obtaining images using radiology methods, namely magnetic resonance imaging (MRI), computed tomography (CT), and positron emission tomography combined with computed tomography (PET/CT) (Fig. 1). Radiology methods provide various and often complementary information about physical and kinetic properties of tissues, metabolism, etc. For example, analysis based on the size or volume of the pathological structure can be obtained using anatomical MRI or CT. Perfusion can be determined by a series of dynamic MRI or contrast-enhanced CT scans. Diffusion-weighted MRI can be used to assess tissue microcirculation and assess cellularity. Metabolic changes such as glucose metabolic rate can be measured using PET/CT and fluorodeoxyglucose. In addition, other additional biomarkers may be proposed in the course of clinical trials [9, 10].

Historically, imaging devices were developed for subjective interpretation of images, for clinicians to determine the presence of lesion and its location. Subsequent technical innovations are focused on image quality improvement, scan times reduction, or processing machines integration. These devices were not primarily intended to provide quantitative measurement in a reproducible manner. Standardization protocols for image acquisition are unavailable. In addition, significant differences may be present in reconstruction
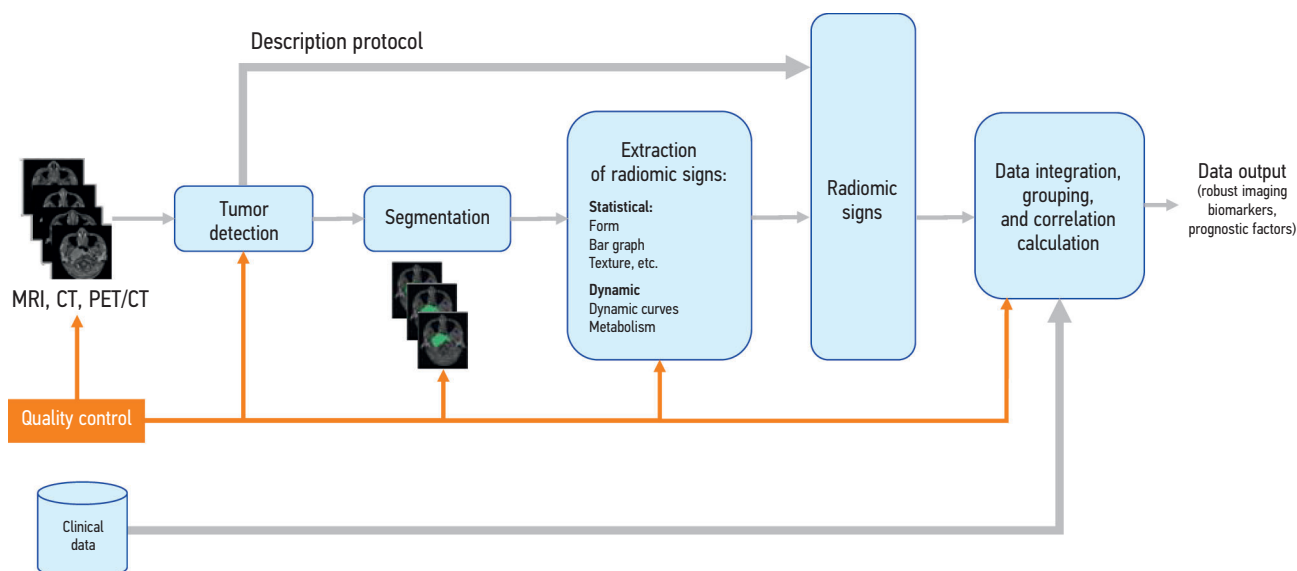
Fig. 1. Scheme of radiomics analysis of radiation diagnostic images indicating the role of quality control system.

parameters. H. Kim et al. [11] studied the effect of recon- struction filters on radiomic signs identified from CT im- ages of patients with lung cancer and concluded that the relationship was statistically significant and reconstruction settings should not be used interchangeably. N. Ohri et al. [12] assessed the variability of radiomic characteristics ob- tained from PET/CT under different modes of data collection, algorithms reconstruction, post-filtration, and number of it- erations. A total of 40 out of 50 signs were demonstrated to have significant (up to 30%) variability. Variability of signs can vary more significantly when performing MRI due to the amplitude of the scanner gradient magnetic field, used pulse sequence, contrast agent administration method, trajectory sampling in k-space, and other factors [13]. Data quality depends on reliability of data collection protocols used in clinical centers, thus the effect of these changes on the sta- bility of radiomic signs needs to be carefully investigated and analyzed in future studies.

New methods of image processing

Image processing is the next step in radiomic signs ex- traction. Thus, identification of a region of interest (ROI) and volume of interest (VOI) is a fundamental task in oncological practice [14]. Manual description by experienced roentgen- ologists or radiologists is considered the gold standard, but is time-consuming with a high degree of inter- or even intra- operator variability. Automated or semi-automated methods are often used, such as determining threshold values, clas- sifiers, clustering, Markov models of random fields, artificial neural networks, deformable models, and some others to determine ROI [15].

Automation can provide new opportunities for segmenta- tion techniques standardization; however, problems associ- ated with complex anatomy or areas of low soft tissue con- trast are still present, therefore manual adjustments by an experienced physician are often required. One of the meth- ods of semi-automatic segmentation, which avoids errors, is the use of digital biopsy, in which only certain segments are sampled based on intensity and texture values [16]. For segmentation or selection of images, advanced machine learning methods also emerged and used [17].

Several major initiatives aimed to develop automatic segmentation solutions using deep learning. These include, Google DeepMind, Microsoft Project InnerEye, and Mirada DLCExpert. These automated segmentation tools showed to increase efficiency in structure reconstruction, especially for organs at risk [18, 19]. In the near future, deep learning- based segmentation tools may become reliable enough for routine research.

Extraction of signs, grouping, and data integration

Extraction of multidimensional datasets (radiomics signs) is the main stage of radiomics to quantify the VOI highlighted in the image [20]. Signs extracted from images can be di- vided into static and dynamic groups.

Characteristics of static signs. Static signs multitude comprises two categories, morphological and statistical [21]. Morphological signs are used to define three-dimensional (3D) shape characteristics such as volume and surface area, as well as sphericity (the extent a 3D volume resembles a sphere). Statistical signs are used to mathematically evalu- ate the distribution of grayscale within an ROI or VOI. There- fore, the first-order signs include the mean value, standard deviation, percentiles, kurtosis, and asymmetry, which are used to characterize the overall variability in intensity. Sec- ond-order signs characterize the texture of selected area by analyzing the relationship between individual voxels within the ROI or area, i.e., exhibit local distribution.

Aspects of dynamic signs. Pharmacokinetic modeling is commonly used to quantify the dynamic distribution of a contrast agent or other indicator within a region (which may be one or more voxels). In general, pharmacokinetic modeling considers the contrast agent concentration as a function of arterial input and residual contrast agent decay within the ROI. The intravascular and interstitial space can be modeled under different assumptions. For example, the most widely used kinetic model, the Toft model, assumes instant mixing of contrast in the intravascular and interstitial space, whereas the extended Toft model takes into account the effect of delayed contrast agent concentration in tissue. The model of homogeneity of adiabatic tissue is explained by the fact that contrast agent concentration in distribution volume outside the vessels changes more slowly compared to the intravascular space concentration. Thus, the model assumes a finite transit time for contrast agents from arte- rial phase to venous phase.

In general, existing analytical pipeline typically includes thousands of extracted radiomics characteristics, and this number is expected to grow with new available data. How- ever, clinically significant signs include not all selected ones, but the most reliable signs, correlating with clinical data for the possibility of disease course prediction.

Calculation of correlations, identification of prognostic factors

As in many other fields where the -omics suffix is used, the number of input variables often far exceeds the num- ber of patients. In order to reduce the probability of false positive results, specific sign selection or search area size reduction is required, and filter-based scoring approaches are commonly used, such as Wilcoxon analysis and principal component analysis. This can be implemented using either one-dimensional methods, when the evaluation criterion de- pends only on the object relevance, or multivariate methods, when a weighted sum is used to maximize relevance and minimize redundancy [22–25]. Object selection can also be combined with object classification into one model.

Once a set of characteristics is obtained, a data-driven model can be created. These models include controlled and

uncontrolled approaches [21, 26]. Unmanaged analysis does not provide a result variable, but rather a summary of information. Most often, a thermal map is used for its graphical display, on which cluster structures in data matrix are simultaneously detected. In contrast, in the course of monitored analysis, models are created, that attempt to divide the treatment outcome data. Typical classification methods include traditional logistic regression or more advanced machine learning methods.

Isolated radiomic signs that correlate closely with clinical data and molecular analysis results can be classified as imaging biomarkers, whereas classical biomarkers are obtained by histological and molecular examination of tumor tissues, i.e., using invasive method, imaging biomarkers provide non-invasive characterization of the pathology. In addition, reliable indicators of normal or pathological processes in tissues or tumor responses are available for any intervention.

QUALITY CONTROL AND STANDARDIZATION OF PARAMETERS IN RADIOMICS

Measurement accuracy improvement is necessary (Fig. 2) to ensure radiomic signs quality and imaging biomarkers reliability, which is determined by the magnitude of bias or absolute error of obtained data and variability of values (repeatability and reproducibility, defined as dispersion of measured values). These indicators are achieved

by introducing quality control tests in radiation diagnostic departments, namely acceptance tests, periodic, and internal control tests (tests for parameter constancy) [27]. Acceptance tests are performed during equipment installation to establish the compliance of tested characteristics with the manufacturer's limit values. In case of confirmation of parameter conformity, the medical organization personnel perform the first tests for parameter constancy, during which base values are established for further quality control. Internal control or parameter constancy testing is essential in the quality control system as it predicts deterioration in diagnostic image quality. In Russia, periodic tests include monitoring of extended list of parameters, and are performed by certified testing laboratories.

In international practice, inclusion of technical personnel in the staff of MRI, CT, PET/CT offices is common. For example, a large role is assigned to medical physicists, whose important task consist research optimization and standardization, as well as radiation diagnostics equipment quality monitoring and safe system organization during research [28]. In Russia presence of such personnel in the staff of radiation diagnostics rooms are currently not required, and competencies to implement quality control for radiomics are unnecessary for medical personnel.

Measures to ensure quality control of radiological diagnostic equipment are required to achieve reliability and clinically acceptable repeatability of measurements, which is supported by the Radiological Society of North America (RSNA), the European Society of Radiology, etc. Thus, collaboration between members of the Quantitative Imaging
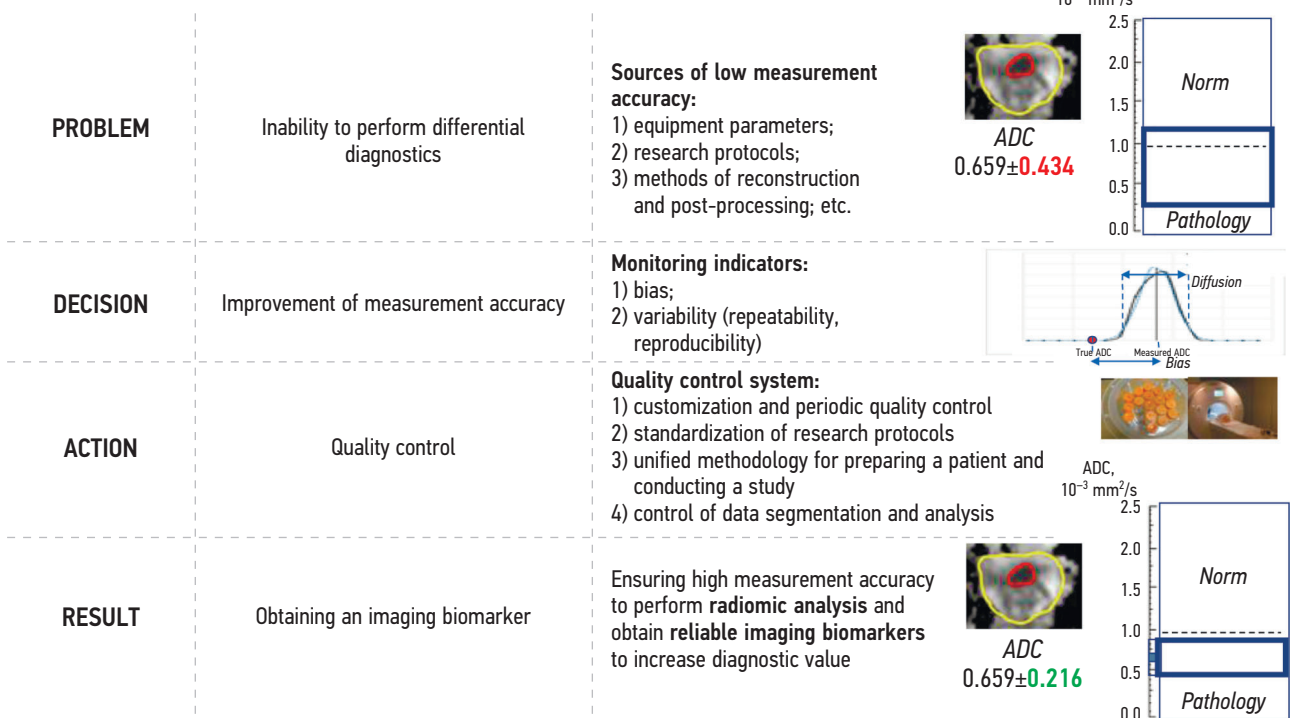
Fig. 2. Justification for quality control system implementation in radiomics.

Network (QIN; USA) and National Institute of Standards and Technology phantoms was developed for quality control in clinical trials [29, 30].

Relationships are formed between revealed signs and clinical data as a result of radiomic analysis to check the model constructed and assess output information reliability; it is validated for new patients [31, 32]. Literature data are used, as well as dataset validation testing, or data from other healthcare organizations to gain generalization possibility [31].

Standardization of study protocols

Following the standard methods of examination preparation, namely exclude foreign objects from the scan area that contribute to distortion is necessary since MRI, CT, and PET/CT images are susceptible to artifacts and noise; make sure that the established rules for positioning the patient are followed for better visualization. The patient should feel comfortably motionless for a long time.

In addition, the voxel size and signal intensity have a great influence on radiomic signs, therefore, ensuring the standardization of protocols is important when setting up the scan [32, 33]. The effect of reconstruction filters on image quality and signal intensity should also be taken into account, namely a filter should be chosen that does not lose the useful signal and ensure high reproducibility of radiomic signs when performing PET/CT and CT [34].

The image matrix is scaled and reduced to an isotropic (square) form as part of image preprocessing [35]. Signal intensity normalization to one scale is also recommended, especially for MRI. For this purpose, statistical methods are used, for example ANTsR and WhiteStripe [36]. Signal intensity inhomogeneity phenomena may be encountered when performing MRI, which are caused not by biological properties of tissues, but by technical factors. In such cases, correction for this heterogeneity is required, which should be included in the quality control system of performed procedures.

Post–processing control

Tools and algorithms with proven accuracy of their work should be used for post-processing process [36]. For example, for the subsequent correct analysis of radiomic signs, it is important to use high-quality tools at the segmentation stage. Previously semi-automatic algorithms with manual segmentation correction were used, but now more and more algorithms based on artificial intelligence technologies [37] appear, which must undergo appropriate tests [38].

Monitoring of isolated radiomic signs and validation of imaging biomarkers

Principles of standardization and quality control of studies and procedures for pre- and post-processing of images are required to ensure the quality (bias and variability) of radiomic signs, as well as reliability of imaging biomarkers [39].

At this stage, quality control tools are used, such as phantoms, which enable the assessment of bias and reproducibility of distinguished signs. Phantoms can be both digital and physical, made using substances of specified parameters [40, 41]. For example, for multicenter studies of breast cancer, an appropriate phantom is used, which enables the evaluation of study reproducibility and accuracy [42].

The phantom is scanned repeatedly under different conditions, after which the variability of measurements is calculated and compared with the threshold value that the European Medicines Agency recommends, which is no more than 15% to analyze the effect of the scanning parameters on variability and methodology of study and post-processing performance [39].

Accuracy is assessed in the process of studies on phantoms or on tissue samples and corresponds to the relative error when the true value of signs (ground truth) and measured ones are compared. Setting the threshold value for successful completion of assessment at the level of 15% is recommended in the process of imaging biomarker validation [39].

This field of radiomics is under development, which may become an effective method for diagnosing tumors and predicting process analysis in the near future. We believe that the number of studies in this field will increase with the introduction of artificial intelligence algorithms to create relationships between the selected signs and clinical data. However, without the implementation of the described quality control approaches at all stages, obtaining a solid evidence is impossible, i.e., data reproducible on other populations, other equipment with a bias indicators within the established limit. Phantoms were previously developed for monitoring quantitative modes of MRI (with diffusion indicators) and CT (with indicators of bone mineral density) at the Center for Diagnostics and Telemedicine. From our point of view, interaction with technical specialists (medical physicists, engineers) and medical personnel is necessary to develop phantoms with specified measurement accuracy in planning a study of radiomic signs and further obtaining imaging biomarkers in this work.

ROLE OF DEVELOPMENT OF VISUALIZATION BIOMARKERS

In recent years, efforts were made to improve approaches to standardization of radiomic signs by defining standard data collection protocols. Particular efforts for this were made by the QIN created by the National Cancer Institute (NCI), as well as RSNA, the Quantitative Imaging Biomarkers Alliance (QIBA) and others. In 2010, NCI launched an initiative of the Cancer Institute Centers for Quantitative Image Excellence, and the creation of a National Clinical Trials Network has become a key focus of this effort [43]. Centers for

quantitative image improvement create PET/CT, CT, and MR phantoms, as well as protocols for standardization, and QIBA provides consensus decisions on the accuracy of quantitative biomarker imaging measurements and requirements/procedures necessary to achieve this level of accuracy [29, 35, 36, 44, 45].

Since the term "radiomics" appeared in the scientific literature, hundreds of published radiomics studies aimed to improve the quality of diagnostics, treatment, and prognosis of cancer. An increasing number of works demonstrate the value of imaging biomarkers as an additional tool for clinical decision-making and role of machine learning algorithms in it [46].

One of the earliest applications of the radiomics-based method is the successful detection of tumors in the imaging of lung and breast cancers.

Breast cancer is a pathology that most often occurs in women worldwide. Accurate diagnosis and early prediction of treatment response are key aspects in clinical practice since it is a well-known heterogeneous disease [47]. Several studies used radiomics to predict breast cancer subtype or ER, PR, Ki67, and HER2 status on mammography [48], PET/CT [49, 50], and MRI [51, 52]. In addition to characterizing breast cancer, radiomics may also provide a non-invasive approach to predict metastases in the sentinel lymph nodes [53].

Most radiological research on breast cancer focuses on therapy response evaluation. H.M. Chan et al. [54] developed an automated method using MRI to predict the absence or insufficient response to treatment in patients with early breast cancer. Most other studies attempted to obtain a pathologic complete response (pCR) biomarker with neoadjuvant chemotherapy, a hot topic of discussion in studies on breast cancer. Thus, N.M. Braman et al. [55] revealed that intra- and peri-tumor characteristics found on dynamic contrast-enhanced MRI can predict pCR prior to treatment. Other studies also showed that T1WI, T2WI, and DWI can aid in pCR detection [56, 57].

Radiological studies focused on the prognosis of breast cancer are performed more and more frequently. For example, H. Park et al. [58] developed an algorithm combining MRI imaging biomarkers and clinical information to individually assess the survival ability of patients with breast cancer.

Lung cancer is the most dangerous type of cancer, and its prevalence also continues to increase worldwide. Lung cancer screening is one of the most important diagnostic applications of radiomics. N. Nasrullah et al. [59] proposed a deep learning model based on chest CT studies from the LIDC-IDRI dataset and achieved good results in detecting malignant lung nodules with a sensitivity of 94% and specificity of 91%. B.W. Carter et al. [60] conducted a screening study of patients diagnosed with lung cancer in the National Lung Screening Trial dataset using low-dose CT. They were able to obtain predictive accuracy of 80% and 79% for nodules that develop into malignant neoplasms in one or two years, respectively.

Radiomics enables the determination at the preoperative stage in staging lung cancer by tumor nodules metastasis (TNM) [61, 62], which is important for making a decision about surgical intervention. In addition, the technique can be used to detect specific genetic mutations in lung cancer, such as the status for the *Estimated glomerular filtration rate* gene [63] which can help medical specialists choose the optimal therapeutic approach. X. Fave et al. used delta-radiomic characteristics to predict outcomes in patients with stage III non-small cell lung cancer during radiation therapy [64]. Their results suggest that changes in radiomic characteristics due to radiation therapy will be indicative of tumor response. T.P. Coroller et al. [65] established that radiomic signs of CT before treatment can predict a pathological response after neoadjuvant chemoradiation therapy in patients with advanced non-small cell lung cancer.

In recent years, radiomics are increasingly used for diagnostics, treatment response prediction, and long-term outcomes of tumors of the nervous system [26, 66, 67], head and neck [68, 69], gastrointestinal tract [70, 71], prostate cancer [72, 73], and some other forms of oncological diseases [74].

CONCLUSION

Early detection and identification of tumors, their heterogeneity, and phenotypic signs can be invaluable in patient stratification, subsequent treatment options determination, and effects prediction. Radiomic analysis of diagnostic studies provides information necessary for this, but only under conditions of high-quality collected and processed data. All of these processes need to be standardized and optimized using a variety of quality control methods, and at each stage, from image acquisition to validation of imaging biomarkers. In addition, clinical information must be taken into account, based on which the search for clinical correlations is performed to establish the prognostic value of biomarkers. Only the qualitative fulfillment of all these criteria can make the biomarker imaging tool really useful for doctors and necessary for patients.

ADDITIONAL INFORMATION

REFERENCES

1. Kumar V, Gu Y, Basu S, et al. Radiomics: The process and the challenges. *Magn Reson Imaging*. 2012;30(9):1234–1248. doi: 10.1016/j.mri.2012.06.010

2. Papanikolaou N, Matos C, Koh DM. How to develop a meaningful radiomic signature for clinical use in oncologic patients. *Cancer Imaging*. 2020;20(1):33. doi: 10.1186/s40644-020-00311-4

3. Aerts HJ, Grossmann P, Tan Y, et al. Defining a radiomic response phenotype: A pilot study using targeted therapy in NSCLC. *Sci Rep*. 2016;6:33860. doi: 10.1038/srep33860

4. Coroller TP, Grossmann P, Hou Y, et al. CT-based radiomic signature predicts distant metastasis in lung adenocarcinoma. *Radiother Oncol*. 2015;114(3):345–350. doi: 10.1016/j.radonc.2015.02.015

5. Lopez CJ, Nagornaya N, Parra NA, et al. Association of radiomics and metabolic tumor volumes in radiation treatment of glioblastoma multiforme. *Int J Radiat Oncol Biol Phys*. 2017;97(3):586–595. doi: 10.1016/j.ijrobp.2016.11.011

6. De Souza NM, Achten E, Alberich-Bayarri A, et al. Validated imaging biomarkers as decision-making tools in clinical trials and routine practice: current status and recommendations from the EIBALL* subcommittee of the European Society of Radiology (ESR). *Insights Imaging*. 2019;10(1):87. doi: 10.1186/s13244-019-0764-0

7. Jones EF, Buatti JM, Shu HK, et al. Clinical trial design and development work group within the quantitative imaging network. *Tomography*. 2020;6(2):60–64. doi: 10.18383/j.tom.2019.00022

8. European Society of Radiology (ESR). ESR statement on the validation of imaging biomarkers. *Insights Imaging*. 2020;11(1):76. doi: 10.1186/s13244-020-00872-9

9. Grimm LJ, Zhang J, Mazurowski MA. Computational approach to radiogenomics of breast cancer: Luminal A and luminal B molecular subtypes are associated with imaging features on routine breast MRI extracted using computer vision algorithms. *J Magn Reson Imaging*. 2015;42(4):902–907. doi: 10.1002/jmri.24879

10. Nie K, Shi L, Chen Q, et al. Rectal cancer: Assessment of neoadjuvant chemoradiation outcome based on radiomics of multiparametric MRI. *Clin Cancer Res*. 2016;22(21):5256–5264. doi: 10.1158/1078-0432.CCR-15-2997

11. Kim H, Park CM, Lee M, et al. Impact of reconstruction algorithms on ct radiomic features of pulmonary tumors: analysis of intra- and inter-reader variability and inter-reconstruction algorithm variability. *PLoS One*. 2016;11(10):e0164924. doi: 10.1371/journal.pone.0164924

12. Ohri N, Duan F, Snyder BS, et al. Pretreatment 18F-FDG PET textural features in locally advanced non-small cell lung cancer: Secondary analysis of ACRIN 6668/RTOG 0235. *J Nucl Med*. 2016; 57(6):842–848. doi: 10.2967/jnumed.115.166934

13. Zhang B, Tian J, Dong D, et al. Radiomics features of multiparametric MRI as novel prognostic factors in advanced nasopharyngeal carcinoma. *Clin Cancer Res*. 2017;23(15):4259–4269. doi: 10.1158/1078-0432.CCR-16-2910

14. Nakatsugawa M, Cheng Z, Goatman KA, et al. Radiomic analysis of salivary glands and its role for predicting xerostomia in irradiated head and neck cancer patients. *Int J Radiat Oncol Biol Phys*. 2016; 96(2 suppl):S217. doi: 10.1016/j.ijrobp.2016.06.539

15. Shafiee MJ, Chung AG, Khalvati F, et al. Discovery radiomics via evolutionary deep radiomic sequencer discovery for pathologically proven lung cancer detection. *J Med Imaging*. 2016;4(4):041305. doi: 10.1117/1.JMI.4.4.041305

16. Echegaray S, Nair V, Kadoch M, et al. A rapid segmentation-insensitive «Digital Biopsy» method for radiomic feature extraction: method and pilot study using ct images of non-small cell lung cancer. *Tomography*. 2016;2(4):283–294. doi: 10.18383/j.tom.2016.00163

17. Li H, Galperin-Aizenberg M, Pryma D, et al. Unsupervised machine learning of radiomic features for predicting treatment response and overall survival of early stage non-small cell lung cancer patients treated with stereotactic body radiation therapy. *Radiother Oncol*. 2018;129(2):218–226. doi: 10.1016/j.radonc.2018.06.025

18. Tajbakhsh N, Shin JY, Gurudu SR, et al. Convolutional neural networks for medical image analysis: full training or fine tuning? *IEEE Transactions on Medical Imaging*. 2016;35(5):1299–1312. doi: 10.1109/TMI.2016.2535302

19. Elguindi S, Zelefsky MJ, Jiang J, et al. Deep learning-based auto-segmentation of targets and organs-at-risk for magnetic resonance imaging only planning of prostate radiotherapy. *Phys Imaging Radiat Oncol*. 2019;12:80–86. doi: 10.1016/j.phro.2019.11.006

20. Gillies RJ, Kinahan PE, Hricak H. Radiomics: images are more than pictures, they are data. *Radiology*. 2016;278(2):563–577. doi: 10.1148/radiol.2015151169

21. Buckler AJ, Bresolin L, Dunnick NR, et al. Quantitative imaging test approval and biomarker qualification: Interrelated but distinct activities. *Radiology*. 2011;259(3):875–884. doi: 10.1148/radiol.10100800

22. Alobaidli S, McQuaid S, South C, et al. The role of texture analysis in imaging as an outcome predictor and potential tool in radiotherapy treatment planning. *Br J Radiol*. 2014;87(1042):20140369. doi: 10.1259/bjr.20140369

23. Li H, Giger ML, Lan L, et al. Comparative analysis of image-based phenotypes of mammographic density and parenchymal patterns in distinguishing between BRCA1/2 cases, unilateral cancer cases, and controls. *J Med Imaging*. 2014;1(3):031009. doi: 10.1117/1.JMI.1.3.031009

24. Goh V, Ganeshan B, Nathan P, et al. Assessment of response to tyrosine kinase inhibitors in metastatic renal cell cancer: CT texture as a predictive biomarker. *Radiology*. 2011;261(1):165–171. doi: 10.1148/radiol.11110264

25. Yip C, Davnall F, Kozarski R, et al. Assessment of changes in tumor heterogeneity following neoadjuvant chemotherapy in primary esophageal cancer. *Dis Esophagus*. 2015;28(2):172–179. doi: 10.1111/dote.12170

26. Park JE, Kim HS. Radiomics as a quantitative imaging biomarker: practical considerations and the current standpoint in neurooncologic studies. *Nucl Med Mol Imaging*. 2018;52(2):99–108. doi: 10.1007/s13139-017-0512-7

27. Sergunova KA, Akhmad ES, Semenov DS, et al. Medical physicist's participation in quality assurance and safety in magnetic resonance imaging. *Medical physics*. 2020;(3):78–85. (In Russ).

28. Clements JB, Baird CT, de Boer SF, et al. AAPM medical physics practice guideline 10.a.: Scope of practice for clinical medical physics. *J Appl Clin Med Phys*. 2018;19(6):11–25. doi: 10.1002/acm2.12469

29. Shukla-Dave A, Obuchowski NA, Chenevert TL, et al. Quantitative imaging biomarkers alliance (QIBA) recommendations for improved precision of DWI and DCE-MRI derived biomarkers in multicenter oncology trials. *J Magn Reson Imaging*. 2019;49(7):e101–e121. doi: 10.1002/jmri.26518

30. Russek SE, Boss M, Jackson EF, et al. Characterization of NIST/ISMRM MRI System Phantom. *Proc Intl Soc Mag Reson Med.* 2012;20:2456.

31. Kuo MD, Jamshidi N. Behind the numbers: Decoding molecular phenotypes with radiogenomics –guiding principles and technical considerations. *Radiology.* 2014;270(2):320–325. doi: 10.1148/radiol.13132195

32. Narang S, Lehrer M, Yang D, et al. Radiomics in glioblastoma: current status, challenges and potential opportunities. *Transl Cancer Res.* 2016;5(4):383–397. doi: 10.21037/tcr.2016.06.31

33. O'Connor JP, Aboagye EO, Adams JE, et al. Imaging biomarker roadmap for cancer studies. *Nat Rev Clin Oncol.* 2017;14(3):169–186. doi: 10.1038/nrclinonc.2016.162

34. Buizza G, Toma-Dasu I, Lazzeroni M, et al. Early tumor response prediction for lung cancer patients using novel longitudinal pattern features from sequential PET/CT image scans. *Phys Med.* 2018;54:21–29. doi: 10.1016/j.ejmp.2018.09.003

35. Raunig DL, McShane LM, Pennello G, et al. Quantitative imaging biomarkers: a review of statistical methods for technical performance assessment. *Stat Methods Med Res.* 2015;24(1):27–67. doi: 10.1177/0962280214537344

36. Obuchowski NA, Reeves AP, Huang EP, et al. Quantitative imaging biomarkers: a review of statistical methods for computer algorithm comparisons. *Stat Methods Med Res.* 2015;24(1):68–106. doi: 10.1177/0962280214537390

37. Elguindi S, Zelefsky MJ, Jiang J, et al. Deep learning-based auto-segmentation of targets and organs-at-risk for magnetic resonance imaging only planning of prostate radiotherapy. *Phys Imaging Radiat Oncol.* 2019;12:80–86. doi: 10.1016/j.phro.2019.11.006

38. Morozov SP, Vladzimirsky AV, Klyashtorny VG, et al. Clinical trials of software based on intelligent technologies (radiation diagnostics). Methodological recommendations. Moscow; 2019. 33 p. (In Russ.).

39. Sullivan DC, Obuchowski NA, Kessler LG, et al. Metrology standards for quantitative imaging biomarkers. *Radiology.* 2015;277(3):813–825. doi: 10.1148/radiol.2015142202

40. Shur J, Blackledge M, D'Arcy J, et al. MRI texture feature repeatability and image acquisition factor robustness, a phantom study and in silico study. *Eur Radiol Exp.* 2021;5(1):2. doi: 10.1186/s41747-020-00199-6

41. Bane O, Hectors SJ, Wagner M, et al. Accuracy, repeatability, and interplatform reproducibility of T1 quantification methods used for DCE-MRI: Results from a multicenter phantom study. *Magn Reson Med.* 2018;79(5):2564–2575. doi: 10.1002/mrm.26903

42. He Y, Liu Y, Dyer BA, et al. 3D-printed breast phantom for multipurpose and multi-modality imaging. *Quant Imaging Med Surg.* 2019;9(1):63–74. doi: 10.21037/qims.2019.01.05

43. Scheuermann JS, Reddin JS, Opanowski A, et al. Qualification of national cancer institute-designated cancer centers for quantitative PET/CT imaging in clinical trials. *J Nucl Med.* 2017;58(7):1065–1071. doi: 10.2967/jnumed.116.186759

44. Obuchowski NA, Barnhart HX, Buckler AJ, et al. Statistical issues in the comparison of quantitative imaging biomarker algorithms using pulmonary nodule volume as an example. *Stat Methods Med Res.* 2015;24(1):107–140. doi: 10.1177/0962280214537392

45. Kessler LG, Barnhart HX, Buckler AJ, et al. The emerging science of quantitative imaging biomarkers terminology and definitions for scientific studies and regulatory submissions. *Stat Methods Med Res.* 2015;24(1):9–26. doi: 10.1177/0962280214537333

46. Napel S, Mu W, Jardim-Perassi BV, et al. Quantitative imaging of cancer in the postgenomic era: Radio(geno)mics, deep learning, and habitats. *Cancer.* 2018;124(24):4633–4649. doi: 10.1002/cncr.31630

47. Rozhkova NI, Bozhenko VK, Burdina II, et al. Radiogenomics of breast cancer as new vector of interdisciplinary integration of radiation and molecular biological technologies (literature review). *Medical alphabet.* 2020;(20):21–29. (In Russ). doi: 10.33667/2078-5631-2020-20-21-29

48. Antropova N, Huynh BQ, Giger ML. A deep feature fusion methodology for breast cancer diagnosis demonstrated on three imaging modality datasets. *Med Phys.* 2017;44(10):5162–5171. doi: 10.1002/mp.12453

49. Antunovic L, Gallivanone F, Sollini M, et al. [^{18}F]FDG PET/CT features for the molecular characterization of primary breast tumors. *Eur J Nucl Med Mol Imaging.* 2017;44(12):1945–1954. doi: 10.1007/s00259-017-3770-9

50. Ha S, Park S, Bang JI, et al. Metabolic radiomics for pretreatment ^{18}F-FDG PET/CT to characterize locally advanced breast cancer: histopathologic characteristics, response to neoadjuvant chemotherapy, and prognosis. *Sci Rep.* 2017;7(1):1556. doi: 10.1038/s41598-017-01524-7

51. Guo W, Li H, Zhu Y, et al. Prediction of clinical phenotypes in invasive breast carcinomas from the integration of radiomics and genomics data. *J Med Imaging (Bellingham).* 2015;2(4):041007. doi: 10.1117/1.JMI.2.4.041007

52. Saha A, Harowicz MR, Grimm LJ, et al. A machine learning approach to radiogenomics of breast cancer: a study of 922 subjects and 529 DCE-MRI features. *Br J Cancer.* 2018;119(4):508–516. doi: 10.1038/s41416-018-0185-8

53. Dong Y, Feng Q, Yang W, et al. Preoperative prediction of sentinel lymph node metastasis in breast cancer based on radiomics of T2-weighted fat-suppression and diffusion-weighted MRI. *Eur Radiol.* 2018;28(2):582–591. doi: 10.1007/s00330-017-5005-7

54. Chan HM, van der Velden BH, Loo CE, Gilhuijs KG. Eigentumors for prediction of treatment failure in patients with early-stage breast cancer using dynamic contrast-enhanced MRI: a feasibility study. *Phys Med Biol.* 2017;62(16):6467–6485. doi: 10.1088/1361-6560/aa7dc5

55. Braman NM, Etesami M, Prasanna P, et al. Intratumoral and peritumoral radiomics for the pretreatment prediction of pathological complete response to neoadjuvant chemotherapy based on breast DCE-MRI. *Breast Cancer Res.* 2017;19(1):57. doi: 10.1186/s13058-017-0846-1

56. Chamming's F, Ueno Y, Ferré R, et al. Features from computerized texture analysis of breast cancers at pretreatment MR imaging are associated with response to neoadjuvant chemotherapy. *Radiology.* 2018;286(2):412–420. doi: 10.1148/radiol.2017170143

57. Partridge SC, Zhang Z, Newitt DC, et al. Diffusion-weighted MRI findings predict pathologic response in neoadjuvant treatment of breast cancer: the ACRIN 6698 multicenter trial. *Radiology.* 2018;289(3):618–627. doi: 10.1148/radiol.2018180273

58. Park H, Lim Y, Ko ES, et al. Radiomics signature on magnetic resonance imaging: association with disease-free survival in patients with invasive breast cancer. *Clin Cancer Res.* 2018;24(19):4705–4714. doi: 10.1158/1078-0432.CCR-17-3783

59. Nasrullah N, Sang J, Alam MS, et al. Automated lung nodule detection and classification using deep learning combined

with multiple strategies. *Sensors (Basel)*. 2019;19(17):3722. doi: 10.3390/s19173722

60. Carter BW, Godoy MC, Erasmus JJ. Predicting malignant nodules from screening CTs. *J Thorac Oncol.* 2016;11(12):2045–2047. doi: 10.1016/j.jtho.2016.09.117

61. Aerts HJ, Velazquez ER, Leijenaar RT, et al. Decoding tumour phenotype by noninvasive imaging using a quantitative radiomics approach. *Nat Commun.* 2014;5:4006. doi: 10.1038/ncomms5006

62. Zhou H, Dong D, Chen B, et al. Diagnosis of distant metastasis of lung cancer: based on clinical and radiomic features. *Transl Oncol.* 2018;11(1):31–36. doi: 10.1016/j.tranon.2017.10.010

63. Liu Y, Kim J, Balagurunathan Y, et al. Radiomic features are associated with EGFR mutation status in lung adenocarcinomas. *Clin Lung Cancer.* 2016;17(5):441–448.e6. doi: 10.1016/j.cllc.2016.02.001

64. Fave X, Zhang L, Yang J, et al. Delta-radiomics features for the prediction of patient outcomes in non-small cell lung cancer. *Sci Rep.* 2017;7(1):588. doi: 10.1038/s41598-017-00665-z

65. Coroller TP, Agrawal V, Narayan V, et al. Radiomic phenotype features predict pathological response in non-small cell lung cancer. *Radiother Oncol.* 2016;119(3):480–486. doi: 10.1016/j.radonc.2016.04.004

66. Kickingereder P, Neuberger U, Bonekamp D, et al. Radiomic subtyping improves disease stratification beyond key molecular, clinical, and standard imaging characteristics in patients with glioblastoma. *Neuro Oncol.* 2018;20(6):848–857. doi: 10.1093/neuonc/nox188

67. Pérez-Beteta J, Molina-García D, Ortiz-Alhambra JA, et al. Tumor surface regularity at MR imaging predicts survival and response to surgery in patients with glioblastoma. *Radiology.* 2018;288(1):218–225. doi: 10.1148/radiol.2018171051

68. Zhou Z, Chen L, Sher D, et al. Predicting lymph node metastasis in head and neck cancer by combining many-objective radiomics and 3-dimensioal convolutional neural network through evidential reasoning. *Annu Int Conf IEEE Eng Med Biol Soc.* 2018;2018:1–4. doi: 10.1109/EMBC.2018.8513070

69. Wang G, He L, Yuan C, et al. Pretreatment MR imaging radiomics signatures for response prediction to induction chemotherapy in patients with nasopharyngeal carcinoma. *Eur J Radiol.* 2018;98:100–106. doi: 10.1016/j.ejrad.2017.11.007

70. Chen X, Oshima K, Schott D, et al. Assessment of treatment response during chemoradiation therapy for pancreatic cancer based on quantitative radiomic analysis of daily CTs: An exploratory study. *PLoS One.* 2017;12:e0178961. doi: 10.1371/journal.pone.0178961

71. Huang YQ, Liang CH, He L, et al. Development and validation of a radiomics nomogram for preoperative prediction of lymph node metastasis in colorectal cancer. *J Clin Oncol.* 2016;34(18):2157–2164. doi: 10.1200/JCO.2015.65.9128

72. Lin YC, Lin G, Hong JH, et al. Diffusion radiomics analysis of intratumoral heterogeneity in a murine prostate cancer model following radiotherapy: Pixelwise correlation with histology. *J Magn Reson Imaging.* 2017;46(2):483–489. doi: 10.1002/jmri.25583

73. Chaddad A, Kucharczyk MJ, Niazi T. Multimodal radiomic features for the predicting gleason score of prostate cancer. *Cancers (Basel).* 2018;10(8):249. doi: 10.3390/cancers10080249

74. Ognerubov NA, Shatov IA, Shatov AV. Radiogenomics and radiomics in the diagnostics of malignant tumours: a literary review. *Tambov University Reports.* Series: Natural and Technical Sciences. 2017;22(6):1453–1460. (In Russ). doi: 10.20310/1810-0198-2017-22-6-1453-1460

СПИСОК ЛИТЕРАТУРЫ

1. Kumar V., Gu Y., Basu S., et al. Radiomics: The process and the challenges // Magn Reson Imaging. 2012. Vol. 30, N 9. P. 1234–1248. doi: 10.1016/j.mri.2012.06.010

2. Papanikolaou N., Matos C., Koh D.M. How to develop a meaningful radiomic signature for clinical use in oncologic patients // Cancer Imaging. 2020. Vol. 20, N 1. P. 33. doi: 10.1186/s40644-020-00311-4

3. Aerts H.J., Grossmann P., Tan Y., et al. Defining a radiomic response phenotype: A pilot study using targeted therapy in NSCLC // Sci Rep. 2016. Vol. 6. P. 33860. doi: 10.1038/srep33860

4. Coroller T.P., Grossmann P., Hou Y., et al. CT-based radiomic signature predicts distant metastasis in lung adenocarcinoma // Radiother Oncol. 2015. Vol. 114, N 3. P. 345–350. doi: 10.1016/j.radonc.2015.02.015

5. Lopez C.J., Nagornaya N., Parra N.A., et al. Association of radiomics and metabolic tumor volumes in radiation treatment of glioblastoma multiforme // Int J Radiat Oncol Biol Phys. 2017. Vol. 97, N 3. P. 586–595. doi: 10.1016/j.ijrobp.2016.11.011

6. De Souza N.M., Achten E., Alberich-Bayarri A., et al. Validated imaging biomarkers as decision-making tools in clinical trials and routine practice: current status and recommendations from the EIBALL* subcommittee of the European Society of Radiology (ESR) // Insights Imaging. 2019. Vol. 10, N 1. P. 87. doi: 10.1186/s13244-019-0764-0

7. Jones E.F., Buatti J.M., Shu H.K., et al. Clinical trial design and development work group within the quantitative imaging network // Tomography. 2020. Vol. 6, N 2. P. 60–64. doi: 10.18383/j.tom.2019.00022

8. European Society of Radiology (ESR). ESR Statement on the validation of imaging biomarkers // Insights Imaging. 2020. Vol. 11, N 1. P. 76. doi: 10.1186/s13244-020-00872-9

9. Grimm L.J., Zhang J., Mazurowski M.A. Computational approach to radiogenomics of breast cancer: Luminal A and luminal B molecular subtypes are associated with imaging features on routine breast MRI extracted using computer vision algorithms // J Magn Reson Imaging. 2015. Vol. 42, N 4. P. 902–907. doi: 10.1002/jmri.24879

10. Nie K., Shi L., Chen Q., et al. Rectal cancer: Assessment of neoadjuvant chemoradiation outcome based on radiomics of multiparametric MRI // Clin Cancer Res. 2016. Vol. 22, N 21. P. 5256–5264. doi: 10.1158/1078-0432.CCR-15-2997

11. Kim H., Park C.M., Lee M., et al. Impact of reconstruction algorithms on ct radiomic features of pulmonary tumors: analysis of intra- and inter-reader variability and inter-reconstruction algorithm variability // PLoS One. 2016. Vol. 11, N 10. P. e0164924. doi: 10.1371/journal.pone.0164924

12. Ohri N., Duan F., Snyder B.S., et al. Pretreatment 18F-FDG PET textural features in locally advanced non-small cell lung cancer: Secondary analysis of ACRIN 6668/RTOG 0235 // J Nucl Med. 2016. Vol. 57, N 6. P. 842–848. doi: 10.2967/jnumed.115.166934

13. Zhang B., Tian J., Dong D., et al. Radiomics features of multiparametric MRI as novel prognostic factors in advanced nasopharyngeal carcinoma // Clin Cancer Res. 2017. Vol. 23, N 15. P. 4259–4269. doi: 10.1158/1078-0432.CCR-16-2910

14. Nakatsugawa M., Cheng Z., Goatman K.A., et al. Radiomic analysis of salivary glands and its role for predicting xerostomia in irradiated head and neck cancer patients // Int J Radiat Oncol Biol Phys. 2016. Vol. 96, N 2, Suppl. P. S217. doi: 10.1016/j.ijrobp.2016.06.539

15. Shafiee M.J., Chung A.G., Khalvati F., et al. Discovery radiomics via evolutionary deep radiomic sequencer discovery for pathologically proven lung cancer detection // J Med Imaging. 2016. Vol. 4, N 4. P. 041305. doi: 10.1117/1.JMI.4.4.041305

16. Echegaray S., Nair V., Kadoch M., et al. A rapid segmentation-insensitive "Digital Biopsy" method for radiomic feature extraction: method and pilot study using ct images of non-small cell lung cancer // Tomography. 2016. Vol. 2, N 4. P. 283–294. doi: 10.18383/j.tom.2016.00163

17. Li H., Galperin-Aizenberg M., Pryma D., et al. Unsupervised machine learning of radiomic features for predicting treatment response and overall survival of early stage non-small cell lung cancer patients treated with stereotactic body radiation therapy // Radiother Oncol. 2018. Vol. 129, N 2. P. 218–226. doi: 10.1016/j.radonc.2018.06.025

18. Tajbakhsh N., Shin J.Y., Gurudu S.R., et al. Convolutional neural networks for medical image analysis: full training or fine tuning? // IEEE Transactions on Medical Imaging. 2016. Vol. 35, N 5. P. 1299–1312. doi: 10.1109/TMI.2016.2535302

19. Elguindi S., Zelefsky M.J., Jiang J., et al. Deep learning-based auto-segmentation of targets and organs-at-risk for magnetic resonance imaging only planning of prostate radiotherapy // Phys Imaging Radiat Oncol. 2019. Vol. 12. P. 80–86. doi: 10.1016/j.phro.2019.11.006

20. Gillies R.J., Kinahan P.E., Hricak H. Radiomics: images are more than pictures, they are data // Radiology. 2016. Vol. 278, N 2. P. 563–577. doi: 10.1148/radiol.2015151169

21. Buckler A.J., Bresolin L., Dunnick N.R., et al. Quantitative imaging test approval and biomarker qualification: Interrelated but distinct activities // Radiology. 2011. Vol. 259, N 3. P. 875–884. doi: 10.1148/radiol.10100800

22. Alobaidli S., McQuaid S., South C., et al. The role of texture analysis in imaging as an outcome predictor and potential tool in radiotherapy treatment planning // Br J Radiol. 2014. Vol. 87, N 1042. P. 20140369. doi: 10.1259/bjr.20140369

23. Li H., Giger M.L., Lan L., et al. Comparative analysis of image-based phenotypes of mammographic density and parenchymal patterns in distinguishing between BRCA1/2 cases, unilateral cancer cases, and controls // J Med Imaging. 2014. Vol. 1, N 3. P. 031009. doi: 10.1117/1.JMI.1.3.031009

24. Goh V., Ganeshan B., Nathan P., et al. Assessment of response to tyrosine kinase inhibitors in metastatic renal cell cancer: CT texture as a predictive biomarker // Radiology. 2011. Vol. 261, N 1. P. 165–171. doi: 10.1148/radiol.11110264

25. Yip C., Davnall F., Kozarski R., et al. Assessment of changes in tumor heterogeneity following neoadjuvant chemotherapy in primary esophageal cancer // Dis Esophagus. 2015. Vol. 28, N 2. P. 172–179. doi: 10.1111/dote.12170

26. Park J.E., Kim H.S. Radiomics as a quantitative imaging biomarker: practical considerations and the current standpoint in neuro-oncologic studies // Nucl Med Mol Imaging. 2018. Vol. 52, N 2. P. 99–108. doi: 10.1007/s13139-017-0512-7

27. Сергунова К.А., Ахмад Е.С., Семенов Д.С., и др. Участие медицинских физиков в обеспечении контроля качества оборудования и безопасности пациентов при магнитно-резонансной томографии // Медицинская физика. 2020. № 3. С. 78–85.

28. Clements J.B., Baird C.T., de Boer S.F., et al. AAPM medical physics practice guideline 10.a.: Scope of practice for clinical medical physics // J Appl Clin Med Phys. 2018. Vol. 19, N 6. P. 11–25. doi: 10.1002/acm2.12469

29. Shukla-Dave A., Obuchowski N.A., Chenevert T.L., et al. Quantitative imaging biomarkers alliance (QIBA) recommendations for improved precision of DWI and DCE-MRI derived biomarkers in multicenter oncology trials // J Magn Reson Imaging. 2019. Vol. 49, N 7. P. e101–e121. doi: 10.1002/jmri.26518

30. Russek S.E., Boss M., Jackson E.F., et al. Characterization of NIST/ISMRM MRI System Phantom // Proc Intl Soc Mag Reson Med. 2012. Vol. 20. P. 2456.

31. Kuo M.D., Jamshidi N. Behind the numbers: Decoding molecular phenotypes with radiogenomics –guiding principles and technical considerations // Radiology. 2014. Vol. 270, N 2. P. 320–325. doi: 10.1148/radiol.13132195

32. Narang S., Lehrer M., Yang D., et al. Radiomics in glioblastoma: current status, challenges and potential opportunities // Transl Cancer Res. 2016. Vol. 5, N 4. P. 383–397. doi: 10.21037/tcr.2016.06.31

33. O'Connor J.P., Aboagye E.O., Adams J.E., et al. Imaging biomarker roadmap for cancer studies // Nat Rev Clin Oncol. 2017. Vol. 14, N 3. P. 169–186. doi: 10.1038/nrclinonc.2016.162

34. Buizza G., Toma-Dasu I., Lazzeroni M., et al. Early tumor response prediction for lung cancer patients using novel longitudinal pattern features from sequential PET/CT image scans // Phys Med. 2018. Vol. 54. P. 21–29. doi: 10.1016/j.ejmp.2018.09.003

35. Raunig D.L., McShane L.M., Pennello G., et al. Quantitative imaging biomarkers: a review of statistical methods for technical performance assessment // Stat Methods Med Res. 2015. Vol. 24, N 1. P. 27–67. doi: 10.1177/0962280214537344

36. Obuchowski N.A., Reeves A.P., Huang E.P., et al. Quantitative imaging biomarkers: a review of statistical methods for computer algorithm comparisons // Stat Methods Med Res. 2015. Vol. 24, N 1. P. 68–106. doi: 10.1177/0962280214537390

37. Elguindi S., Zelefsky M.J., Jiang J., et al. Deep learning-based auto-segmentation of targets and organs-at-risk for magnetic resonance imaging only planning of prostate radiotherapy // Phys Imaging Radiat Oncol. 2019. Vol. 12. P. 80–86. doi: 10.1016/j.phro.2019.11.006

38. Морозов С.П., Владзимирский А.В., Кляшторный В.Г., и др. Клинические испытания программного обеспечения на основе интеллектуальных технологий (лучевая диагностика). Методические рекомендации. Москва, 2019. 33 с.

39. Sullivan D.C., Obuchowski N.A., Kessler L.G., et al. Metrology standards for quantitative imaging biomarkers // Radiology. 2015. Vol. 277, N 3. P. 813–825. doi: 10.1148/radiol.2015142202

40. Shur J., Blackledge M., D'Arcy J., et al. MRI texture feature repeatability and image acquisition factor robustness, a phantom study and in silico study // Eur Radiol Exp. 2021. Vol. 5, N 1. P. 2. doi: 10.1186/s41747-020-00199-6

41. Bane O., Hectors S.J., Wagner M., et al. Accuracy, repeatability, and interplatform reproducibility of T1 quantification methods used for DCE-MRI: Results from a multicenter phantom study // Magn Reson Med. 2018. Vol. 79, N 5. P. 2564–2575. doi: 10.1002/mrm.26903

42. He Y., Liu Y., Dyer B.A., et al. 3D-printed breast phantom for multi-purpose and multi-modality imaging // Quant Imaging Med Surg. 2019. Vol. 9, N 1. P. 63–74. doi: 10.21037/qims.2019.01.05

43. Scheuermann J.S., Reddin J.S., Opanowski A., et al. Qualification of national cancer institute-designated cancer centers for quantitative PET/CT imaging in clinical trials // J Nucl Med. 2017. Vol. 58, N 7. P. 1065–1071. doi: 10.2967/jnumed.116.186759

44. Obuchowski N.A., Barnhart H.X., Buckler A.J., et al. Statistical issues in the comparison of quantitative imaging biomarker algorithms using pulmonary nodule volume as an example // Stat Methods Med Res. 2015. Vol. 24, N 1. P. 107–140. doi: 10.1177/0962280214537392

45. Kessler L.G., Barnhart H.X., Buckler A.J., et al. The emerging science of quantitative imaging biomarkers terminology and definitions for scientific studies and regulatory submissions // Stat Methods Med Res. 2015. Vol. 24, N 1. P. 9–26. doi: 10.1177/0962280214537333

46. Napel S., Mu W., Jardim-Perassi B.V., et al. Quantitative imaging of cancer in the postgenomic era: Radio(geno)mics, deep learning, and habitats // Cancer. 2018. Vol. 124, N 24. P. 4633–4649. doi: 10.1002/cncr.31630

47. Рожкова Н.И., Боженко В.К., Бурдина И.И., и др. Радиогеномика рака молочной железы — новый вектор междисциплинарной интеграции лучевых и молекулярно-биологических технологий (обзор литературы) // Медицинский алфавит. 2020. № 20. С. 21–29. doi: 10.33667/2078-5631-2020-20-21-29

48. Antropova N., Huynh B.Q., Giger M.L. A deep feature fusion methodology for breast cancer diagnosis demonstrated on three imaging modality datasets // Med Phys. 2017. Vol. 44, N 10. P. 5162–5171. doi: 10.1002/mp.12453

49. Antunovic L., Gallivanone F., Sollini M., et al. [18F]FDG PET/CT features for the molecular characterization of primary breast tumors // Eur J Nucl Med Mol Imaging. 2017. Vol. 44, N 12. P. 1945–1954. doi: 10.1007/s00259-017-3770-9

50. Ha S., Park S., Bang J.I., et al. Metabolic radiomics for pretreatment 18F-FDG PET/CT to characterize locally advanced breast cancer: histopathologic characteristics, response to neoadjuvant chemotherapy, and prognosis // Sci Rep. 2017. Vol. 7, N 1. P. 1556. doi: 10.1038/s41598-017-01524-7

51. Guo W., Li H., Zhu Y., et al. Prediction of clinical phenotypes in invasive breast carcinomas from the integration of radiomics and genomics data // J Med Imaging (Bellingham). 2015. Vol. 2, N 4. P. 041007. doi: 10.1117/1.JMI.2.4.041007

52. Saha A., Harowicz M.R., Grimm L.J., et al. A machine learning approach to radiogenomics of breast cancer: a study of 922 subjects and 529 DCE-MRI features // Br J Cancer. 2018. Vol. 119, N 4. P. 508–516. doi: 10.1038/s41416-018-0185-8

53. Dong Y., Feng Q., Yang W., et al. Preoperative prediction of sentinel lymph node metastasis in breast cancer based on radiomics of T2-weighted fat-suppression and diffusion-weighted MRI // Eur Radiol. 2018. Vol. 28, N 2. P. 582–591. doi: 10.1007/s00330-017-5005-7

54. Chan H.M., van der Velden B.H., Loo C.E., Gilhuijs K.G. Eigentumors for prediction of treatment failure in patients with early-stage breast cancer using dynamic contrast-enhanced MRI: a feasibility study // Phys Med Biol. 2017. Vol. 62, N 16. P. 6467–6485. doi: 10.1088/1361-6560/aa7dc5

55. Braman N.M., Etesami M., Prasanna P., et al. Intratumoral and peritumoral radiomics for the pretreatment prediction of pathological complete response to neoadjuvant chemotherapy based on breast DCE-MRI // Breast Cancer Res. 2017. Vol. 19, N 1. P. 57. doi: 10.1186/s13058-017-0846-1

56. Chamming's F., Ueno Y., Ferré R., et al. Features from computerized texture analysis of breast cancers at pretreatment MR imaging are associated with response to neoadjuvant chemotherapy // Radiology. 2018. Vol. 286, N 2. P. 412–420. doi: 10.1148/radiol.2017170143

57. Partridge S.C., Zhang Z., Newitt D.C., et al. Diffusion-weighted MRI findings predict pathologic response in neoadjuvant treatment of breast cancer: the ACRIN 6698 multicenter trial // Radiology. 2018. Vol. 289, N 3. P. 618–627. doi: 10.1148/radiol.2018180273

58. Park H., Lim Y., Ko E.S., et al. Radiomics signature on magnetic resonance imaging: association with disease-free survival in patients with invasive breast cancer // Clin Cancer Res. 2018. Vol. 24, N 19. P. 4705–4714. doi: 10.1158/1078-0432.CCR-17-3783

59. Nasrullah N., Sang J., Alam M.S., et al. Automated lung nodule detection and classification using deep learning combined with multiple strategies // Sensors (Basel). 2019. Vol. 19, N 17. P. 3722. doi: 10.3390/s19173722

60. Carter B.W., Godoy M.C., Erasmus J.J. Predicting malignant nodules from screening CTs // J Thorac Oncol. 2016. Vol. 11, N 12. P. 2045–2047. doi: 10.1016/j.jtho.2016.09.117

61. Aerts H.J., Velazquez E.R., Leijenaar R.T., et al. Decoding tumour phenotype by noninvasive imaging using a quantitative radiomics approach // Nat Commun. 2014. Vol. 5. P. 4006. doi: 10.1038/ncomms5006

62. Zhou H., Dong D., Chen B., et al. Diagnosis of distant metastasis of lung cancer: based on clinical and radiomic features // Transl Oncol. 2018. Vol. 11, N 1. P. 31–36. doi: 10.1016/j.tranon.2017.10.010

63. Liu Y., Kim J., Balagurunathan Y., et al. Radiomic features are associated with EGFR mutation status in lung adenocarcinomas // Clin Lung Cancer. 2016. Vol. 17, N 5. P. 441–448.e6. doi: 10.1016/j.cllc.2016.02.001

64. Fave X., Zhang L., Yang J., et al. Delta-radiomics features for the prediction of patient outcomes in non-small cell lung cancer // Sci Rep. 2017. Vol. 7, N 1. P. 588. doi: 10.1038/s41598-017-00665-z

65. Coroller T.P, Agrawal V., Narayan V., et al. Radiomic phenotype features predict pathological response in non-small cell lung cancer // Radiother Oncol. 2016. Vol. 119, N 3. P. 480–486. doi: 10.1016/j.radonc.2016.04.004

66. Kickingereder P., Neuberger U., Bonekamp D., et al. Radiomic subtyping improves disease stratification beyond key molecular, clinical, and standard imaging characteristics in patients with glioblastoma // Neuro Oncol. 2018. Vol. 20, N 6. P. 848–857. doi: 10.1093/neuonc/nox188

67. Pérez-Beteta J., Molina-García D., Ortiz-Alhambra J.A., et al. Tumor surface regularity at MR imaging predicts survival and response to surgery in patients with glioblastoma // Radiology. 2018. Vol. 288, N 1. P. 218–225. doi: 10.1148/radiol.2018171051

68. Zhou Z., Chen L., Sher D., et al. Predicting lymph node metastasis in head and neck cancer by combining many-objective radiomics and 3-dimensioal convolutional neural network through evidential reasoning // Annu Int Conf IEEE Eng Med Biol Soc. 2018. Vol. 2018. P. 1–4. doi: 10.1109/EMBC.2018.8513070

69. Wang G., He L., Yuan C., et al. Pretreatment MR imaging radiomics signatures for response prediction to induction chemotherapy in patients with nasopharyngeal carcinoma // Eur J Radiol. 2018. Vol. 98. P. 100–106. doi: 10.1016/j.ejrad.2017.11.007

70. Chen X., Oshima K., Schott D., et al. Assessment of treatment response during chemoradiation therapy for pancreatic cancer based on quantitative radiomic analysis of daily CTs: An exploratory study // PLoS One. 2017. Vol. 12. P. e0178961. doi: 10.1371/journal.pone.0178961

71. Huang Y.Q., Liang C.H., He L., et al. Development and validation of a radiomics nomogram for preoperative prediction of lymph node metastasis in colorectal cancer // J Clin Oncol. 2016. Vol. 34, N 18. P. 2157–2164. doi: 10.1200/JCO.2015.65.9128

72. Lin Y.C., Lin G., Hong J.H., et al. Diffusion radiomics analysis of intratumoral heterogeneity in a murine prostate cancer model follow-ing radiotherapy: Pixelwise correlation with histology // J Magn Reson Imaging. 2017. Vol. 46, N 2. P. 483–489. doi: 10.1002/jmri.25583

73. Chaddad A., Kucharczyk M.J., Niazi T. Multimodal radiomic features for the predicting gleason score of prostate cancer // Cancers (Basel). 2018. Vol. 10, N 8. P. 249. doi: 10.3390/cancers10080249

74. Огнерубов Н.А., Шатов И.А., Шатов А.В. Радиогеномика и радиомика в диагностике злокачественных опухолей: обзор литературы // Вестник Тамбовского университета. Серия: Естественные и технические науки. 2017. Т. 22, № 6-2. С. 1453–1460. doi: 10.20310/1810-0198-2017-22-6-1453-1460

AUTHORS' INFO

* Anna N. Khoruzhaya, MD;
address: 28-1 Srednyaya Kalitnikovskaya str., 109029 Moscow, Russia; ORCID: https://orcid.com/0000-0003-4857-5404;
eLibrary SPIN: 7948-6427; e-mail: a.khoruzhaya@npcmr.ru

Ekaterina S. Akhmad;
ORCID: https://orcid.com/0000-0002-8235-9361;
eLibrary SPIN: 5891-4384

Dmitry S. Semenov;
ORCID: https://orcid.com/0000-0002-4293-2514;
eLibrary SPIN: 2278-7290

ОБ АВТОРАХ

* Хоружая Анна Николаевна;
адрес: Россия, 109029, Москва, Средняя Калитниковская ул., д. 28, стр. 1; ORCID: https://orcid.com/0000-0003-4857-5404;
eLibrary SPIN: 7948-6427; e-mail: a.khoruzhaya@npcmr.ru

Ахмад Екатерина Сергеевна;
ORCID: https://orcid.com/0000-0002-8235-9361;
eLibrary SPIN: 5891-4384

Семенов Дмитрий Сергеевич;
ORCID: https://orcid.com/0000-0002-4293-2514;
eLibrary SPIN: 2278-7290

* Corresponding author / Автор, ответственный за переписку

Роль маммографии в радиомике рака молочной железы

В.Г. Говорухина[1], С.С. Семенов[2, 3], П.Б. Гележе[2], В.В. Диденко[2, 4], С.П. Морозов[2], А.Е. Андрейченко[2]

[1] Московский государственный университет имени М.В. Ломоносова, Москва, Российская Федерация

[2] Научно-практический клинический центр диагностики и телемедицинских технологий Департамента здравоохранения города Москвы, Москва, Российская Федерация

[3] Московский клинический научно-практический центр имени А.С. Логинова, Москва, Российская Федерация

[4] Городская клиническая онкологическая больница № 1, Москва, Российская Федерация

АННОТАЦИЯ

Маммография — в настоящее время единственный способ скрининга рака молочной железы (РМЖ). Хотя цифровая маммография служит основным и наиболее широкодоступным методом для выявления РМЖ, её эффективность в обнаружении и оценке внутриопухолевой гетерогенности опухоли ограничена. Пункционная биопсия не может отразить гистологической картины опухоли в целом из-за небольшого размера образца ткани или опухоли. По этой причине выбор подходящего лечения и определение прогноза становится затруднительным. В этом случае такой неинвазивный подход, как медицинская визуализация, даёт более полное представление об опухоли, перспективен при «виртуальной биопсии», а также в контроле прогрессирования заболевания и ответа на терапию.

Радиомика с помощью текстурного анализа позволяет взглянуть на снимок как на группу числовых характеристик, выйти за пределы привычного качественного зрительного восприятия интенсивностей и перейти к более глубокому анализу цифровых, пиксельных данных с целью повышения точности дифференциальной диагностики. Метод радиогеномики, являясь естественным продолжением радиомики, фокусируется на определении экспрессии генов исходя из лучевого фенотипа опухоли. В обзоре рассматриваются возможности применения маммографии в радиомике и радиогеномике РМЖ.

В статье представлен обзор литературы баз данных PubMed, Medline, Springer, eLibrary, а также найденных с помощью Google Scholar актуальных российских научных статей. Полученная релевантная информация объединена, структурирована и проанализирована с целью изучения роли маммографии в радиомике РМЖ.

Ключевые слова: рак молочной железы; маммография; радиомика; радиогеномика; искусственный интеллект.

The role of mammography in breast cancer radiomics

Veronika G. Govorukhina[1], Serafim S. Semenov[2, 3], Pavel B. Gelezhe[2], Vera V. Didenko[2, 4], Sergey P. Morozov[2], Anna E. Andreychenko[2]

[1] Lomonosov Moscow State University, Moscow, Russian Federation
[2] Research and Practical Clinical Center for Diagnostics and Telemedicine Technologies of Moscow Health Care, Moscow, Russian Federation
[3] Moscow Clinical Scientific Center named after A.S. Loginov, Moscow, Russian Federation
[4] City Clinical Oncology Hospital № 1, Moscow, Russian Federation

ABSTRACT

Mammography is still the only screening method for breast cancer. Although digital mammography is the most common and widely used method for detecting breast cancer, it is ineffective at detecting and assessing intratumoral heterogeneity. Due to the small size of the tissue sample or tumor, biopsies often fail to represent the entire tumor. For this reason, selecting a treatment and determining a patient's prognosis becomes difficult. In this case, medical imaging is a noninvasive approach that can provide a more comprehensive view of the entire tumor, act as a "virtual biopsy," and be useful for monitoring disease progression and response to therapy.

Radiomics with texture analysis allows you to look at an image as a group of numerical data, moving beyond the usual visual perception and into a deeper analysis of digital, pixel data to improve the accuracy of differential diagnosis. Radioge-nomics is a natural extension of radiomics that focuses on determining gene expression based on radiologic tumor phenotype. The purpose of this review is to evaluate the role of mammography in breast cancer radiomics and radiogenomics.

The article presents a literature review of relevant Russian scientific articles found in databases such as PubMed, Medline, Springer, eLibrary, and Google Scholar. The information obtained was then pooled, structured, and analyzed to examine the role of mammography in breast cancer screening radiomics.

Keywords: breast cancer; mammography; radiomics; radiogenomics; artificial intelligence.

乳房造影检查在乳腺癌放射学中的作用

Veronika G. Govorukhina[1], Serafim S. Semenov[2, 3], Pavel B. Gelezhe[2], Vera V. Didenko[2, 4],
Sergey P. Morozov[2], Anna E. Andreychenko[2]

[1] Lomonosov Moscow State University, Moscow, Russian Federation
[2] Research and Practical Clinical Center for Diagnostics and Telemedicine Technologies of Moscow Health Care, Moscow, Russian Federation
[3] Moscow Clinical Scientific Center named after A.S. Loginov, Moscow, Russian Federation
[4] City Clinical Oncology Hospital № 1, Moscow, Russian Federation

简评

乳房造影检查是目前筛查乳腺癌的唯一方法。尽管数字乳房x线照相术是检测乳腺癌的主要和最广泛可用的方法，但其在检测和评估肿瘤的肿瘤内异质性方面的有效性有限。由于组织样本或肿瘤体积小，穿刺活检不能反映整个肿瘤的组织学图片。由于这个原因，选择适当的治疗方法和确定预后变得复杂。在这种情况下，医学成像这样的非侵入性方法给出了肿瘤的更完整的画面，是有希望的»虚拟活检»，以及用于监测疾病的进展和对治疗的反应。

使用纹理分析的放射学允许您将图像视为一组数值特征，超越通常的定性视觉感知强度，并继续深入分析数字，像素数据，以提高差分诊断的准确性。放射基因组学方法是放射组学的自然延伸，侧重于根据肿瘤的放射表型确定基因的表达。该综述探讨了在乳腺癌的放射组学和放射基因组学中使用乳房造影照相术的可能性。

本文概述了PubMed，Medline，Springer，eLibrary数据库的文献，以及使用Google学术搜索找到的相关俄罗斯科学文章。将获得的相关信息组合，结构与分析，以研究乳房造影照相术在乳腺癌放射组学中的作用。

关键词：乳腺癌;乳房x光检查;放射学;放射基因组学;人工智能。

BREAST CANCER: RELEVANCE AND CHARACTERISTICS

Breast cancer (BC) is a pressing issue in modern oncology since it ranks first in terms of prevalence among all malignant neoplasms in women [1]. In Russia, the incidence of BC was 89.8 cases per 100,000 female population in 2018 [1]; in 2019, 73,366 breast cancer cases were detected, with 27.7% of patients in stages III and IV [2].

BC is a heterogeneous disease, which means that tumor morphology and expression subtypes differ depending on the receptor status of BC [3, 4]. Further, the expression of the estrogen receptor (ER), progesterone receptor (PR), and human epidermal growth factor receptor 2 (HER2) determines BC receptor status. The proliferation marker Ki-67 and the epidermal growth factor receptor are also immunochemically stained to determine the molecular subtype of BC [4].

The following are the five molecular subtypes of BC:

1) Luminal A [ER+, PR+ high (≥20%), HER2-, Ki-67 low (≤20%)]: estrogen-dependent low-aggressive tumors with no overexpression of HER2 protein receptors; characterized by high expression of the ER gene
2) Luminal B [ER+, PR+ low (≤20%), HER2-, Ki-67 high]: estrogen-dependent tumors with no overexpression of HER2 protein receptors
3) Luminal B [ER+, HER2+, any Ki-67 level, any PR]: estrogen-dependent aggressive tumors; expressed amplification of the HER2 oncogene; apparent expression of the ER gene
4) HER2 positive [ER- and PR-, any Ki-67, HER2+]: estrogen-independent aggressive tumors; expressed amplification of the HER2 oncogene
5) Triple negative (basal-like): estrogen-independent aggressive tumors with the worst survival rates (ER-, PR-, HER2-) [3–5]

Tumor biology is known to influence the selection of therapy as well as the outcome prognosis, with ER+ and PR+ patients having a longer relapse-free survival ability, while triple-negative BC (TNBC) (ER-, PR-, HER2-) has the most aggressive course and the worst survival rates [3, 6]. The use of biological markers to identify BC subtypes improves patient survival by allowing for more accurate disease diagnosis. For example, patients with ER and PR expression in their tumors should receive endocrine therapy, while patients with HER2 expression should receive anti-HER2 therapy [7].

Intratumoral heterogeneity is defined as the heterogeneity of the morphological structure and the variability in the expression of various markers by individual groups of cells within the same tumor [8, 9]. On the other hand, morphological intratumoral heterogeneity can be defined as diversity in different areas of the tumor, i.e., spatial heterogeneity, or as tumor progression in time, i.e., heterogeneity in time [8]. Due to such heterogeneity of neoplasms and the small size of the puncture tissue sample, the biopsy cannot reflect the histological presentation of the tumor as a whole. Therefore, choosing the appropriate treatment and determining the prognosis becomes difficult. When the tumor is small, biopsies can be difficult. In this case, a noninvasive approach such as medical imaging provides a more consistent view of the tumor and holds promise for "virtual biopsy," as well as monitoring disease progression and response to therapy [7, 10–12].

EARLY DIAGNOSTICS OF BREAST CANCER AND PREDICTION OF THE OUTCOME OF THERAPY

Cancer detection at an early stage is an effective method to reduce patient mortality [13]. Mammography is still the only method for screening and diagnosing BC [10]. Although digital mammography is the most commonly used method for early detection of BC, its efficiency in detecting findings is limited, and mammography has a lower sensitivity in patients with high mammary gland density (ACR-C and D) [14], since the pathological lesion can be overlapped by fibroglandular structures in the image [15, 16]. Despite the reduced sensitivity in one of the groups of patients, digital mammography currently has the best combination of sensitivity and specificity in diagnostics of BC, but these two indicators vary between 75%–90% and 80%–90%, respectively, depending on the country [15]. In their recent study, O. Demircioglu et al. [17] showed that the interpretation of low-quality images by radiologists with limited experience leads to overdiagnosis and unnecessary painful invasive procedures in roughly half of clinical cases [6, 15, 17].

Recent advances in artificial intelligence (AI) technologies used for image analysis hold promise for detecting tumors and reducing the burden on doctors, evaluating treatment, and monitoring disease progression [6]. However, in BC, the primary tasks of clinical practice and research are early detection of the disease prognosis and prediction of the response to therapy. From this point of view, other applications of AI are possible, such as using texture analysis to determine the cancer subtypes and predict treatment response [6, 18, 19].

The interpretation of images by a radiologist with an assessment of the tumor structure, its relationship to the surrounding tissues, special aspects of the location, and structure of microcalcifications are all part of the mammographic study analysis. To create truly personalized therapy, a quantitative (objective) assessment of the lesion is also required [6].

Intratumoral heterogeneity is important for accurate diagnosis, clinical prognosis (response to treatment, survival rate, disease progression, etc.), and treatment of oncological diseases [20, 21]. Early detection of tumor resistance to therapy is critical for improving outcomes, allowing for timely treatment regimen changes [6].

Thus, there is a need to improve the efficiency of detection, prediction of outcome, and response to treatment of BC. A unique set of techniques, combined in radiomics and radiogenomics, is gaining traction as a tool for maximizing the information that can be extracted from virtually any modality of digital medical imaging [15].

RADIOMICS AND RADIOGENOMICS

Radiation diagnostic images contain information that indicates pathophysiological processes, and this relationship can be identified using quantitative image analysis [22]. To put it another way, tumor characteristics at the cellular and genetic levels are reflected in the phenotypic patterns of the tumor, which can be manifested and detected in images [23].

Radiomics is a process that includes the stages of preparation and subsequent quantitative analysis of multidimensional data obtained from digital medical images (the "omic" suffix appears in the names of molecular biology fields that deal with large amounts of data [24]). Radiomics is defined as image analysis that uses specific algorithms to extract numerical characteristics of images in order to create classification models to improve medical decision-making support, as well as to determine the disease prognosis [25, 26] and treatment [27], which is especially significant for personalized therapy. In radiomics, one area of interest in an image is used to obtain a set (sometimes tens or hundreds) of numerical characteristics, each of which can hold a certain information and theoretical aspect (often referred to as a "radiomic sign"), which is not available in normal viewing of images [15]. Radiomics transforms medical imaging data into a dataset of order statistics by using automatic texture sign extraction algorithms for digital medical images [28]. In other words, radiomics with the use of texture analysis allows you to think of an image as a collection of numerical characteristics, go beyond the usual visual perception, and analyze multidimensional data.

Radiogenomics is a technology that connects a patient's genotype to an imaging phenotype. It should be noted that the term "radiogenomics" can also refer to genetic variability and its relationship with response to radiation therapy [29, 30], but it is more often used to assess the relationship between the image characteristics of a tumor or any other disease and its gene expression patterns and gene mutations [25, 26].

Radiogenomics is a method for determining gene expression in a tumor based on its radiation phenotype. This is important because tumors are heterogeneous, and radiomics data are extracted from the region of interest (tumor) as a whole rather than from a separate sample [22]. Radiogenomics also allows for the assessment of treatment response that is not solely based on the traditional measurement of tumor size over time [25]. The combination of radiomics and radiogenomics can detect gene abnormalities in images [6]. Radiomics and radiogenomics improve the accuracy of clinical diagnosis and have prognostic value by identifying relationships between various types of clinical data [22].

STAGES OF RADIOMICS

When considering radiomics as a process, several major stages can be distinguished, namely, image acquisition, highlighting the area of interest, extraction of radiomic signs from the area of interest (texture analysis of images), analysis of textural signs, and construction of various prediction and classification models using the obtained radiomic data with the option of including additional information (e.g., clinical, demographic, or genomic data; the presence of comorbid conditions) [22, 23, 31]. The stages of radiomics are depicted in Fig. 1, and their more detailed characteristics are discussed further below:

1. Determination of the clinical problem and *acquisition of digital medical images*, excluding low-quality studies.
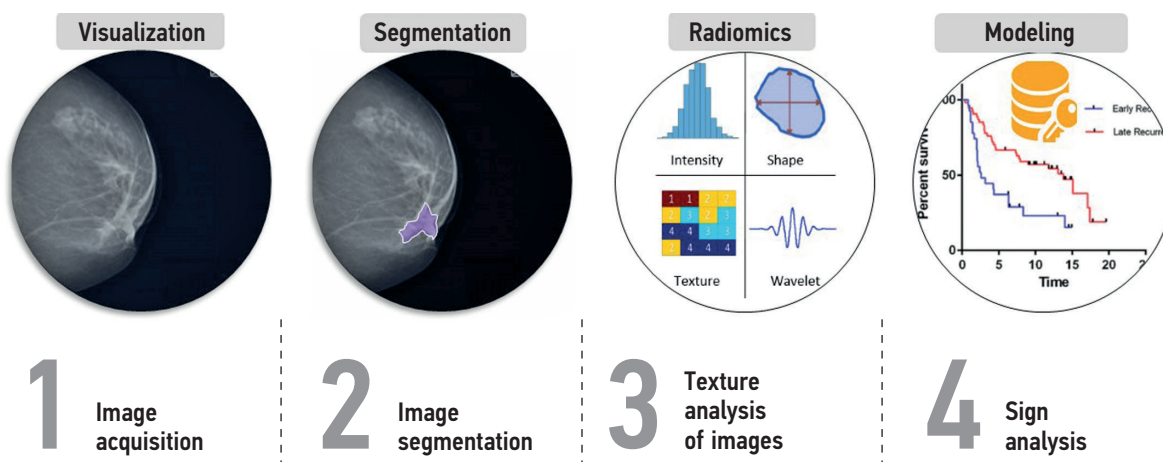
Fig. 1. The diagram illustrates the typical stages in radiomics. After obtaining medical images (1), they are manually or automatically segmented (2). Using special software or programming language modules, radiomic signs of the first and higher orders are extracted from segmented regions of interest (3). Next, the analysis and selection of the most significant textural signs obtained are carried out. Finally, based on the analyzed radiomic data, various clinical and diagnostic models of classification or prediction are constructed (4)

2. ***Segmentation of images*** to the main analyzed areas of interest [32], such as a malignant neoplasm, to assess intratumoral heterogeneity. Many tumors have indistinct boundaries, which complicates the reproducibility of their segmentation [33]. Although it is preferable to use semiautomatic or fully automatic selection of the area of interest using special software, in some cases, expert specification and manual selection are required [23, 34]. The selection process of the region of interest is not standardized, and the region of interest may contain the entire tumor or some of its parts [35, 36]. Manually determining the region of interest is time-consuming and variable due to differences in image interpretation by different radiologists [33], which ultimately affects the accuracy of the radiomic models constructed; however, modern deep learning technologies using big data are capable of mitigating this effect [37].

3. ***Extraction of a variety of radiomic signs*** from a segmented region of interest using mathematical operations involving numerical values of intensities and relative positions of pixels or voxels in images. The extracted quantitative signs are classified into two categories: morphological signs (volume and shape) and histogram signs (description of the intensity of gray tone levels) of the first, second, and higher orders [26, 34].

Morphological signs reflect the shape of the region of interest. For planar images, 2D signs of shape are relevant, such as the perimeter-to-surface ratio and roundness as a measure of the approximation of the shape of the region of interest to the shape of a circle. For example, a stellate tumor will have a higher surface-to-volume ratio than a round tumor [31].

First-order histogram signs [38] indicate the distribution of gray-level intensities for pixels in the region of interest. The most common signs (mean and median) in this category indicate the width of the range of intensities; entropy is a measure of irregularity in the distribution of intensities (higher values indicate a more heterogeneous region) [39]. However, first-order statistics do not account for the spatial arrangement of pixels.

Second-order histogram signs [38], also known as texture signs, indicate the spatial relationship between two adjacent pixels with the same or different brightness values. The most common technique for extracting texture signs is based on a gray-level co-occurrence matrix, which is a matrix whose rows and columns represent gray intensity-level values; the matrix cells indicate the number of times the corresponding gray values are in a certain relationship (angle and distance between the pixels analyzed). For example, signs obtained by using such a matrix include second-order entropy, which indicates heterogeneity; energy, which describes image homogeneity; and contrast range, which determines the local change in intensities [10]. In radiomics, texture analysis provides information on the measure of intratumoral heterogeneity [22, 40].

Figure 2 shows a comparison of the histogram signs of the first and second orders, as well as the formation of the adjacency matrix of the gray tone level, where Fig. 2 (*a*) presents two original images, Fig. 2 (*b*) histograms of the
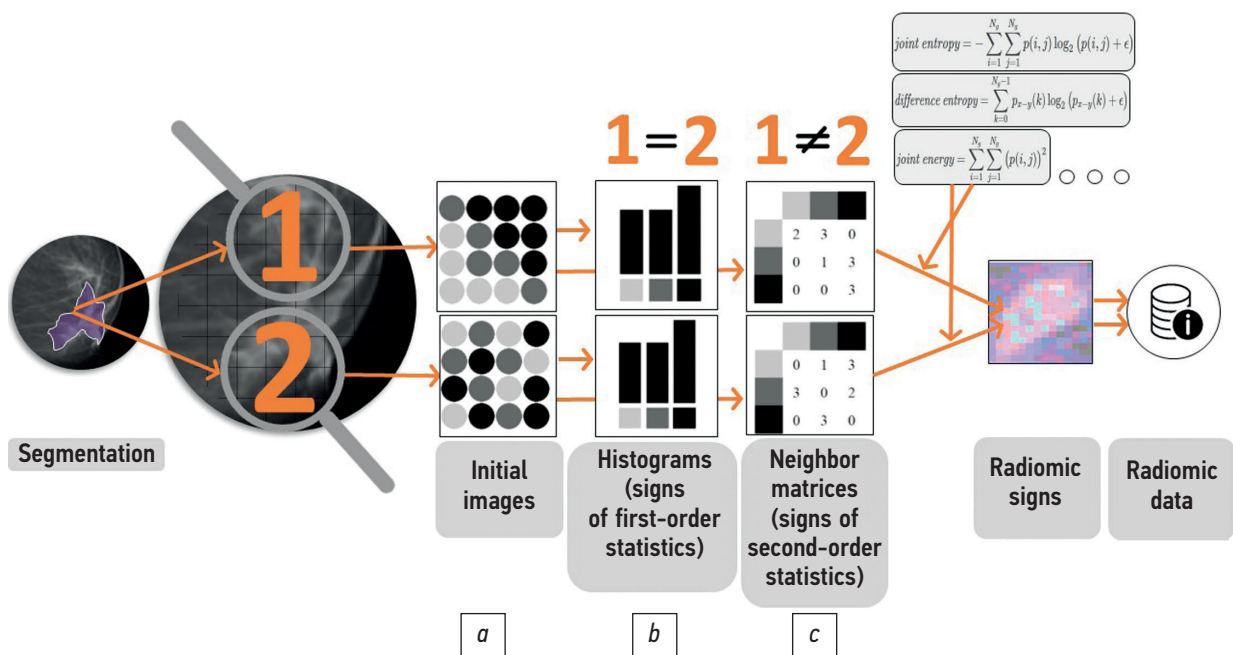
Fig. 2. Comparison of histogram signs of the first and second orders. The two different initial regions of interest of the segmented image (*a*) comprise an equal number of pixels in light gray, dark gray, and black shades. Brightness histograms based on the number of pixels of certain shades (histogram signs of the first order) are the same (*b*). These signs do not indicate the mutual arrangement of the pixels. Adjacency matrices (second-order histogram signs) reflect the heterogeneity of images (*c*). In the future, mathematical algorithms derived from the obtained histograms of intensities and adjacency matrices of the gray level will be used to calculate a variety of radiomic signs for analysis and modeling

first order, and Fig. 2 (*c*) grayscale adjacency matrices obtained for the original images. The row and column headings of these matrices contain the shade of gray numbers. Each cell of the table contains the number of horizontal pairs of pixels, in which pixels with the shade indicated in the header of the row and column of this cell are located relative to each other at an angle of 0º [41]. Subsequently, mathematical algorithms from the obtained histograms of intensities and adjacency matrices of the gray level are used to calculate a set of radiomics signs for analysis and modeling.

4. *Analysis and modeling*: the radiomic signs obtained, depending on the question posed, can be analyzed in various ways, ranging from statistical models to machine learning methods.

Given the large amount of data extracted from the images, step 1 is selection or reduction of signs. Irreproducible signs should be excluded, since they most probably lead to false results of the models constructed [42, 43].

Step 2 is multivariate data analysis [31] and the construction of models classified into three main groups: predictive, explanatory, and descriptive [15]. Descriptive models are used to obtain a broad representation of each sign, summarizing its key characteristics. Thus, explanatory methods often used for biomedical data frequently focus on the ability of the model to establish a relationship between a sign and an outcome, such as the relationship between the texture characteristics of the gray-level co-incidence matrix and the morphological type of BC within the region of interest. Further, machine learning methods are used to create predictive models, which analyze the probability of certain outcomes based on the input data obtained [15], such as a radiomic model for predicting the lack of response to neoadjuvant BC chemotherapy. Before using the models in clinical settings, the quality and reproducibility of the results of operation obtained should be assessed [31].

EXPERIENCE, POSSIBILITIES, AND PROSPECTS FOR USING MAMMOGRAPHY IN RADIOMICS AND RADIOGENOMICS OF BREAST CANCER

Recognition of a malignant neoplasm

The most difficult and crucial step in mammography is classifying mammogram findings as benign or malignant [44]. In their recent study, N. Mao et al. [45] demonstrated that using quantitative signs in conjunction with AI can provide greater diagnostic efficiency when using mammography compared to the efficiency of diagnostics performed by experienced radiologists [15].

The process of classifying microcalcifications as benign or malignant based on images is still a difficult task for radiologists [46]. When suspicious calcifications are detected,

texture analysis of images can be performed in conjunction with AI methods, potentially reducing the number of unnecessary biopsies [47, 48].

Specific features of the mammary gland parenchyma may reflect biological risk factors for BC. H. Li et al. [49] showed that using textural signs extracted from mammograms of the affected and contralateral (with normal parenchyma) glands improves the accuracy of digital mammography in the diagnosis of BC. Studies reveal that radiomics with high sensitivity and specificity can distinguish between malignant and benign mammary gland neoplasms [50].

Definition of BC subtypes

Recent radiogenomics studies have confirmed the relationship between MR signs of BC imaging and molecular subtypes, namely, luminal A, luminal B, HER2, and TNBC [51]. Although mammography images provide less information than magnetic resonance imaging (MRI), several studies are currently underway to demonstrate the potential of mammography in radiomics and radiogenomics of BC. In their study, W. Ma et al. [10] demonstrated the possibility of predicting the molecular subtype of BC by extracting radiomic characteristics from mammographic images. The most significant signs were roundness, concavity, mean gray value, and correlation. The results revealed that luminal subtypes and TNBC have distinct textural signs, in contrast to other subtypes, which allow them to be quantitatively distinguished using radiomics.

In some BC patients, the use of neoadjuvant chemotherapy does not provide an effective therapeutic response, resulting in delayed surgery, poor prognosis, and increase in treatment costs. Moreover, the use of radiomics in conjunction with independent clinical risk factors (e.g., Ki-67 index, HER2 status) has been shown to improve the predictive model of nonresponse to neoadjuvant chemotherapy [52].

Early detection of a more aggressive subtype of BC, namely, TNBC, using medical imaging will allow clinicians to prescribe treatment prior to definitive biopsy confirmation [53]. In a study by H.X. Zhang et al. [53], TNBC had greater roundness and concavity compared to other subtypes; the area under the ROC curve (receiver operating characteristic curve; classic ROC curve, a graph of sensitivity versus specificity [54]) was used to assess the accuracy of these two signs in differentiating TNBC from other BC subtypes and was greater than 0.70 [53, 55]. In this study, the skewness coefficient (a histogram attribute reflecting the skewness of the distribution of values relative to the mean) of all subtypes was less than 0 (negative or left-sided skewness). Further, the asymmetry coefficient of TNBC was found to be lower than the coefficients of the other subtypes under study. Therefore, the above radiomic signs can be considered as potential markers of differences between TNBC and other subtypes of BC in the future [53].

Predicting the development of BC and the possibility of personalized screening

Radiomics-based technologies can help advance personalized screening by developing tools for individual risk assessment and including them in decision-making support tools for mammographic screening, as well as individual screening intervals [56–58]. A higher density of mammary glands has been linked to an increased risk of BC development [59]. The term "density" refers to the degree of attenuation of X-ray radiation as it passes through the gland and reflects the distribution of fibroglandular tissue. However, the definition of density alone does not represent the entire complexity of the gland structure. Image-derived textural signs have been proposed as markers of changes in the parenchyma, indicating a link to the development of BC [57, 59]. In their study, D. Kontos et al. [59] (2019) identified radiomic phenotypes on mammograms that reflect the complexity of the parenchyma (in addition to density) and are independently associated with BC. In contrast to the conventional definition of density, textural signs indicated a subtler and more localized complexity of the parenchymal pattern. The density of the mammary glands differed between the phenotypes of low and medium complexity of the parenchyma but was similar for the other phenotypes. There are interesting data on the phenotype with the least complexity (parenchyma complexity) in women with high mammary gland density due to their greater homogeneity, whereas the phenotype with low and medium parenchyma complexity included a small number of high-density images [59].

Preoperative detection of axillary lymph node metastases

BC metastases are most commonly found in the axillary lymph nodes. Axillary lymph node status is an important factor in determining overall and relapse-free survival in BC patients [60]. An accurate preoperative determination of the status of the axillary lymph nodes can provide doctors with information that allows them to decide whether or not to perform lymphadenectomy and prescribe adjuvant therapy. Currently, the status is determined by biopsy of the sentinel lymph node, which can lead to complications, such as damage to blood vessels and nerves, as well as the development of lymphedema; and diagnostics using imaging methods has a low sensitivity [60]. J. Yang et al. [60] developed a model that includes radiomic signs extracted from mammograms, which can be used as a noninvasive method for determining metastases in the axillary lymph nodes prior to surgery when combined with additional clinical and pathological information.

LIMITATIONS ON THE APPLICATION OF RADIOMICS

Although radiomics and radiogenomics hold great promise for the advancement of personalized medicine, they must be validated on an independent dataset to confirm their diagnostic and predictive value. It will take time for these technologies to gain significant practical value in cancer research and even more time before they can be applied in clinical practice. These limitations are due to the fact that the available large amounts of data do not currently contain the full characteristics of patients [6]. The complexity of the reproducibility of radiomics results is associated with disadvantages at each stage, namely, different textural signs are obtained on different equipment and visualization protocols [61, 62]; the gold standard for manual tumor segmentation is time-consuming and operator-dependent [63]; semiautomatic and automatic segmentations, which reduce variability [64, 65], are not standardized; there is obvious repeatability between texture signs, necessitating the reduction of the size of the data [66, 67]; and there is no clear explanation of the relationship between the unit of radiomics (the basic unit of the texture) and human tissues. Furthermore, any "meaningful" research results obtained should be reviewed when the underlying theory is unclear and technical methods are not standardized [68].

PROSPECTS FOR USING MAGNETIC RESONANCE IMAGING IN BREAST CANCER RADIOMICS

Convincing evidence have been accumulated that MRI of the mammary glands is superior in diagnostic accuracy to traditional diagnostic methods such as mammography [69]. Aside from detecting more cases of duct carcinoma in situ, MRI of the mammary glands often changes the stage of the oncological process, which helps to optimize the treatment process.

It has been established that radiomic signs extracted from MR images of mammary glands indicate tumor heterogeneity and vascularization [70], as well as enable to differentiate duct carcinoma from a benign focus [71]. Existing radiomic models continue to lag behind expert mammologists in terms of area under the curve for differentiating benign from malignant lesions [72]. However, promising results in identifying suspicious (BI-RADS 4 and 5) lesions using diffusion-weighted imaging radiomics have been obtained [73].

Radiomics appears to be capable of assisting in clinical decision-making while avoiding potentially invasive interventions in the armpit. Two different studies have shown that the radiomic model can predict sentinel lymph node metastases [74, 75], which is extremely important in clinical practice.

Another application of radiomics is associated with the Ki-67 proliferation index, which is used as a prognostic marker in BC [72]. Recent studies have investigated the possibility of predicting the expression of the Ki-67 proliferation marker using radiomics of a series of dynamic contrast enhancements [76–79].

CONCLUSION

One of the key concepts in radiomics is that ray diagnostic images contain data that can provide more information about the region of interest than previously believed. Mammography is the most effective method for early detection of BC. Mammographic images can be used for radiomic analysis, which can be used to identify malignant neoplasms, BC subtypes, disease progression, and response to treatment.

Radiomics-based technologies, such as in the field of mammography, may be incorporated into medical decision-making support tools in the future to determine strategies for individual screening, follow-up, and possibly preventive therapy. However, it should be noted that radiomics is still in its early stages of development, with much more research needed before clinical application.

Radiomics mammography provides important diagnostic and prognostic information about BC, which has the potential to reduce the need for invasive and often complicated procedures. Although radiomics-based techniques will not replace biopsy in the near future, pending support with new research, the integration of radiomics and radiogenomics into clinical practice will be one of the most important and promising tasks in achieving the goal of reducing BC mortality.

ADDITIONAL INFORMATION

REFERENCES

1. Kaprin AD, Starinsky VV, Petrova GV. Malignant neoplasms in Russia in 2018 (morbidity and mortality). Moscow : P.A. Herzen Moscow State Research Institute; 2019. 250 p. (In Russ).

2. Kaprin AD, Starinsky VV. The state of oncological care for the population of Russia in 2019. Moscow : P.A. Herzen Moscow State Research Institute; 2020. 239 p. (In Russ).

3. Grishina KA, Muzaffarova TA, Khailenko VA, Karpukhin AV. Molecular genetic markers of breast cancer. *Tumors of the female reproductive system*. 2016;12(3):36–42. (In Russ). doi: 10.17650/1994-4098-2016-12-3-36-42

4. Wu M, Ma J. Association between imaging characteristics and different molecular subtypes of breast cancer. *Acad Radiol*. 2017;24(4):426–434. doi: 10.1016/j.acra.2016.11.012

5. Stenina MB, Zhukova LG, Koroleva IA, et al. Practical recommendations for the drug treatment of breast cancer. *Malig tumours*. 2021;10(3). (In Russ).

6. Pesapane F, Suter MB, Rotili A, et al. Will traditional biopsy be substituted by radiomics and liquid biopsy for breast cancer diagnosis and characterisation? *Med Oncol*. 2020;37(4):29. doi: 10.1007/s12032-020-01353-1

7. Januškevičienė I, Petrikaitė V. Heterogeneity of breast cancer: the importance of interaction between different tumor cell populations. *Life Sci*. 2019;(239):117009. doi: 10.1016/j.lfs.2019.117009

8. Turashvili G, Brogi E. Tumor heterogeneity in breast cancer. *Front Med*. 2017;4:227. doi: 10.3389/fmed.2017.00227

9. Zavyalova MV, Vtorushin SV, Tsyganov MM. Intra-tumor heterogeneity: nature and biological significance. Review. *Biochemistry*. 2013;78(11):1531–1549. (In Russ).

10. Ma W, Zhao Y, Ji Y, et al. Breast cancer molecular subtype prediction by mammographic radiomic features. *Acad Radiol*. 2019;26(2):196–201. doi: 10.1016/j.acra.2018.01.023

11. Aerts HJ, Velazquez ER, Leijenaar RT, et al. Decoding tumour phenotype by noninvasive imaging using a quantitative radiomics approach. *Nat Commun*. 2014;5:4006. doi: 10.1038/ncomms5006

12. Lin F, Wang Z, Zhang K, et al. Contrast-Enhanced spectral mammography-based radiomics nomogram for identifying benign and malignant breast lesions of Sub-1 cm. *Front Oncol*. 2020;10:573630. doi: 10.3389/fonc.2020.573630

13. Li X, Qin G, He Q, et al. Digital breast tomosynthesis versus digital mammography: integration of image modalities enhances deep learning-based breast mass classification. *Eur Radiol*. 2020;30(2):778–788. doi: 10.1007/s00330-019-06457-5

14. Nazari SS, Mukherjee P. An overview of mammographic density and its association with breast cancer. *Breast Cancer*. 2018;25(3):259–267. doi: 10.1007/s12282-018-0857-5

15. Conti A, Duggento A, Indovina I, et al. Radiomics in breast cancer classification and prediction. *Semin Cancer Biol*. 2021;72:238–250. doi: 10.1016/j.semcancer.2020.04.002

16. Hogg P, Kelly J, Mercer C. Digital mammography: A holistic approach. Springer; 2015. 309 p.

17. Demircioglu O, Uluer M, Aribal E. How many of the biopsy decisions taken at inexperienced breast radiology units were correct? *J Breast Heal*. 2017;13(1):23–26. doi: 10.5152/tjbh.2016.2962

18. Valdora F, Houssami N, Rossi F, et al. Rapid review: radiomics and breast cancer. *Breast Cancer Res Treat*. 2018;169(2):217–229. doi: 10.1007/s10549-018-4675-4

19. Mayerhoefer ME, Materka A, Langset G, et al. Intro-duction to radiomics. *J Nucl Med.* 2020;61(4):488–495. doi: 10.2967/jnumed.118.222893

20. Lambin P, Zindler J, Vanneste BG, et al. Decision support systems for personalized and participative radiation oncology. *Adv Drug Deliv Rev.* 2017;109:131–153. doi: 10.1016/j.addr.2016.01.006

21. Wen YL, Leech M. Review of the role of radiomics in tumour risk classification and prognosis of cancer. *Anticancer Research.* 2020;40(7):3605–3618. doi: 10.21873/anticanres.14350

22. Gillies RJ, Kinahan PE, Hricak H. Radiomics: Images are more than pictures, they are data. *Radiology.* 2016;278(2):563–577. doi: 10.1148/radiol.2015151169

23. Lambin P, Leijenaar RT, Deist TM, et al. Radiomics: The bridge between medical imaging and personalized medicine. *Nat Rev Clin Oncol.* 2017;14(12):749–762. doi: 10.1038/nrclinonc.2017.141

24. Vailati-Riboni M, Palombo V, Loor JJ. What are omics sciences? Periparturient diseases of dairy cows: a systems biology approach. 2017. P. 1–7. doi: 10.1007/978-3-319-43033-1_1

25. Porcu M, Solinas C, Mannelli L, et al. Radiomics and "radi-omics" in cancer immunotherapy: a guide for clinicians. *Crit Rev Oncol Hematol.* 2020;154:103068. doi: 10.1016/j.critrevonc.2020.103068

26. Ognerubov NA, Shatov IA, Shatov AV. Radiogenomics and radiomics in the diagnostics of malignant tumours: a literary review. *Tambov Univ Reports Ser Nat Tech Sci.* 2017;22(6-2):1453–1460. doi: 10.20310/1810-0198-2017-22-6-1453-1460

27. Nasief H, Hall W, Zhenget C, et al. Improving treatment response prediction for chemoradiation therapy of pancreatic cancer using a combination of delta-radiomics and the clinical biomarker CA19-9. *Front Oncol.* 2020;9:1464. doi: 10.3389/fonc.2019.01464

28. Lambin P, Rios-Velazquez E, Leijenaar R, et al. Radiomics: Extracting more information from medical images using advanced feature analysis. *Eur J Cancer.* 2012;48(4):441–446. doi: 10.1016/j.ejca.2011.11.036

29. Kerns SL, Ostrer H, Rosenstein BS. Radiogenomics: Using genetics to identify cancer patients at risk for development of adverse effects following radiotherapy. *Cancer Discovery.* 2014;4(2):155–165. doi: 10.1158/2159-8290

30. Neri E, Del Re M, Paiar F, et al. Radiomics and liquid biopsy in oncology: the holons of systems medicine. *Insights Imaging.* 2018;9(6):915–924. doi: 10.1007/s13244-018-0657-7

31. Rizzo S, Botta F, Raimondi S, et al. Radiomics: the facts and the challenges of image analysis. *Eur Radiol Exp.* 2018;2(1):36. doi: 10.1186/s41747-018-0068-z

32. Kumar V, Gu Y, Basu S, et al. Radiomics: The process and the challenges. *Magn Reson Imaging.* 2012;30(9):1234–1248. doi: 10.1016/j.mri.2012.06.010

33. Sala E, Mema E, Himoto Y, et al. Unravelling tumour heterogeneity using next-generation imaging: radiomics, radiogenomics, and habitat imaging. *Clinical Radiology.* 2017;72(1):3–10. doi: 10.1016/j.crad.2016.09.013

34. Lee SH, Park H, Ko ES. Radiomics in breast imaging from techniques to clinical applications: A review. *Korean J Radiol.* 2020;21(7):779–792. doi: 10.3348/kjr.2019.0855

35. Tagliafico AS, Piana M, Schenone D, et al. Overview of radiomics in breast cancer diagnosis and prognostication. *Breast.* 2020;(49):74–80. doi: 10.1016/j.breast.2019.10.018

36. Li H, Giger ML, Huo Z, et al. Computerized analysis of mammographic parenchymal patterns for assessing breast cancer risk:

Effect of ROI size and location. *Med Phys.* 2004;31(3):549–555. doi: 10.1118/1.1644514

37. Holbrook MD, Blocker SJ, Mowery YM, et al. Mri-based deep learning segmentation and radiomics of sarcoma in mice. *Tomography.* 2020;6(1):23–33. doi: 10.18383/j.tom.2019.00021

38. Pratt W. Digital Image Processing. Moscow : World; 1982. 480 p.

39. Santos JM, Oliveira BC, de Araujo-Filho J, et al. State-of-the-art in radiomics of hepatocellular carcinoma: a review of basic principles, applications, and limitations. *Abdom Radiol.* 2020;45(2):342–353. doi: 10.1007/s00261-019-02299-3

40. Avanzo M, Stancanello J, El Naqa I. Beyond imaging: The promise of radiomics. *Phys Medica.* 2017;(38):122–139. doi: 10.1016/j.ejmp.2017.05.071

41. Verma M, Raman B, Murala S. Local extrema co-occurrence pattern for color and texture image retrieval. *Neurocomputing.* 2015;165:255–269. doi: 10.1016/j.neucom.2015.03.015

42. Tunali I, Hall LO, Napel S, et al. Stability and reproducibility of computed tomography radiomic features extracted from peritumoral regions of lung cancer lesions. *Med Phys.* 2019;46(11):5075–5085. doi: 10.1002/mp.13808

43. Nasief H, Zheng C, Schott D, et al. A machine learning based delta-radiomics process for early prediction of treatment response of pancreatic cancer. *NPJ Precis Oncol.* 2019;3(1):25. doi: 10.1038/s41698-019-0096-z

44. Cui Y, Li Y, Xing D, et al. Improving the prediction of benign or malignant breast masses using a combination of image biomarkers and clinical parameters. *Front Oncol.* 2021;11:629321. doi: 10.3389/fonc.2021.629321

45. Mao N, Yin P, Wang Q, et al. Added value of radiomics on mammography for breast cancer diagnosis: a feasibility study. *J Am Coll Radiol.* 2019;16(4 Pt A):485–491. doi: 10.1016/j.jacr.2018.09.041

46. Fanizzi A, TM, Losurdo L, et al. A machine learning approach on multiscale texture analysis for breast microcalcification diagnosis. *BMC Bioinformatics.* 2020;21(Suppl 2):91. doi: 10.1186/s12859-020-3358-4

47. Stelzer PD, Steding O, Raudner MW, et al. Combined texture analysis and machine learning in suspicious calcifications detected by mammography: Potential to avoid unnecessary stereotactical biopsies. *Eur J Radiol.* 2020;132:109309. doi: 10.1016/j.ejrad.2020.109309

48. Karahaliou A, Skiadopoulos S, Boniatis I, et al. Texture analysis of tissue surrounding microcalcifications on mammograms for breast cancer diagnosis. *Br J Radiol.* 2007;80(956):648–656. doi: 10.1259/bjr/30415751

49. Li H, Mendel KR, Lan L, et al. Digital mammography in breast cancer: Additive value of radiomics of breast parenchyma. Radiology. 2019;291(1):15–20. doi: 10.1148/radiol.2019181113

50. Parekh VS, Jacobs MA. MPRAD: A multiparametric radiomics framework. *arXiv.* 2018.

51. Rozhkova NI, Bozhenko VK, Burdina II, et al. Radiogenomics of breast cancer as new vector of interdisciplinary integration of radiation and molecular biological technologies (literature review). *Med Alph.* 2020;(20):21–29. doi: 10.33667/2078-5631-2020-20-21-29

52. Wang Z, Lin F, Ma H, et al. Contrast-Enhanced spectral mammography-based radiomics nomogram for the prediction of neo-adjuvant chemotherapy-insensitive breast cancers. *Front Oncol.* 2021;11:605230. doi: 10.3389/fonc.2021.605230

53. Zhang HX, Sun ZQ, Cheng YG, et al. A pilot study of radiomics technology based on X-ray mammography in patients with triple-

negative breast cancer. *J Xray Sci Technol*. 2019;27(3):485–492. doi: 10.3233/XST-180488

54. Morozov SP, Vladzimirsky AV, Klyashtornyy VG, et al. Clinical acceptance of software based on artificial intelligence technologies (Radiology). Moscow: Research and Practical Clinical Center for Diagnostics and Telemedicine Technologies; 2019. 45 p.

55. Mandrekar JN. Receiver operating characteristic curve in diagnostic test assessment. *J Thorac Oncol*. 2010;5(9):1315–1316. doi: 10.1097/JTO.0b013e3181ec173d

56. Rahbar H, McDonald ES, Lee JM, et al. How can advanced imaging be used to mitigate potential breast cancer overdiagnosis? *Academic Radiology*. 2016;23(6):768–773. doi: 10.1016/j.acra.2016.02.008

57. Pinker K. Beyond breast density: Radiomic phenotypes enhance assessment of breast cancer risk. *Radiology*. 2019;290(1):50–51. doi: 10.1148/radiol.2018182296

58. Sun W, Tseng TL, Qian W, et al. Using multiscale texture and density features for near-term breast cancer risk analysis. *Med Phys*. 2015;42(6):2853–2862. doi: 10.1118/1.4919772

59. Kontos D, Winham SJ, Oustimov A, et al. Radiomic phenotypes of mammographic parenchymal complexity: Toward augmenting breast density in breast cancer risk assessment. *Radiology*. 2019;290(1):41–49. doi: 10.1148/radiol.2018180179

60. Yang J, Wang T, Yang L, et al. Preoperative prediction of axillary lymph node metastasis in breast cancer using mammography-based radiomics method. *Sci Rep*. 2019;9(1):4429. doi: 10.1038/s41598-019-40831-z

61. Zhao B, Tan Y, Tsai WY, et al. Reproducibility of radiomics for deciphering tumor phenotype with imaging. *Sci Rep*. 2016;6:23428. doi: 10.1038/srep23428

62. Lu L, Ehmke RC, Schwartz LH, Zhao B. et al. Assessing agreement between radiomic features computed for multiple CT imaging settings. *PLoS One*. 2016;11(12):e0166550. doi: 10.1371/journal.pone.0166550

63. Velazquez ER, Parmar C, Jermoumi M, et al. Volumetric CT-based segmentation of NSCLC using 3D-Slicer. *Sci Rep*. 2013;3:3529. doi: 10.1038/srep03529

64. Qiu Q, Duan J, Gong G, et al. Reproducibility of radiomic features with GrowCut and GraphCut semiautomatic tumor segmentation in hepatocellular carcinoma. *Transl Cancer Res*. 2017;6(5). doi: 10.21037/tcr.2017.09.47

65. Qiu Q, Duan J, Duan Z, et al. Reproducibility and non-redundancy of radiomic features extracted from arterial phase CT scans in hepatocellular carcinoma patients: Impact of tumor segmentation variability. *Quant Imaging Med Surg*. 2019;9(3):453–464. doi: 10.21037/qims.2019.03.02

66. Hunter LA, Krafft S, Stingo F, et al. High quality machine-robust image features: Identification in nonsmall cell lung cancer computed tomography images. *Med Phys*. 2013;40(12):121916. doi: 10.1118/1.4829514

67. O'Connor JP, Aboagye EO, Adams JE, et al. Imaging biomarker roadmap for cancer studies. *Nat Rev Clin Oncol*. 2017;14(3):169–186. doi: 10.1038/nrclinonc.2016.162

68. Chalkidou A, O'Doherty M, Marsden PK. False discovery rates in PET and CT studies with texture features: a systematic review. *PLoS One*. 2015;10(5):e0124165. doi: 10.1371/journal.pone.0124165

69. Mann RM, Kuhl CK, Moy L. Contrast-enhanced MRI for breast cancer screening. *J Magn Reson Imaging*. 2019;50(2):377–390. doi: 10.1002/jmri.26654

70. Parekh VS, Jacobs MA. Integrated radiomic framework for breast cancer and tumor biology using advanced machine learning and multiparametric MRI. *NPJ Breast Cancer*. 2017;3:43. doi: 10.1038/s41523-017-0045-3

71. Whitney HM, Taylor NS, Drukker K, et al. Additive benefit of radiomics over size alone in the distinction between benign lesions and luminal a cancers on a large clinical breast MRI dataset. *Acad Radiol*. 2019;26(2):202–209. doi: 10.1016/j.acra.2018.04.019

72. Crivelli P, Ledda RE, Parascandolo N, et al. A new challenge for radiologists: radiomics in breast cancer. *BioMed Research International*. 2018;2018:6120703. doi: 10.1155/2018/6120703

73. Bickelhaupt S, Paech D, Kickingereder P, et al. Prediction of malignancy by a radiomic signature from contrast agent-free diffusion MRI in suspicious breast lesions found on screening mammography. *J Magn Reson Imaging*. 2017;46(2):604–616. doi: 10.1002/jmri.25606

74. Han L, Zhu Y, Liu Z, et al. Radiomic nomogram for prediction of axillary lymph node metastasis in breast cancer. *Eur Radiol*. 2019;29(7):3820–3829. doi: 10.1007/s00330-018-5981-2

75. Dong Y, Feng Q, Yang W, et al. Preoperative prediction of sentinel lymph node metastasis in breast cancer based on radiomics of T2-weighted fat-suppression and diffusion-weighted MRI. *Eur Radiol*. 2018;28(2):582–591. doi: 10.1007/s00330-017-5005-7

76. Ma W, Ji Y, Qi L, et al. Breast cancer Ki67 expression prediction by DCE-MRI radiomics features. *Clin Radiol*. 2018;73(10):909.e1–909.e5. doi: 10.1016/j.crad.2018.05.027

77. Jagadish K, Sheela GM, Naidu BP, et al. Big data analytics and radiomics to discover diagnostics and therapeutics for gastric cancer. In: Recent Advancements in Biomarkers and Early Detection of Gastrointestinal Cancers. 2020. P. 213–219. doi: 10.1007/978-981-15-4431-6_12

78. Scheckenbach K. Radiomics: Big data instead of biopsies in the future? *Laryngorhinootologie*. 2018;97(S 01):S114–S141. doi: 10.1055/s-0043-121964

79. European Society of Radiology (ESR). Medical imaging in personalised medicine: a white paper of the research committee of the European Society of Radiology (ESR). *Insights Imaging*. 2015;6(2):141–155. doi: 10.1007/s13244-015-0394-0

СПИСОК ЛИТЕРАТУРЫ

1. Каприн, А.Д., Старинский, В.В., Петрова Г.В. Злокачественные новообразования в России в 2018 году (заболеваемость и смертность). Москва: МНИОИ им. П.А. Герцена, 2019. 250 с.

2. Каприн А.Д., Старинский В.В. Состояние онкологической помощи населению России в 2019 году. Москва: МНИОИ им. П.А. Герцена, 2020. 239 с.

3. Гришина К.А., Музаффарова Т.А., Хайленко В.А., Карпухин А.В. Молекулярно-генетические маркеры рака молочной железы // Опухоли женской репродуктивной системы. 2016. Vol. 12, N 3. P. 36–42. doi: 10.17650/1994-4098-2016-12-3-36-42

4. Wu M., Ma J. Association between imaging characteristics and different molecular subtypes of breast can-

cer // Acad Radiol. 2017. Vol. 24, N 4. P. 426–434. doi: 10.1016/j.acra.2016.11.012

5. Стенина М.Б., Жукова Л.Г., Королева И.А., и соавт. Практические рекомендации по лекарственному лечению рака молочной железы // Malig tumours. 2021. Vol. 10. N 3.

6. Pesapane F., Suter M.B., Rotili A., et al. Will traditional biopsy be substituted by radiomics and liquid biopsy for breast cancer diagnosis and characterisation? // Med Oncol. 2020. Vol. 37, N 4. P. 29. doi: 10.1007/s12032-020-01353-1

7. Januškevičienė I., Petrikaitė V. Heterogeneity of breast cancer: The importance of interaction between different tumor cell populations // Life Sci. 2019. Vol. 239. P. 117009. doi: 10.1016/j.lfs.2019.117009

8. Turashvili G., Brogi E. Tumor heterogeneity in breast cancer // Front Med. 2017. Vol. 4. P. 227. doi: 10.3389/fmed.2017.00227

9. Завьялова М.В., Вторушин С.В., Цыганов М.М. Внутриопухолевая гетерогенность : природа и биологическое значение. Обзор // Биохимия. 2013. Т. 78, № 11. С. 1531–1549.

10. Ma W., Zhao Y., Ji Y., et al. Breast cancer molecular subtype prediction by mammographic radiomic features // Acad Radiol. 2019. Vol. 26, N 2. P. 196–201. doi: 10.1016/j.acra.2018.01.023

11. Aerts H.J., Velazquez E.R., Leijenaar R.T., et al. Decoding tumour phenotype by noninvasive imaging using a quantitative radiomics approach // Nat Commun. 2014. Vol. 5. P. 4006. doi: 10.1038/ncomms5006

12. Lin F., Wang Z., Zhang K., et al. Contrast-Enhanced spectral mammography-based radiomics nomogram for identifying benign and malignant breast lesions of Sub-1 cm // Front Oncol. 2020. Vol. 10. P. 573630. doi: 10.3389/fonc.2020.573630

13. Li X., Qin G., He Q., et al. Digital breast tomosynthesis versus digital mammography: integration of image modalities enhances deep learning-based breast mass classification // Eur Radiol. 2020. Vol. 30, N 2. P. 778–788. doi: 10.1007/s00330-019-06457-5

14. Nazari S.S., Mukherjee P. An overview of mammographic density and its association with breast cancer // Breast Cancer. 2018. Vol. 25, N 3. P. 259–267. doi: 10.1007/s12282-018-0857-5

15. Conti A., Duggento A., Indovina I., et al. Radiomics in breast cancer classification and prediction // Semin Cancer Biol. 2021. Vol. 72. P. 238–250.

16. Hogg P., Kelly J., Mercer C. Digital mammography: A holistic approach // Springer. 2015. 309 p.

17. Demircioglu O., Uluer M., Aribal E. How many of the biopsy decisions taken at inexperienced breast radiology units were correct? // J Breast Heal. 2017. Vol. 13, N 1. P. 23–26. doi: 10.5152/tjbh.2016.2962

18. Valdora F., Houssami N., Rossi F., et al. Rapid review: radiomics and breast cancer // Breast Cancer Res Treat. 2018. Vol. 169, N 2. P. 217–229. doi: 10.1007/s10549-018-4675-4

19. Mayerhoefer M.E., Materka A., Langset G., et al. Introduction to radiomics // J Nucl Med. 2020. Vol. 61, N 4. P. 488–495. doi: 10.2967/jnumed.118.222893

20. Lambin P., Zindler J., Vanneste B.G., et al. Decision support systems for personalized and participative radiation oncology // Adv Drug Deliv Rev. 2017. Vol. 109. P. 131–153. doi: 10.1016/j.addr.2016.01.006

21. Wen Y.L., Leech M. Review of the role of radiomics in tumour risk classification and prognosis of cancer // Anticancer Research. 2020. Vol. 40, N 7. P. 3605–3618. doi: 10.21873/anticanres.14350

22. Gillies R.J., Kinahan P.E., Hricak H. Radiomics: Images are more than pictures, they are data // Radiology. 2016. Vol. 278, N 2. P. 563–577. doi: 10.1148/radiol.2015151169

23. Lambin P., Leijenaar R.T., Deist T.M., et al. Radiomics: The bridge between medical imaging and personalized medicine // Nat Rev Clin Oncol. 2017. Vol. 14, N 12. P. 749–762. doi: 10.1038/nrclinonc.2017.141

24. Vailati-Riboni M., Palombo V., Loor J.J. What are omics sciences? // Periparturient Diseases of Dairy Cows: A Systems Biology Approach. 2017. P. 1–7. doi: 10.1007/978-3-319-43033-1_1

25. Porcu M., Solinas C., Mannelli L., et al. Radiomics and "radi-omics" in cancer immunotherapy: a guide for clinicians // Crit Rev Oncol Hematol. 2020. Vol. 154. P. 103068. doi: 10.1016/j.critrevonc.2020.103068

26. Ognerubov N.A., Shatov I.A., Shatov A.V. Radiogenomics and radiomics in the diagnostics of malignant tumours: a literary review // Tambov Univ Reports Ser Nat Tech Sci. 2017. Vol. 22, N 6-2. P. 1453–1460. doi: 10.20310/1810-0198-2017-22-6-1453-1460

27. Nasief H., Hall W, Zhenget C, al. Improving treatment response prediction for chemoradiation therapy of pancreatic cancer using a combination of delta-radiomics and the clinical biomarker CA19-9 // Front Oncol. 2020. Vol. 9. P. 1464. doi: 10.3389/fonc.2019.01464

28. Lambin P., Rios-Velazquez E., Leijenaar R., et al. Radiomics: Extracting more information from medical images using advanced feature analysis // Eur J Cancer. 2012. Vol. 48, N 4. P. 441–446. doi: 10.1016/j.ejca.2011.11.036

29. Kerns S.L., Ostrer H., Rosenstein B.S. Radiogenomics: Using genetics to identify cancer patients at risk for development of adverse effects following radiotherapy // Cancer Discovery. 2014. Vol. 4, N 2. P. 155–165. doi: 10.1158/2159-8290

30. Neri E., Del Re M., Paiar F., et al. Radiomics and liquid biopsy in oncology: the holons of systems medicine // Insights Imaging. 2018. Vol. 9, N 6. P. 915–924. doi: 10.1007/s13244-018-0657-7

31. Rizzo S., Botta F., Raimondi S., et al. Radiomics: the facts and the challenges of image analysis // Eur Radiol Exp. 2018. Vol. 2, N 1. P. 36. doi: 10.1186/s41747-018-0068-z

32. Kumar V., Gu Y., Basu S., et al. Radiomics: The process and the challenges // Magn Reson Imaging. 2012. Vol. 30, N 9. P. 1234–1248. doi: 10.1016/j.mri.2012.06.010

33. Sala E., Mema E., Himoto Y., et al. Unravelling tumour heterogeneity using next-generation imaging: radiomics, radiogenomics, and habitat imaging // Clinical Radiology. 2017. Vol. 72, N 1. P. 3–10. doi: 10.1016/j.crad.2016.09.013

34. Lee S.H., Park H., Ko E.S. Radiomics in breast imaging from techniques to clinical applications: A review // Korean J Radiol. 2020. Vol. 21, N 7. P. 779–792. doi: 10.3348/kjr.2019.0855

35. Tagliafico A.S., Piana M., Schenone D., et al. Overview of radiomics in breast cancer diagnosis and prognostication // Breast. 2020. Vol. 49. P. 74–80. doi: 10.1016/j.breast.2019.10.018

36. Li H., Giger M.L., Huo Z., et al. Computerized analysis of mammographic parenchymal patterns for assessing breast cancer risk: effect of ROI size and location // Med Phys. 2004. Vol. 31, N 3. P. 549–555. doi: 10.1118/1.1644514

37. Holbrook M.D., Blocker S.J., Mowery Y.M., et al. Mri-based deep learning segmentation and radiomics of sarcoma in mice // Tomography. 2020. Vol. 6, N 1. P. 23–33. doi: 10.18383/j.tom.2019.00021

38. Прэтт У. Цифровая обработка изображений. Москва : Мир, 1982. 480 с.

39. Santos J.M., Oliveira B.C., de Araujo-Filho J., et al. State-of-the-art in radiomics of hepatocellular carcinoma: a review of basic principles, applications, and limitations // Abdom Radiol. 2020. Vol. 45, N 2. P. 342–353. doi: 10.1007/s00261-019-02299-3

40. Avanzo M., Stancanello J., El Naqa I. Beyond imaging: the promise of radiomics // Phys Medica. 2017. Vol. 38. P. 122–139. doi: 10.1016/j.ejmp.2017.05.071

41. Verma M., Raman B., Murala S. Local extrema co-occurrence pattern for color and texture image retrieval // Neurocomputing. 2015. Vol. 165. P. 255–269. doi: 10.1016/j.neucom.2015.03.015

42. Tunali I., Hall L.O., Napel S., et al. Stability and reproducibility of computed tomography radiomic features extracted from peritumoral regions of lung cancer lesions // Med Phys. 2019. Vol. 46, N 11. P. 5075–5085. doi: 10.1002/mp.13808

43. Nasief H., Zheng C., Schott D., et al. A machine learning based delta-radiomics process for early prediction of treatment response of pancreatic cancer // NPJ Precis Oncol. 2019. Vol. 3, N 1. P. 25. doi: 10.1038/s41698-019-0096-z

44. Cui Y., Li Y., Xing D., et al. Improving the prediction of benign or malignant breast masses using a combination of image biomarkers and clinical parameters // Front Oncol. 2021. Vol. 11. P. 629321. doi: 10.3389/fonc.2021.629321

45. Mao N., Yin P., Wang Q., et al. Added value of radiomics on mammography for breast cancer diagnosis: a feasibility study // J Am Coll Radiol. 2019. Vol. 16, N 4, Pt A. P. 485–491. doi: 10.1016/j.jacr.2018.09.041

46. Fanizzi A., Basile T.M., Losurdo L., et al. A machine learning approach on multiscale texture analysis for breast microcalcification diagnosis // BMC Bioinformatics. 2020. Vol. 21, Suppl 2. P. 91. doi: 10.1186/s12859-020-3358-4

47. Stelzer P.D., Steding O., Raudner M.W., et al. Combined texture analysis and machine learning in suspicious calcifications detected by mammography: Potential to avoid unnecessary stereotactical biopsies // Eur J Radiol. 2020. Vol. 132. P. 109309. doi: 10.1016/j.ejrad.2020.109309

48. Karahaliou A., Skiadopoulos S., Boniatis I., et al. Texture analysis of tissue surrounding microcalcifications on mammograms for breast cancer diagnosis // Br J Radiol. 2007. Vol. 80, N 956. P. 648–656. doi: 10.1259/bjr/30415751

49. Li H., Mendel K.R., Lan L., et al. Digital mammography in breast cancer: Additive value of radiomics of breast parenchyma // Radiology. 2019. Vol. 291, N 1. P. 15–20. doi: 10.1148/radiol.2019181113

50. Parekh V.S., Jacobs M.A. MPRAD: A multiparametric radiomics framework // arXiv. 2018.

51. Rozhkova N.I., Bozhenko V.K., Burdina I.I., et al. Radiogenomics of breast cancer as new vector of interdisciplinary integration of radiation and molecular biological technologies (literature review) // Med Alph. 2020. N 20. P. 21–29. doi: 10.33667/2078-5631-2020-20-21-29

52. Wang Z., Lin F., Ma H., et al. Contrast-Enhanced spectral mammography-based radiomics nomogram for the prediction of neoadjuvant chemotherapy-insensitive breast cancers // Front Oncol. 2021. Vol. 11. P. 605230. doi: 10.3389/fonc.2021.605230

53. Zhang H.X., Sun Z.Q., Cheng Y.G., et al. A pilot study of radiomics technology based on X-ray mammography in patients with triple-negative breast cancer // J Xray Sci Technol. 2019. Vol. 27, N 3. P. 485–492. doi: 10.3233/XST-180488

54. Morozov S.P., Vladzimirsky A.V., Klyashtornyy V.G., et al. Clinical acceptance of software based on artificial intelligence technologies (Radiology). Moscow: Research and Practical Clinical Center for Diagnostics and Telemedicine Technologies; 2019. 45 p.

55. Mandrekar J.N. Receiver operating characteristic curve in diagnostic test assessment // J Thorac Oncol. 2010. Vol. 5, N 9. P. 1315–1316. doi: 10.1097/JTO.0b013e3181ec173d

56. Rahbar H., McDonald E.S., Lee J.M., et al. How can advanced imaging be used to mitigate potential breast cancer overdiagnosis? // Academic Radiology. 2016. Vol. 23, N 6. P. 768–773. doi: 10.1016/j.acra.2016.02.008

57. Pinker K. Beyond breast density: Radiomic phenotypes enhance assessment of breast cancer risk // Radiology. 2019. Vol. 290, N 1. P. 50–51. doi: 10.1148/radiol.2018182296

58. Sun W., Tseng T.L., Qian W., et al. Using multiscale texture and density features for near-term breast cancer risk analysis // Med Phys. 2015. Vol. 42, N 6. P. 2853–2862. doi: 10.1118/1.4919772

59. Kontos D., Winham S.J., Oustimov A., et al. Radiomic phenotypes of mammographic parenchymal complexity: Toward augmenting breast density in breast cancer risk assessment // Radiology. 2019. Vol. 290, N 1. P. 41–49. doi: 10.1148/radiol.2018180179

60. Yang J., Wang T., Yang L., et al. Preoperative prediction of axillary lymph node metastasis in breast cancer using mammography-based radiomics method // Sci Rep. 2019. Vol. 9, N 1. P. 4429. doi: 10.1038/s41598-019-40831-z

61. Zhao B., Tan Y., Tsai W.Y., et al. Reproducibility of radiomics for deciphering tumor phenotype with imaging // Sci Rep. 2016. Vol. 6. P. 23428. doi: 10.1038/srep23428

62. Lu L., Ehmke R.C., Schwartz L.H., Zhao B. Assessing agreement between radiomic features computed for multiple CT imaging settings // PLoS One. 2016. Vol. 11, N 12. P. e0166550. doi: 10.1371/journal.pone.0166550

63. Velazquez E.R., Parmar C., Jermoumi M., et al. Volumetric CT-based segmentation of NSCLC using 3D-Slicer // Sci Rep. 2013. Vol. 3. P. 3529. doi: 10.1038/srep03529

64. Qiu Q., Duan J., Gong G., et al. Reproducibility of radiomic features with GrowCut and GraphCut semiautomatic tumor segmentation in hepatocellular carcinoma // Transl Cancer Res. 2017. Vol. 6, N 5. doi: 10.21037/tcr.2017.09.47

65. Qiu Q., Duan J., Duan Z., et al. Reproducibility and non-redundancy of radiomic features extracted from arterial phase CT scans in hepatocellular carcinoma patients: Impact of tumor segmentation variability // Quant Imaging Med Surg. 2019. Vol. 9, N 3. P. 453–464. doi: 10.21037/qims.2019.03.02

66. Hunter L.A., Krafft S., Stingo F., et al. High quality machine-robust image features: Identification in nonsmall cell lung cancer computed tomography images // Med Phys. 2013. Vol. 40, N 12. P. 121916. doi: 10.1118/1.4829514

67. O'Connor J.P., Aboagye E.O., Adams J.E., et al. Imaging biomarker roadmap for cancer studies // Nat Rev Clin Oncol. 2017. Vol. 14, N 3. P. 169–186. doi: 10.1038/nrclinonc.2016.162

68. Chalkidou A., O'Doherty M.J., Marsden P.K. False discovery rates in PET and CT studies with texture features: A systematic review // PLoS One. 2015. Vol. 10, N 5. P. e0124165. doi: 10.1371/journal.pone.0124165

69. Mann R.M., Kuhl C.K., Moy L. Contrast-enhanced MRI for breast cancer screening // J Magn Reson Imaging. 2019. Vol. 50, N 2. P. 377–390. doi: 10.1002/jmri.26654

70. Parekh V.S., Jacobs M.A. Integrated radiomic framework for breast cancer and tumor biology using advanced machine learning and multiparametric MRI // NPJ Breast Cancer. 2017. Vol. 3. P. 43. doi: 10.1038/s41523-017-0045-3

71. Whitney H.M., Taylor N.S., Drukker K., et al. Additive benefit of radiomics over size alone in the distinction between benign lesions and luminal a cancers on a large clinical breast MRI dataset // Acad Radiol. 2019. Vol. 26, N 2. P. 202–209. doi: 10.1016/j.acra.2018.04.019

72. Crivelli P., Ledda R.E., Parascandolo N., et al. A new challenge for radiologists: radiomics in breast cancer // BioMed Research International. 2018. Vol. 2018. P. 6120703. doi: 10.1155/2018/6120703

73. Bickelhaupt S., Paech D., Kickingereder P., et al. Prediction of malignancy by a radiomic signature from contrast agent-free diffusion MRI in suspicious breast lesions found on screening mammography // J Magn Reson Imaging. 2017. Vol. 46, N 2. P. 604–616. doi: 10.1002/jmri.25606

74. Han L., Zhu Y., Liu Z., et al. Radiomic nomogram for prediction of axillary lymph node metastasis in breast cancer // Eur Radiol. 2019. Vol. 29, N 7. P. 3820–3829. doi: 10.1007/s00330-018-5981-2

75. Dong Y., Feng Q., Yang W., et al. Preoperative prediction of sentinel lymph node metastasis in breast cancer based on radiomics of T2-weighted fat-suppression and diffusion-weighted MRI // Eur Radiol. 2018. Vol. 28, N 2. P. 582–591. doi: 10.1007/s00330-017-5005-7

76. Ma W., Ji Y., Qi L., et al. Breast cancer Ki67 expression prediction by DCE-MRI radiomics features // Clin Radiol. 2018. Vol. 73, N 10. P. 909.e1–909.e5. doi: 10.1016/j.crad.2018.05.027

77. Jagadish K., Sheela G.M., Naidu B.P., et al. Big data analytics and radiomics to discover diagnostics and therapeutics for gastric cancer // Recent Advancements in Biomarkers and Early Detection of Gastrointestinal Cancers. 2020. P. 213–219. doi: 10.1007/978-981-15-4431-6_12

78. Scheckenbach K. Radiomics: Big data instead of biopsies in the future? // Laryngorhinootologie. 2018. Vol. 97, S 01. P. S114–S141. doi: 10.1055/s-0043-121964

79. European Society of Radiology (ESR). Medical imaging in personalised medicine: a white paper of the research committee of the European Society of Radiology (ESR) // Insights Imaging. 2015. Vol. 6, N 2. P. 141–155. doi: 10.1007/s13244-015-0394-0

AUTHORS' INFO

* Serafim S. Semenov, MD;
address: 24-1 Petrovka street, 127051 Moscow, Russia;
ORCID: https://orcid.org/0000-0003-2585-0864;
eLibrary SPIN: 4790-0416; e-mail: s.semenov@npcmr.ru

Veronika G. Govorukhina, MD;
e-mail: govorukhinaver@gmail.com;
ORCID: https://orcid.org/0000-0002-1611-9618;
eLibrary SPIN: 7038-8580

Pavel B. Gelezhe, MD, Cand. Sci. (Med.);
e-mail: gelezhe.pavel@gmail.com;
ORCID: https://orcid.org/0000-0003-1072-2202;
eLibrary SPIN: 4841-3234

Vera V. Didenko, MD;
e-mail: didenko@npcmr.ru;
ORCID: https://orcid.org/0000-0001-9068-1273;
eLibrary SPIN: 5033-8376

Sergey P. Morozov, MD, Dr. Sci. (Med.), Professor;
e-mail: morozov@npcmr.ru;
ORCID: https://orcid.org/0000-0001-6545-6170;
eLibrary SPIN: 8542-1720

Anna E. Andreychenko, Cand. Sci. (Phys.-Math.);
e-mail: a.andreychenko@npcmr.ru;
ORCID: https://orcid.org/0000-0001-6359-0763;
eLibrary SPIN: 6625-4186

ОБ АВТОРАХ

* Семенов Серафим Сергеевич;
адрес: Россия, 127051, Москва, ул. Петровка, д. 24, стр. 1;
ORCID: https://orcid.org/0000-0003-2585-0864;
eLibrary SPIN: 4790-0416; e-mail: s.semenov@npcmr.ru

Говорухина Вероника Георгиевна;
e-mail: govorukhinaver@gmail.com;
ORCID: https://orcid.org/0000-0002-1611-9618;
eLibrary SPIN: 7038-8580

Гележе Павел Борисович, к.м.н.;
e-mail: gelezhe.pavel@gmail.com;
ORCID: https://orcid.org/0000-0003-1072-2202;
eLibrary SPIN: 4841-3234

Диденко Вера Владимировна;
e-mail: didenko@npcmr.ru;
ORCID: https://orcid.org/0000-0001-9068-1273;
eLibrary SPIN: 5033-8376

Морозов Сергей Павлович, д.м.н., профессор;
e-mail: morozov@npcmr.ru;
ORCID: https://orcid.org/0000-0001-6545-6170;
eLibrary SPIN: 8542-1720

Андрейченко Анна Евгеньевна, к.физ.-мат.н.;
e-mail: a.andreychenko@npcmr.ru;
ORCID: https://orcid.org/0000-0001-6359-0763;
eLibrary SPIN: 6625-4186

* Corresponding author / Автор, ответственный за переписку

Кавернозные мальформации головного мозга и современные взгляды на их лечение

Е.Н. Гиря[1], В.Е. Синицын[2], А.С. Токарев[1, 3]

[1] Научно-исследовательский институт скорой помощи имени Н.В. Склифосовского, Москва, Российская Федерация
[2] Московский государственный университет имени М.В. Ломоносова, Москва, Российская Федерация
[3] Департамент здравоохранения города Москвы, Москва, Российская Федерация

АННОТАЦИЯ

Кавернозные мальформации головного мозга благодаря развитию современных методов нейровизуализации являются в последние годы всё чаще обнаруживаемой патологией. Несмотря на доброкачественный характер течения в большинстве случаев, данные образования могут приводить к развитию судорожного синдрома и серьёзным неврологическим нарушениям. Как правило, причинами клинических симптомов являются кровоизлияния в структуру каверном и окружающую паренхиму головного мозга. Выбор тактики ведения пациентов с кавернозными мальформациями головного мозга зависит от типа мальформации, её размеров, локализации, наличия повторных кровоизлияний и клинической картины.

Данный обзор литературы посвящён современным методам лечения кавернозных мальформаций головного мозга, в частности хирургическим подходам. В случаях глубинного расположения очагов в функционально значимых зонах головного мозга, для которых характерен максимальный риск осложнений при хирургическом вмешательстве, альтернативными выступают методы лучевой терапии, такие как стереотаксическая радиохирургия, протонная терапия. Рассматриваются возможности, эффективность и безопасность стереотаксического радиохирургического лечения, использование протонной терапии в лечении кавернозных мальформаций. Выявлены преимущества лучевых методов лечения кавернозных мальформаций.

Ключевые слова: кавернозные мальформации; лучевая диагностика; МРТ; обзор; аппарат Гамма-нож; протонная терапия; радиохирургическое лечение; стереотаксическая лазерная абляция.

Cavernous malformations of the brain and modern views on their treatment

Elena N. Girya[1], Valentin E. Sinitsyn[2], Aleksei S. Tokarev[1, 3]

[1] Sklifosovsky Research Institute for Emergency Medicine, Moscow, Russian Federation
[2] Lomonosov Moscow State University, Moscow, Russian Federation
[3] Moscow Health Department, Moscow, Russian Federation

ABSTRACT

Cavernous malformations of the brain have become an increasingly common pathology in recent years, thanks to the advancement of modern methods of neuroimaging. Despite the benign nature of the course in most cases, these formations can cause convulsions and serious neurological disorders. Typically, clinical manifestations are caused by hemorrhages in the structure of the cavernous and surrounding parenchyma of the brain. The management strategy chosen for patients with cerebral cavernous malformations is determined by the type of malformation, its size, localization, the presence of repeated hemorrhages, and the clinical picture.

This literature review focuses on modern methods of treating cerebral cavernous malformations. The main methods of treatment for cavernous malformations of the brain, particularly surgical treatment, have been analyzed. If surgical intervention is not possible, alternative methods of treatment include radiation therapy, such as stereotaxic radiosurgery, and proton therapy, in cases of deep location of foci in functionally significant areas of the brain, which are characterized by the highest risk of complications. The possibilities, efficacy, and safety of stereotactic radiosurgical treatment are discussed, as well as the use of proton therapy in the treatment of cavernous malformations. Furthermore, radiation therapy has been shown to be beneficial for cavernous malformations.

Keywords: cavernous malformations; radiation diagnostics; MRI; review; Gamma knife; proton therapy; radiosurgical treatment; stereotaxic laser ablation.

大脑海绵状畸形及其治疗的现代观点

Elena N. Girya[1], Valentin E. Sinitsyn[2], Aleksei S. Tokarev[1, 3]

[1] Sklifosovsky Research Institute for Emergency Medicine, Moscow, Russian Federation
[2] Lomonosov Moscow State University, Moscow, Russian Federation
[3] Moscow Health Department, Moscow, Russian Federation

简评

由于现代神经影像学方法的发展，近年来大脑海绵状畸形已成为越来越可检测的病理。尽管在大多数情况下病程的性质是良性的，但这些形成可导致惊厥综合征和严重神经系统疾病的发展。基本上临床症状的原因是洞穴结构和大脑周围实质的出血。大脑海绵状畸形患者的管理策略的选择取决于畸形的类型，其大小，定位，反复出血的存在和临床情况。

这篇文献综述致力于海绵体畸形的现代治疗方法。我们分析治疗脑海绵状畸形的主要方法，特别是手术治疗。无法手术干预的时候，在大脑功能显着区域的病灶深度定位的情况下，其特征在于并发症的最大风险，放射治疗的替代方法是如立体定向放射外。同时审查立体定向放射外科治疗的可能性，有效性和安全性，使用质子治疗治疗海绵体畸形。揭示了治疗海绵体畸形的辐射方法的优点。

关键词：海绵体畸形；放射诊断；MRI；综述；伽玛刀装置；质子治疗；放射外科治疗；立体定向激光消融。

INTRODUCTION

Cavernous malformations (CM) are vascular lesions of the brain and spinal cord with less blood supply and consist of caverns with an endothelial lining [1–4]. CMs are detected both in the supra- and infratentorial regions of the brain and less often in the spinal cord [5–8].

These lesions are the second most common vascular malformations of the central nervous system after developmental venous anomalies [9–11].

The prevalence of CM in men and women is comparable. Although CM can also be found in children, the diagnosis is usually established at age 20–40 years. In most cases, CM may not manifest clinically; however, over time, it can cause serious focal and cerebral neurological symptoms because of CM rupture and hemorrhage into the structure of the lesions and the surrounding brain tissues [12].

Although several studies have reported that the levels of risks of hemorrhages and seizures in this patient population have been established to date, a clear identification of modifiable risk factors is a significant challenge. Management of patients with CM includes monitoring or performing surgery [13, 14].

SURGICAL TREATMENT OF BRAIN CM

Microsurgical resection remains the "gold" standard of CM treatment, which can permanently relieve the patient of the concomitant manifestations of CM and the risks of developing neurological deficits associated with hemorrhages. Assessment of the risk of surgical intervention depends on the size and location of the lesion, proximity to the brain surface, and experience of the surgeon [15]. Surgical treatment is aimed at total removal of the CM and surrounding potential epileptogenic zones [16]. However, if these lesions are located close to vital structures (distance of <1 cm), complete resection can lead to postoperative neurological damage. In CMs localized in brain areas such as the thalamus, basal ganglia, or brainstem, surgery is usually performed only with frequent recurrent hemorrhages or with a significant deterioration in the patient's condition.

Several authors note that the relatively low incidence of complications of surgical treatment exceeds the risk of hemorrhage in patients without previous diagnosis. Thus, surgical removal of asymptomatic foci, especially in cases of deep localization or localization in the brainstem, is unreasonable.

Foci that are deeply located in the basal ganglia or thalamus require a technically complex surgery, in which critical structures of the brain, including the nuclei and tracts of the white matter, can be affected; there is a risk of damage to the perforating arteries. Postoperative complications of this surgical intervention, even among experienced specialists, occur in 5%–18% of cases, and lethal outcomes occur in approximately 2% [17].

Despite the progress and improvement of surgical techniques, many patients still do not qualify for surgery or have received incomplete treatment, so CM remains untreated. As treatment for this patient population, stereotactic irradiation, such as radiosurgery and stereotactic radiation therapy, is gaining increasing significance.

POSSIBILITIES, EFFICIENCY, AND SAFETY OF RADIOSURGICAL TREATMENT OF BRAIN CM

Numerous studies have focused on the use of radiation therapy for arteriovenous malformations and dural arteriovenous fistulas [18–20]. Some studies have also demonstrated the possibility of applying this method to treat CM. Radiation therapy is mainly indicated for CM up to 3 cm in diameter and located in deep brain areas, such as those with the highest risk of complications. At present, stereotactic radiosurgical treatment is one of the main radiation therapy methods used to treat CM. Several uncontrolled studies have reported that the risk of recurrent hemorrhage after radiosurgery is reduced in patients after 2 years.

Lee et al. examined the efficacy and safety of radiosurgical treatment using the Gamma Knife in patients with brain CM [21] by analyzing the results of treatment of 261 patients with 331 symptomatic CM (average age, 39.9 years; average CM volume, 3.1 ml). The average radiation dose throughout the treatment period was 11.9 Gy. Patients were followed up for 69 months. Several patients were diagnosed with CM after an initial hemorrhage. In total, 136 hemorrhages were diagnosed before treatment.

Researchers concluded that radiosurgical treatment reduced the risk of hemorrhage in patients with CM; therefore, this method is considered an effective alternative treatment for patients with difficult surgical access or with severe concomitant diseases.

Kefeli et al. attempted to evaluate the results of treatment of brainstem CM using the Gamma Knife [22]. Their study included 82 patients with 1–3 hemorrhagic events confirmed by X-ray imaging before treatment. After the treatment, the average target volume was 0.3 ml, and the maximum radiation dose was 12 Gy. The average follow-up durations were 25.5 months before surgery and 50.3 months after surgery. The annual pretreatment hemorrhage rate was 8.6%. In the post-treatment follow-up, only three patients experienced recurrence of hemorrhage; thus, the frequency of recurrent hemorrhage within 1 year after treatment was 0.87%, i.e., the risk of such complications was significantly reduced with this therapeutic approach.

The magnitude of hemorrhage risk in CM has not been clearly defined so far. During the natural course of CM, the annual risk of hemorrhage ranges from 2.3% to 4.1%, while in surgical treatment, the risk ranges from 2.7% to 6.8%

[23, 24]. However, the risk of recurrent hemorrhage in CM increases after the initial hemorrhage, reaching 40% [25].

Wen et al. performed a meta-analysis to assess the clinical efficacy of radiosurgical treatment of CM using the Gamma Knife and revealed no significant differences in the frequency of hemorrhages between the first 2 years of the postoperative period and the subsequent 2 years (RR 2.81; 95% confidence interval 0.20–13.42) [26].

Recent studies have established an annual decrease in the frequency of hemorrhage from 39.5% to 7.2% during the first 2 years after CM treatment using the Gamma Knife and from 3.6% to 1% in subsequent years [22, 27, 28].

Kondziolka et al. studied the frequency of hemorrhages by monitoring CM and revealed that the annual frequency of hemorrhage was 5.9% before radiosurgery and 1.1% at 2 years after surgery [29]. Aboukais et al. demonstrated a decrease in this indicator from 3.16% to 2.46% [30]. Moreover, Lopez-Serrano et al. reported annual hemorrhage rates of 3.06% and 1.4% before and after radiosurgical treatment [31].

Some authors believe that the efficiency of using the Gamma Knife is apparent 2–3 years after radiosurgical treatment, which is due to a decrease in the CM volume over time caused by sclerosis and vascular thrombobliteration after irradiation [31, 32]. However, whether the decrease in the frequency of hemorrhages is associated with radiosurgical interventions or is a consequence of the natural course of CM is under discussion [21].

The assumption was that the mechanisms of radiosurgical treatment of vascular malformations are based on processes such as the proliferation of endothelial cells and hyalinization, which causes the closure of the vessel lumen. Gewirtz et al. and Nyáry et al. performed histological examinations of CM tissues in patients undergoing radiosurgical treatment, which revealed signs of fibrinoid necrosis, destruction of endothelial cells, and pronounced fibrosis in the connective tissue stroma [33, 34].

Park et al. analyzed long-term results of radiosurgical treatment of symptomatic brainstem CM using the Gamma Knife in 45 patients (14 men, 31 women) [27]. The follow-up duration was more than 5 years, with an average of 9.31 (range, 5.1–19.4) years. All patients had a history of one or more episodes of symptomatic hemorrhage before radiosurgical treatment. These hemorrhages were accompanied by manifestations of neurological deficit, including cranial nerve dysfunction, hemiparesis, hemisensory deficiency, spasticity, and chorea. The average target CM volume was 1.82 cm^3, and the median radiation dose limit was 13 Gy. Finally, the authors concluded that radiosurgical treatment with Gamma Knife is safe and clinically effective for treating CM, which reduced the recurrence rate of hemorrhage.

Until 2019, three major studies were conducted on the use of the Gamma Knife (with >100 cases and at least 4 years of follow-up) in the treatment of recurrent hemorrhagic or symptomatic CMs [35–37]. These studies enrolled a total of 530 patients. Kida showed that the annual incidence of hemorrhages after using the Gamma Knife decreased from 9.5% within 1 year to 4.7% within 2 years [37]. In other studies, the annual hemorrhage rate after treatment decreased from 15% within 2 years to 2.4% after 2 years [35].

Some researchers consider gender, severity of neurological manifestations before the intervention, CM size, degree of edema of the surrounding tissues, and radiation dose as factors that influence the frequency of hemorrhages in patients undergoing radiosurgical treatment [36]. Moreover, Kim et al. did not reveal significant differences in the frequency of hemorrhages depending on the CM volume, radiation dose, gender, and patient age at the time of treatment with the use of Gamma Knife [38].

A common complication for most patients with CM is epileptic seizures, and a correlation between the development of hemorrhages and seizures is suggested. Patients with CM often experience concomitant headaches or dizziness with hemorrhages [37]. Experimental studies have revealed that the deposition of blood clot metabolites, especially iron, can be a similar epileptogenic factor. Studies using magnetic resonance imaging (MRI) have confirmed the relationship between the development of seizures and hemorrhages in time in these patients. Another risk factor for the occurrence of seizures is the localization of the CM, primarily supratentorial, archicortical, and mesiotemporal. In comparison with MRI data, Menzler et al. demonstrated that 49 of 81 patients with CM with involvement of the cerebral cortex had seizures, while none of the 17 patients with exclusively subcortical localization of CM had seizures [39].

Considering the complications of radiosurgical treatment of CM, the risk of radiation-induced brain damage with the emergence of neurological disorders, including headache, dizziness, facial nerve palsy, facial paresthesia, diplopia, dysarthria, and asthenia in the extremities, should be noted [30]. Another serious side effect is radiation necrosis, which can promote tumor development [40].

Some researchers express concern about the ability of radiation exposure to induce the formation of new CMs, especially in children and individuals with familial illness [41].

The optimal radiation dose limit during radiosurgical treatment of brainstem CM is not clearly defined; however, Lee et al. and Kim et al. believed that the dose limit of 11 Gy is sufficient to reduce the risk of radiation complications [21, 38]. The use of a level dose is effective, while a decrease in the risk of hemorrhage to 2.4% was recorded 2 years after Gamma Knife application, including improvement in neurological status, and the rate of radiation-induced complications was 2.32%.

In general, the therapeutic dose of radiation concerning radiotoxicity in radiosurgical treatment of CM in the brainstem is 11–13 Gy [42].
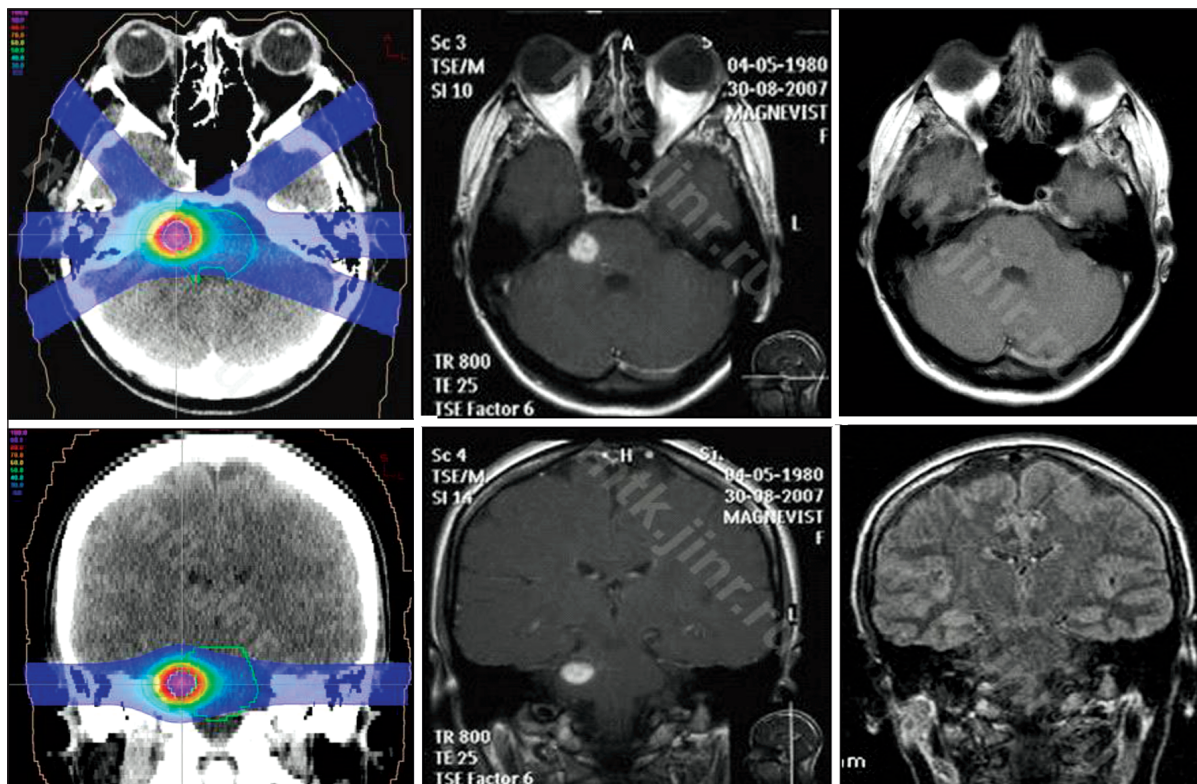
Fig. 1. Plan for proton radiosurgery of a periostemal cavernoma: contrast-enhanced magnetic resonance imaging before treatment and after 3 months showing complete resorption of the cavernoma.

Following current recommendations for radiosurgery, this approach should be considered in treating single CM in patients with a history of hemorrhage in brain areas where the surgical risk of tissue damage is unacceptably high [43]. The expert opinion is that these methods are not recommended in cases where the CM is available for surgical treatment, in asymptomatic cases, and in familial forms of the pathology.

Stereotactic laser ablation of these lesions is also considered a potentially promising method for treating CM with epileptoid manifestations [44].

Thus, radiosurgical treatment of brain CM is a relatively safe approach; as with its use, some complications, such as vascular ruptures and damage to the brain tissue, are not registered. This method implies a single provision of the entire radiation dose, which is required to obtain the desired result and is sufficiently safe for the surrounding brain matter. This approach is characterized by the highest efficiency in the treatment of CM. In some cases, the desired radiation doses cannot be used safely because of the CM size (volume), while a decrease in the dose leads to a decrease in the exposure efficiency [45].

According to Lee et al., in the past, the efficiency of radiosurgical treatment of CM was limited by insufficient capabilities of neuroimaging methods, high doses of radiation (>15 Gy), and incomplete or excessive coverage of the target area [21]. Advances in neuroimaging (such as MRI), optimization of radiation doses, and planning of

interventions using appropriate software have reduced significantly the risk of complications of radiosurgery.

PROTON THERAPY IN THE TREATMENT OF CM

Proton therapy is an even more advanced method of radiation therapy when surgical removal is impossible or the patient refuses to undergo surgery. CM proton therapy, similar to stereotactic radiosurgical treatment, obliterates lesion structures and thereby reduces the risk of subsequent hemorrhages. As an advantage, proton therapy allows sufficient and accurate irradiation of the tumor (accuracy of approximately 0.5 mm) with minimal damage to healthy tissues and a decrease in the risk of side effects [46].

The treatment effect is observed within 5–90 months after application. Complete obliteration of the neoplasm is achieved in 70% of cases. The plan of proton radiosurgery of the cavernoma in the peristem is presented in Fig. 1 [47].

CONCLUSION

CMs are vascular neoplasms of the brain, which mechanism of development is based on vascular proliferation, dysmorphism, and hemorrhagic angiopathy. Clinical symptoms are caused by recurrent hemorrhages in the structure of cavernous angiomas with subsequent

deposition of iron in surrounding brain tissues, which can result in the emergence of epileptogenesis foci, especially when the cavernomas are localized in the mesiotemporal and archicortical regions of the brain. Improvement of diagnostics and treatment methods is a multidisciplinary issue. The treatment method depends on the type, size, and location of the malformation and history of hemorrhages. Since the risk of complications of surgical intervention is high in some patients with CM and patients with a familial form of CM, improvement of alternative surgical treatment methods is extremely important. Stereotactic radiation therapy is currently increasingly used in the treatment of CMs.

REFERENCES

1. Mukha AM, Dashyan VG, Krylov VV. Cavernous malformations of the brain. *Neurological Journal.* 2013;18(5):46–51. (In Russ).
2. Popov VE, Livshits MI, Bashlachev MG, Nalivkin AE. Cavernous malformations in children: a literature review. *Almanac of Clinical Medicine.* 2018;46(2):146–159. (In Russ). doi: 10.18786/2072-0505-2018-46-2-146-159
3. Caton MT, Shenoy VS. Cerebral Cavernous Malformations. Treasure Island (FL): StatPearls Publishing; 2019. doi: 10.20959/wjpr202011-18275
4. Flemming KD, Brown RD Jr. Epidemiology and natural history of intracranial vascular malformations. In: H.R. Winn, ed. Youmans and Winn neurological surgery, 7th ed. Amsterdam: Elsevier; 2017.
5. Gotko AV, Kivelev JV, Sleep AS. Cavernous malformations of the brain and spinal cord. *Ukrainian neurosurgical Journal.* 2013;(3):10–15. (In Russ).
6. Rodich A, Smeyanovich A, Sidorovich R, et al. Modern approaches to the surgical treatment of cavernous angiomas of the brain. *Science and Innovation.* 2018;10(188):70–73. (In Russ).
7. Gross BA, Du R. Natural history of cerebral arteriovenous malformations: a meta-analysis. *J. Neurosurg.* 2013;118(2):437–443. doi: 10.3171/2012.10.JNS121280
8. Kearns KN, Chen CJ, Tvrdik P, et al. Outcomes of surgery for brainstem cavernous malformations: a systematic review. *Stroke.* 2019;50(10):2964–2966. doi: 10.1161/STROKEAHA.119.026120
9. Sazonov IA, Belousova OB. Cavernous malformation, which caused the development of extensive acute subdural hematoma. Case study and literature review. *Questions of neurosurgery named after N.N. Burdenko.* 2019;3(3):73–76. (In Russ). doi: 10.17116/neiro20198303173
10. Mouchtouris N, Chalouhi N, Chitale A, et al. Management of cerebral cavernous malformations: from diagnosis to treatment. *Scientific World Journal.* 2015;2015:808314. doi: 10.1155/2015/808314
11. Negoto T, Terachi S, Baba Y, et al. Symptomatic brainstem cavernoma of elderly patients: timing and strategy of surgical treatment. Two case reports and review of the literature. *World Neurosurg.* 2018;111:227–234. doi: 10.1016/j.wneu.2017.12.111

12. Batra S, Lin D, Recinos PF, et al. Cavernous malformations: natural history, diagnosis and treatment. *Nature Reviews Neurology.* 2009;5(12):659–670. doi: 10.1038/nrneurol.2009.177
13. Al-Shahi Salman R, White PM, Counsell CE, et al. Outcome after conservative management or intervention for unruptured brain arteriovenous malformations. *JAMA.* 2014;311(16):1661–1669. doi: 10.1001/jama.2014.3200
14. Hakim AA, Gralla J, Rozeik C, et al. Anomalies and normal variants of the cerebral arterial supply: A comprehensive pictorial review with a proposed workflow for classification and significance. *J Neuroimaging.* 2018;28(1):14–35. doi: 10.1111/jon.12475
15. Polkovnikov AY. Arteriovenous malformations of the cerebral hemispheres with a small and medium-sized nucleus, features of clinical manifestations and methods of surgical treatment. *Current Issues of Pharmaceutical and Medical Science and Practice.* 2013;2(12):033–038. (In Russ).
16. Chang EF, Wang DD, Barkovich A, et al. Predictors of seizure freedom after surgery for malformations of cortical development. *Ann Neurol.* 2011;70(1):151–162. doi: 10.1002/ana.22399
17. Pasqualin A, Meneghelli P, Giammarusti A, Turazzi S. Results of surgery for cavernomas in critical supratentorial areas. *Acta Neurochir Suppl.* 2014;119:117–123. doi: 10.1007/978-3-319-02411-0_20
18. Maryashev SA. Stereotactic irradiation of arteriovenous malformations of the brain [dissertation abstract]. Moscow; 2016. 26 p. (In Russ).
19. Shimizu K, Kosaka N, Yamamoto T, et al. Arterial spin labeling perfusion-weighted MRI for long-term follow-up of a cerebral arteriovenous malformation after stereotactic radiosurgery. *Acta Radiol Short Rep.* 2014;3(1). doi: 10.1177/2047981613510160
20. Seo Y, Kim DG, Dho YS, et al. A retrospective analysis of the outcomes of dural arteriovenous fistulas treated with gamma knife radiosurgery: a single-institution experience. *Stereotactic Functional Neurosurgery.* 2018;96(1):46–53. doi: 10.1159/000486685
21. Lee CC, Wang WH, Yang HC, et al. Gamma Knife radiosurgery for cerebral cavernous malformation. *Sci Rep.* 2019;9(1):19743. doi: 10.1038/s41598-019-56119-1
22. Kefeli AU, Sengoz M, Peker S. Gamma knife radiosurgery for hemorrhagic brainstem cavernomas. *Turk Neurosurg.* 2018;29(1):14–19. doi: 10.5137/1019-5149.JTN.21690-17.1

23. Cantu C, Murillo-Bonilla L, Arauz A, et al. Predictive factors for intracerebral hemorrhage in patients with cavernous angiomas. *Neurol Res.* 2005;27(3):314–318. doi: 10.1179/016164105X39914

24. Wang CC, Liu A, Zhang J, et al. Surgical management of brainstem cavernous malformations: report of 137 cases. *Surg Neurol.* 2003;59(6):444–454. doi: 10.1016/s0090-3019(03)00187-3

25. Abla AA, Turner JD, Mitha AP, et al. Surgical approaches to brainstem cavernous malformations. *Neurosurgical Focus.* 2010;29(3):E8. doi: 10.3171/2010.6.FOCUS10128

26. Wen R, Shi Y, Gao Y, et al. The efficacy of gamma knife radiosurgery for cavernous malformations: a meta-analysis and review. *World Neurosurgery.* 2019;123:371–377. doi: 10.1016/j.wneu.2018.12.046

27. Park SH, Hwang SK. Gamma knife radiosurgery for symptomatic brainstem intra-axial cavernous malformations. *World Neurosurgery.* 2013;80(6):261–266. doi: 10.1016/j.wneu.2012.09.013

28. Frischer JM, Gatterbauer B, Holzer S, et al. Microsurgery and radiosurgery for brainstem cavernomas: effective and complementary treatment options. *World Neurosurgery.* 2014;81(3-4):520–528 doi: 10.1016/j.wneu.2014.01.004

29. Kondziolka D, Lunsford LD, Flickinger JC, Kestle JR. Reduction of hemorrhage risk after stereotactic radiosurgery for cavernous malformations. *J Neurosurg.* 1995;83(5):825–831. doi: 10.3171/jns.1995.83.5.0825

30. Aboukais R, Estrade L, Devos P, et al. Gamma knife radiosurgery of brainstem cavernous malformations. *Stereotact Funct Neurosurg.* 2016;94(6):397–403. doi: 10.1159/000452844

31. Lopez-Serrano R, Martinez NE, Kusak ME, et al. Significant hemorrhage rate reduction after gamma knife radiosurgery in symptomatic cavernous malformations: long-term outcome in 95 case series and literature review. *Stereotact Funct Neurosurg.* 2017;95(6):369–378. doi: 10.1159/000480664

32. Shin SS, Murdoch G, Hamilton RL, et al. Pathological response of cavernous malformations following radiosurgery. *J Neurosurg.* 2015;123(4):938–944. doi: 10.3171/2014.10.jns14499

33. Gewirtz RJ, Steinberg GK, Crowley R, Levy RP. Pathological changes in surgically resected angiographically occult vascular malformations after radiation. *Neurosurgery.* 1998;42(4):738–741. doi: 10.1097/00006123-199804000-00031

34. Nyary I, Major O, Hanzely Z, Szeifert GT. Histopathological findings in a surgically resected thalamic cavernous hemangioma 1 year afer 40-gy irradiation. *J Neurosurg.* 2005;102(Suppl):56–58. doi: 10.3171/sup.2005.102.s_supplement.0056

35. Monaco EA, Khan AA, Niranjan A, et al. Stereotactic radiosurgery for the treatment of symptomatic brainstem cavern-

ous malformations. *Neurosurgical Focus.* 2010;29(3):E11. doi: 10.3171/2010.7.FOCUS10151

36. Tian KB, Zheng JJ, Ma JP, et al. Clinical course of untreated thalamic cavernous malformations: hemorrhage risk and neurological outcomes. *J Neurosurg.* 2017;127(3):480–491. doi: 10.3171/2016.8.JNS16934

37. Kida Y. Radiosurgery for cavernous malformations in basal ganglia, thalamus and brainstem. *Prog Neurol Surg.* 2009;22:31–37. doi: 10.1159/000163380

38. Kim BS, Yeon JY, Kim JS, et al. Gamma Knife radiosurgery of the symptomatic brain stem cavernous angioma with low marginal dose. *Clin Neurol Neurosurg.* 2014;126:110-114. doi: 10.1016/j.clineuro.2014.08.028

39. Menzler K. Epileptogenicity of cavernomas depends on (archi-) cortical localization. *Neurosurgery.* 2010;67:918–924. doi: 10.1227/NEU.0b013e3181eb5032

40. Liao C, Visocchi M, Zhang W, et al. Management of cerebral radiation necrosis: a retrospective study of 12 patients. *Acta Neurochir Suppl.* 2017;124:195–201. doi: 10.1007/978-3-319-39546-3_30

41. Akers A, Salman RA, Awad I, et al. Synopsis of guidelines for the clinical management of cerebral cavernous malformations: consensus recommendations based on systematic literature review by the angioma alliance scientific advisory board clinical experts panel. *Neurosurgery.* 2017;80(5):665–680. doi: 10.1093/neuros/nyx091

42. Garcia RM, Ivan ME, Lawton MT. Brainstem cavernous malformations: surgical results in 104 patients and a proposed grading system to predict neurological outcomes. *Neurosurgery.* 2015;76(3):265–277. doi: 10.1227/NEU.0000000000000602

43. Krylov VV, Dashyan VG, Shetova IM, et al. Neurosurgical care for patients with cerebral vascular diseases in the Russian Federation. *Neurosurgery.* 2017;(4):11–20. (In Russ).

44. Willie JT, Malcolm JG, Stern MA, et al. Safety and effectiveness of stereotactic laser ablation for epileptogenic cerebral cavernous malformations. *Epilepsia.* 2019;60(2):220–232. doi: 10.1111/epi.14634

45. Amponsah K, Ellis TL, Chan MD, et al. Retrospective analysis of imaging techniques for treatment planning and monitoring of obliteration for gamma knife treatment of cerebral arteriovenous malformation. *Neurosurgery.* 2012;71(4):893–899. doi: 10.1227/neu.0b013e3182672a83

46. Chen CC, Chapman P, Petit J, et al. Proton radiosurgery in neurosurgery. *Neurosurg Focus.* 2007;23(6):E5. doi: 10.3171/FOC-07/12/E5

47. Medical and Technical Complex: Joint Institute for Nuclear Research. Cavernous angiomas (cavernomas) [Internet]. Available from: http://mtk.jinr.ru/index.php?option=com_content&task=view&id=33&Itemid=53

СПИСОК ЛИТЕРАТУРЫ

1. Муха А.М., Дашьян В.Г., Крылов В.В. Кавернозные мальформации головного мозга // Неврологический журнал. 2013. Т. 18, № 5. С. 46–51.

2. Попов В.Е., Лившиц М.И., Башлачев М.Г., Наливкин А.Е. Кавернозные мальформации у детей: обзор литературы // Альманах клинической медицины. 2018. Т. 46, № 2. С. 146–159. doi: 10.18786/2072-0505-2018-46-2-146-159

3. Caton M.T., Shenoy V.S. Cerebral Cavernous Malformations. Treasure Island (FL): StatPearls Publishing; 2019. doi: 10.20959/wjpr202011-18275

4. Flemming K.D., Brown R.D. Epidemiology and natural history of intracranial vascular malformations. In: H.R. Winn, ed. Youmans & Winn neurological surgery, 7th ed. Amsterdam: Elsevier; 2017. P. 3446–3463e7.

5. Готко А.В., Kivelev J.V., Сон А.С. Кавернозные мальформации головного и спинного мозга // Український нейрохірургічний журнал. 2013. № 3. С. 10–15.

6. Родич А., Смеянович А., Сидорович Р., и др. Современные подходы к хирургическому лечению кавернозных ангиом головного мозга // Наука и инновации. 2018. Т. 10, № 188. С. 70–73.

7. Gross B.A., Du R. Natural history of cerebral arteriovenous malformations: a meta-analysis // J Neurosurg. 2013. Vol. 118, N 2. P. 437–443. doi: 10.3171/2012.10.JNS121280

8. Kearns K.N., Chen C.J., Tvrdik P., et al. Outcomes of surgery for brainstem cavernous malformations: a systematic review // Stroke. 2019. Vol. 50, N 10. P. 2964–2966. doi: 10.1161/STROKEAHA.119.026120

9. Сазонов И.А., Белоусова О.Б. Кавернозная мальформация, вызвавшая развитие обширной острой субдуральной гематомы. Случай из практики и обзор литературы // Вопросы нейрохирургии им. Н.Н. Бурденко. 2019. Т. 83, № 3. С. 73–76. doi 10.17116/neiro20198303173

10. Mouchtouris N., Chalouhi N., Chitale A., et al. Management of cerebral cavernous malformations: from diagnosis to treatment // Scientific World Journal. 2015. Vol. 2015, N 808314. doi: 10.1155/2015/808314

11. Negoto T., Terachi S., Baba Y., et al. Symptomatic brainstem cavernoma of elderly patients: timing and strategy of surgical treatment. Two case reports and review of the literature // World Neurosurgery 2018. Vol. 111. P. 227–234. doi: 10.1016/j.wneu.2017.12.111

12. Batra S., Lin D., Recinos P.F., et al. Cavernous malformations: natural history, diagnosis and treatment // Nature Reviews Neurology. 2009. Vol. 5, N 12. P. 659–670. doi: 10.1038/nrneurol.2009.177

13. Al-Shahi Salman R., White P.M., Counsell CE., et al. Outcome after conservative management or intervention for unruptured brain arteriovenous malformations // JAMA. 2014. Vol. 311, N 16. P. 1661–1669. doi: 10.1001/jama.2014.3200

14. Hakim A.A., Gralla J., Rozeik C., et al. Anomalies and normal variants of the cerebral arterial supply: A comprehensive pictorial review with a proposed workflow for classification and significance // J Neuroimaging. 2018. Vol. 28, N 1. P. 14–35. doi: 10.1111/jon.12475

15. Полковников А.Ю. Артериовенозные мальформации полушарий большого мозга с ядром малого и среднего размеров, особенности клинических проявлений и методы хирургического лечения // Актуальні питання фармацевтичної і медичної науки та практики. 2013. Т. 2, № 12. С. 033–038.

16. Chang E.F., Wang D.D., Barkovich A.J., et al. Predictors of seizure freedom after surgery for malformations of cortical development // Ann Neurol. 2011.Vol. 70, N 1. P. 151–162. doi: 10.1002/ana.22399

17. Pasqualin A., Meneghelli P., Giammarusti A., Turazzi S. Results of surgery for cavernomas in critical supratentorial areas // Acta Neurochir Suppl. 2014. Vol. 119. P. 117–123. doi: 10.1007/978-3-319-02411-0_20

18. Маряшев С.А. Стереотаксическое облучение артериовенозных мальформаций головного мозга: Автореф. дис. ... д-ра мед. наук. Москва, 2016. 26 с.

19. Shimizu K., Kosaka N., Yamamoto T., et al. Arterial spin labeling perfusion-weighted MRI for long-term follow-up of a cerebral arteriovenous malformation after stereotactic radiosurgery // Acta Radiol Short Rep. 2014. Vol. 3, N 1. doi: 10.1177/2047981613510160

20. Seo Y., Kim D.G., Dho Y.S., et al. A Retrospective analysis of the outcomes of dural arteriovenous fistulas treated with gamma knife radiosurgery: a single-institution experience // Stereotactic Functional Neurosurgery. 2018. Vol. 96, N 1. P. 46–53. doi: 10.1159/000486685

21. Lee C.C., Wang W.H., Yang H.C., et al. Gamma Knife radiosurgery for cerebral cavernous malformation // Sci Rep. 2019. Vol. 9, N 1. P. 19743. doi: 10.1038/s41598-019-56119-1

22. Kefeli A.U., Sengoz M., Peker S. Gamma knife radiosurgery for hemorrhagic brainstem cavernomas // Turk Neurosurg. 2018. Vol. 29, N 1. P. 14–19. doi: 10.5137/1019-5149.JTN.21690-17.1

23. Cantu C., Murillo-Bonilla L., Arauz A., et al. Predictive factors for intracerebral hemorrhage in patients with cavernous angiomas // Neurol Res. 2005. Vol. 27, N 3. P. 314–318. doi: 10.1179/016164105X39914

24. Wang C.C., Liu A., Zhang J., et al. Surgical management of brainstem cavernous malformations: report of 137 cases // Surg Neurol. 2003. Vol. 59, N 6. P. 444–454. doi: 10.1016/s0090-3019(03)00187-3

25. Abla A.A., Turner J.D., Mitha A.P., et al. Surgical approaches to brainstem cavernous malformations // Neurosurgical Focus. 2010. Vol. 29, N 3. P. E8. doi: 10.3171/2010.6.FOCUS10128

26. Wen R., Shi Y., Gao Y., et al. The efficacy of gamma knife radiosurgery for cavernous malformations: a meta-analysis and review // World Neurosurgery. 2019. Vol. 123. P. 371–377. doi: 10.1016/j.wneu.2018.12.046

27. Park S.H., Hwang S.K. Gamma knife radiosurgery for symptomatic brainstem intra-axial cavernous malformations // World Neurosurgery. 2013. Vol. 80, N 6. P. 261–266. doi: 10.1016/j.wneu.2012.09.013

28. Frischer J.M., Gatterbauer B., Holzer S., et al. Microsurgery and radiosurgery for brainstem cavernomas: effective and complementary treatment options // World Neurosurgery. 2014. Vol. 81, N 3-4. P. 520–528. doi: 10.1016/j.wneu.2014.01.004

29. Kondziolka D., Lunsford L.D., Flickinger J.C., Kestle J.R. Reduction of hemorrhage risk after stereotactic radiosurgery for cavernous malformations // J Neurosurg. 1995. Vol. 83, N 5. P. 825–831. doi: 10.3171/jns.1995.83.5.0825

30. Aboukais R., Estrade L., Devos P., et al. Gamma knife radiosurgery of brainstem cavernous malformations // Stereotact Funct Neurosurg. 2016. Vol. 94, N 6. P. 397–403. doi: 10.1159/000452844

31. Lopez-Serrano R., Martinez N.E., Kusak M.E., et al. Significant hemorrhage rate reduction after gamma knife radiosurgery in symptomatic cavernous malformations: long-term outcome in 95 case series and literature review // Stereotact Funct Neurosurg. 2017. Vol. 95, N 6. P. 369–378. doi: 10.1159/000480664

32. Shin S.S., Murdoch G., Hamilton R.L., et al. Pathological response of cavernous malformations following radiosurgery // J Neurosurg. 2015. Vol. 123, N 4. P. 938–944. doi: 10.3171/2014.10.jns14499

33. Gewirtz R.J., Steinberg G.K., Crowley R., Levy R.P. Pathological changes in surgically resected angiographically occult vascular malformations after radiation // Neurosurgery. 1998. Vol. 42, N 4. P. 738–741. doi: 10.1097/00006123-199804000-00031

34. Nyary I., Major O., Hanzely Z., Szeifert G.T. Histopathological fndings in a surgically resected thalamic cavernous hemangioma 1 year afer 40-gy irradiation // J Neurosurg. 2005. Vol. 102, Suppl. P. 56–58. doi: 10.3171/sup.2005.102.s_supplement.0056

35. Monaco E.A., Khan A.A., Niranjan A., et al. Stereotactic radiosurgery for the treatment of symptomatic brainstem cavernous

malformations // Neurosurgical Focus. 2010. Vol. 29, N 3. E11. doi: 10.3171/2010.7.FOCUS10151

36. Tian K.B., Zheng J.J., Ma J.P., et al. Clinical course of untreated thalamic cavernous malformations: hemorrhage risk and neurological outcomes // J Neurosurg. 2017. Vol. 127, N 3. P. 480–491. doi: 10.3171/2016.8.JNS16934

37. Kida Y. Radiosurgery for cavernous malformations in basal ganglia, thalamus and brainstem // Prog Neurol Surg. 2009. Vol. 22. P. 31–37. doi: 10.1159/00016338

38. Kim B.S., Yeon J.Y., Kim J.S. et al. Gamma Knife radiosurgery of the symptomatic brain stem cavernous angioma with low marginal dose // Clin Neurol Neurosurg. 2014. Vol. 126, P.110-114. doi: 10.1016/j.clineuro.2014.08.028

39. Menzler K. Epileptogenicity of cavernomas depends on (archi-) cortical localization // Neurosurgery. 2010. Vol. 67. P. 918–924. doi: 10.1227/NEU.0b013e3181eb5032

40. Liao C., Visocchi M., Zhang W., et al. Management of cerebral radiation necrosis: a retrospective study of 12 patients // Acta Neurochir Suppl. 2017. Vol. 124. P. 195–201. doi: 10.1007/978-3-319-39546-3_30

41. Akers A., Salman R.A., Awad I., et al. Synopsis of guidelines for the clinical management of cerebral cavernous malformations: consensus recommendations based on systematic literature review by the angioma alliance scientific advisory board clinical experts panel // Neurosurgery. 2017. Vol. 80, N 5. P. 665–680. doi: 10.1093/neuros/nyx091

42. Garcia R.M., Ivan M.E., Lawton M.T. Brainstem cavernous malformations: surgical results in 104 patients and a proposed grading system to predict neurological outcomes // Neurosurgery. 2015. Vol. 76, N 3. P. 265–277. doi: 10.1227/NEU.0000000000000602

43. Крылов В.В., Дашьян В.Г., Шетова И.М., и др. Нейрохирургическая помощь больным с сосудистыми заболеваниями головного мозга в Российской Федерации // Нейрохирургия. 2017. № 4. С. 11–20.

44. Willie J.T., Malcolm J.G., Stern M.A., et al. Safety and effectiveness of stereotactic laser ablation for epileptogenic cerebral cavernous malformations // Epilepsia. 2019. Vol. 60, N 2. P. 220–232. doi: 10.1111/epi.14634

45. Amponsah K., Ellis T.L., Chan M.D., et al. Retrospective analysis of imaging techniques for treatment planning and monitoring of obliteration for gamma knife treatment of cerebral arteriovenous malformation // Neurosurgery. 2012. Vol. 71, N 4. P. 893–899. doi: 10.1227/neu.0b013e3182672a83

46. Chen CC., Chapman P., Petit J., et al. Proton radiosurgery in neurosurgery // Neurosurg Focus. 2007. Vol. 23, N 6. E5. doi: 10.3171/FOC-07/12/E5

47. Медико-технический комплекс: Объединенный институт ядерных исследований. Кавернозные ангиомы (каверномы) [Интернет]. Режим доступа: http://mtk.jinr.ru/index.php?option=com_content&task=view&id=33&Itemid=53. Дата обращения: 14.03.2021.

AUTHORS' INFO

* Elena N. Girya, MD;
address: 3 Bol'shaya Sukharevskaya ploshcad, 129010, Moscow, Russia; tel.: +7 (495) 608-34-50;
ORCID: https://orcid.org/0000-0001-5875-1489;
eLibrary SPIN: 4793-7748; e-mail: mishka_77@list.ru

Valentin E. Sinitsyn, MD, Dr. Sci. (Med.), Professor;
ORCID: https://orcid.org/0000-0002-5649-2193;
eLibrary SPIN: 8449-6590; e-mail: vsini@mail.ru

Alexey S. Tokarev, MD, Cand. Sci. (Med.);
ORCID: https://orcid.com/0000-0002-8415-5602;
eLibrary SPIN: 1608-0630; e-mail: alex_am_00@mail.ru

ОБ АВТОРАХ

* Гиря Елена Николаевна,
адрес: Россия, 129010, Москва, Большая Сухаревская пл., д. 3;
тел.: +7 (495) 608-34-50;
ORCID: https://orcid.org/0000-0001-5875-1489;
eLibrary SPIN: 4793-7748; e-mail: mishka_77@list.ru

Синицын Валентин Евгеньевич, д.м.н., профессор;
ORCID: https://orcid.org/0000-0002-5649-2193;
eLibrary SPIN: 8449-6590; e-mail: vsini@mail.ru

Токарев Алексей Сергеевич, к.м.н.;
ORCID: https://orcid.com/0000-0002-8415-5602;
eLibrary SPIN: 1608-0630; e-mail: alex_am_00@mail.ru

* Corresponding author / Автор, ответственный за переписку

Длительный анамнез бронхоцеле, вызванный типичным карциноидом

К.В. Прусакова, П.В. Гаврилов

Санкт-Петербургский научно-исследовательский институт фтизиопульмонологии, Санкт-Петербург, Российская Федерация

АННОТАЦИЯ

В работе представлен клинический случай с длительным периодом наблюдения одиночного бронхоцеле (бронхогенной ретенционной кисты). При первоначальном комплексном обследовании, включающем такие исследования, как рентгенография, компьютерная томография органов грудной полости, фибробронхоскопия, иммунологические и бактериологические обследования на туберкулёз, данных за онкологическую и инфекционную природу изменений не выявлено. Изменения были расценены как последствия перенесённого неспецифического воспалительного процесса. Через 15 лет при плановом медицинском осмотре по данным рентгенографии органов грудной полости отмечено увеличение размеров бронхоцеле, а также появление округлого образования в медиальных отделах бронхоцеле. С помощью дополнительных методов исследования, таких как компьютерная томография органов грудной полости с внутривенным контрастированием, фибробронхоскопия с биопсией, установлено, что выявленное образование является типичным карциноидом.

Несмотря на то что бронхоцеле в большинстве случаев является доброкачественным изменением, из разнообразия причин, вызывающих его развитие, следует выделить обструкцию бронха новообразованием. Среди новообразований лёгкого типичный карциноид составляет всего 1–2%, характеризуется крайне медленным ростом и отсутствием специфичной клинической симптоматики. Несмотря на это, типичный карциноид относится к злокачественным нейроэндокринным образованиям I типа. В 10–15% случаев выявляются метастазы, преимущественно в медиастинальные лимфатические узлы, а также в печень, кости, реже в мягкие ткани.

Данное клиническое наблюдение говорит о том, что даже при отрицательных результатах первичного обследования локально расположенного бронхоцеле такие изменения требуют онкологической настороженности и периодических обследований в динамике.

Ключевые слова: клинический случай; бронхоцеле; типичный карциноид; компьютерная томография.

Long–term broncocele anamnesis, triggered by typical carcinoid

Kseniya V. Prusakova, Pavel V. Gavrilov

Saint-Petersburg State Research Institute of Phthisiopulmonology, Saint Petersburg, Russian Federation

ABSTRACT

The paper presents a case of a single bronchocele (bronchogenic retention cyst) caused by a typical carcinoid that was observed for a long time. During the initial complex examination, including computed tomography with intravenous contrast, fibrobronchoscopy, and immunological and bacteriological examinations of tuberculosis, there were no changes for the oncological and infectious nature. The changes were interpreted as the result of a postponed nonspecific inflammatory process. Most of them were monitored using chest X-ray and the changes were stable. After 15 years, a control chest X-ray revealed an increase in the size of the compaction in the lung and the appearance of a mass with calcification in the medial sections of the compaction zone. Additional examination, including computed tomography with biopsy, determined that the obstruction of the bronchus was caused by a neoplasm [according to histological examination (typical carcinoid)].

It should be noted that the initial detection of negative study results requires oncological alertness and periodic examinations in dynamics.

Keywords: case report; bronchocele; typical carcinoid; computed tomography.

由典型的类癌引起的支气管囊肿的悠久历史

Kseniya V. Prusakova, Pavel V. Gavrilov

Saint-Petersburg State Research Institute of Phthisiopulmonology, Saint Petersburg, Russian Federation

简评

本文提出了一个长期观察单个支气管囊肿（支气管原性保留囊肿）的临床病例。在最初的全面检查中，包括放射照相术，胸腔计算机断层扫描，纤维支镜检查，结核病的免疫学和细菌学检查等研究，没有发现改变的肿瘤和感染性的数据。这些变化被视为转移非特异性炎症过程的后果。15年后，在常规体检期间，根据胸腔的射线照相，注意到支气管的大小增加，以及支气管囊肿内侧部分圆形出现。在其他研究方法的帮助下（例如胸腔静脉造影的计算机断层扫描，活检的纤维支镜检查），确定检测到的形成是典型的类癌。

尽管在大多数情况下，支气管囊肿是一种良性变化，但从导致其发展的各种原因来看，有必要通过肿瘤来区分支气管囊肿的阻塞。在肺部肿瘤中，典型的类癌仅为1-2％，其特征在于极其缓慢的生长和没有特定的临床症状。尽管如此，典型的类癌属于第一类型恶性神经内分泌形成。在10-15％的病例中，检测到转移，主要在纵隔淋巴结中，以及在肝脏，骨骼中，在软组织中较少。

这一临床观察表明，即使对局部定位的支支气管囊肿的初步检查结果为阴性，这种变化也需要肿瘤警觉性和动态的定期检查。

关键词：临床病例；支气管囊肿；典型类癌；计算机断层扫描。

INTRODUCTION

Bronchocele (bronchogenic retention cyst, mucocele) is a relatively common finding in chest X-ray studies. The morphological substrate of bronchocele is local bronchiectasis in which airways are filled with mucous contents persistently secreted by the mucous membrane and with proximal obstruction of the airways [1]. In radiography and computed tomography, bronchocele is visualized as a tubular branched V- or Y-shaped structure associated with the bronchial tree (finger in glove sign) [2]. The contents have homogeneous structures, but dense inclusions (calcifications) are visualized in 30% of the cases [2, 3]. The contrast agent is not accumulated in computed tomography with intravenous contrast enhancement.

Bronchocele can have an oval or round shape, which depends on the size of the obturated bronchus, amount of contents in the lumen, and state of the surrounding pulmonary parenchyma.

Solitary local retention cysts are asymptomatic. Retention cysts have various causes, such as congenital diseases (bronchial atresia, lung sequestration, and cystic fibrosis), infectious pathologies (nonspecific inflammatory processes, tuberculosis, mycobacteriosis, and allergic bronchopulmonary aspergillosis), obstruction of the bronchus by the lesion (benign or malignant), foreign body, or cicatricial deformity of the bronchus. Differential diagnostics is complicated because bronchocele can have similar radiological semiotics regardless of causes [2].

Bronchocele should be differentiated with arteriovenous malformations in the lungs, such as endobronchial metastasis. In this case, computed tomography with intravenous contrast enhancement is the preferred diagnostic method [2].

In most cases, bronchocele is caused by benign changes in the lungs and does not require case follow-up; however, in a locally located bronchocele, obstructive genesis by the lesion or foreign body should be ruled out. For this purpose, supplementing radiation diagnostic methods with fibrobronchoscopy with biopsy is recommended [4, 5].

Currently, an optimal diagnostic algorithm for identifying the cause of bronchocele development has not been established. Moreover, there are no uniform recommendations for further follow-up of patients with newly diagnosed asymptomatic retention cysts or bronchocele.

CASE DESCRIPTION

A 56-year-old male patient visited the Department of Radiation Diagnostics for computed tomography of the chest cavity organs.

The history assessment revealed that he was examined for pneumonia 15 years ago. Despite the positive dynamics based on clinical studies, during the course of antibiotic therapy, radiological findings did not correspond to the typical course of regression of infiltrative lungs changes in pneumonia. X-ray imaging of the chest revealed an area of induration of a tubular branched structure in the middle section of the right lung (Fig. 1, *a*). Additional studies, including computed tomography of the chest with intravenous contrast enhancement, fibrobronchoscopy, and immunological and bacteriological studies, did not detect tuberculosis or an oncological process. Computed tomography data were presented as selective scans on a film carrier, which revealed a local, single branched structure with smooth, clear contours, located along the subsegmental bronchi of the middle lobe of the right lung (finger in glove sign), with homogeneous contents (Fig. 2), so the patient was diagnosed with bronchogenic retention cyst (bronchocele) on the middle lobe of the right lung. Subsequently, follow-up studies were performed annually by X-ray examination of the chest, and stable changes were observed.
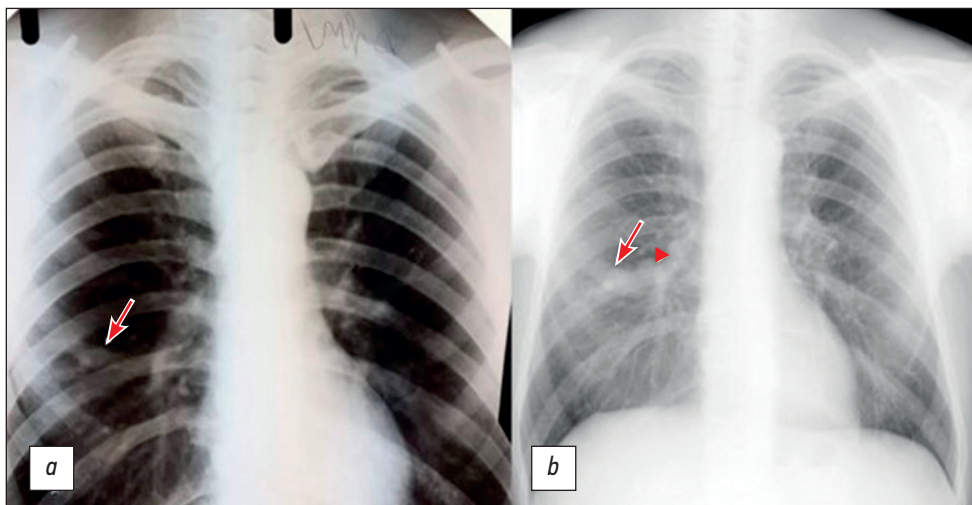
Fig. 1. X-ray image of the chest cavity organs of a 56-year-old patient *a,* At age 41 years, initial examination of the middle section of the right lung revealed a segment of induration of the branched tubular structure (arrow); *b,* 15 years later, the size of the bronchocele (arrow) increased, and a rounded lesion in the medial parts of the bronchocele (arrowhead) emerged.
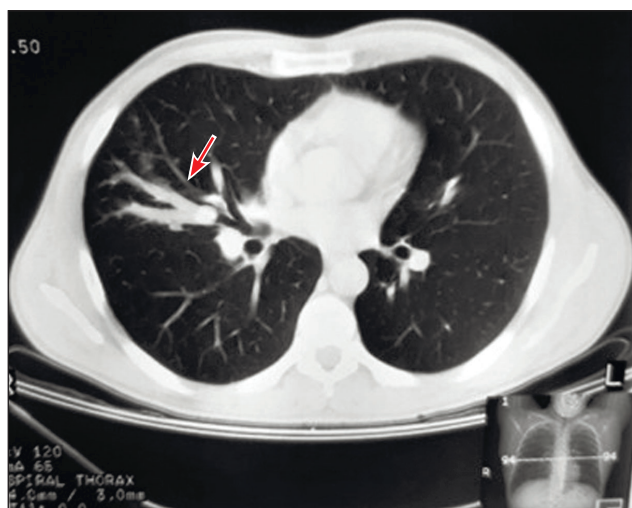
Fig. 2. Selective computed tomography scan of the thoracic cavity organs of the same patient: a homogeneous V-shaped structure in the middle lobe of the right lung with clear contours (arrow).

Prior to the present admission, the patient underwent a medical examination at his workplace with harmful working conditions. X-ray imaging of the chest revealed an increase in the size of the previously determined bronchocele (Fig. 1, *b*), as well as a new round lesion in the medial sections of the bronchocele with calcifications along the lesion contour (Fig. 1, *b*). To clarify the nature of the changes, the patient underwent contrast-enhanced computed tomography of the chest, which detected a single branched V-shaped structure

with a clear contour in the middle lobe of the right lung, and homogeneous contents located along the subsegmental bronchi (finger in glove sign) were preserved. At the base of the bronchocele, a rounded lesion with a smooth, clear contour is noted, almost completely overlapping the bronchus B4 lumen, and single calcifications were found along the periphery with signs of contrast accumulation in the venous phase from +29 HU to +112 HU (Fig. 3). Changes were characteristic of bronchocele caused by neoplastic bronchus obstruction. Fibrobronchoscopy with biopsy was also performed. Bronchoscopy revealed a rounded lesion of the B4 ostium, which completely covered the bronchial lumen (Fig. 4). The lesion is inactive and woundable on contact, and the mucous membrane on the surface is hyperemic and edematous. The biopsy results revealed that the histological presentation of the lesion corresponded to a typical carcinoid. The immunohistochemical study revealed that tumor cells intensely expressed CD56, but not TTF1. The Ki67 proliferative activity index was 2%.

The patient received surgical treatment by resection of the middle lobe of the right lung. On 1-year follow-up examination, no signs of carcinoid recurrence were observed by computed tomography of the chest.

DISCUSSION

The most common causes of multiple bronchocele formation are cystic fibrosis, allergic bronchopulmonary
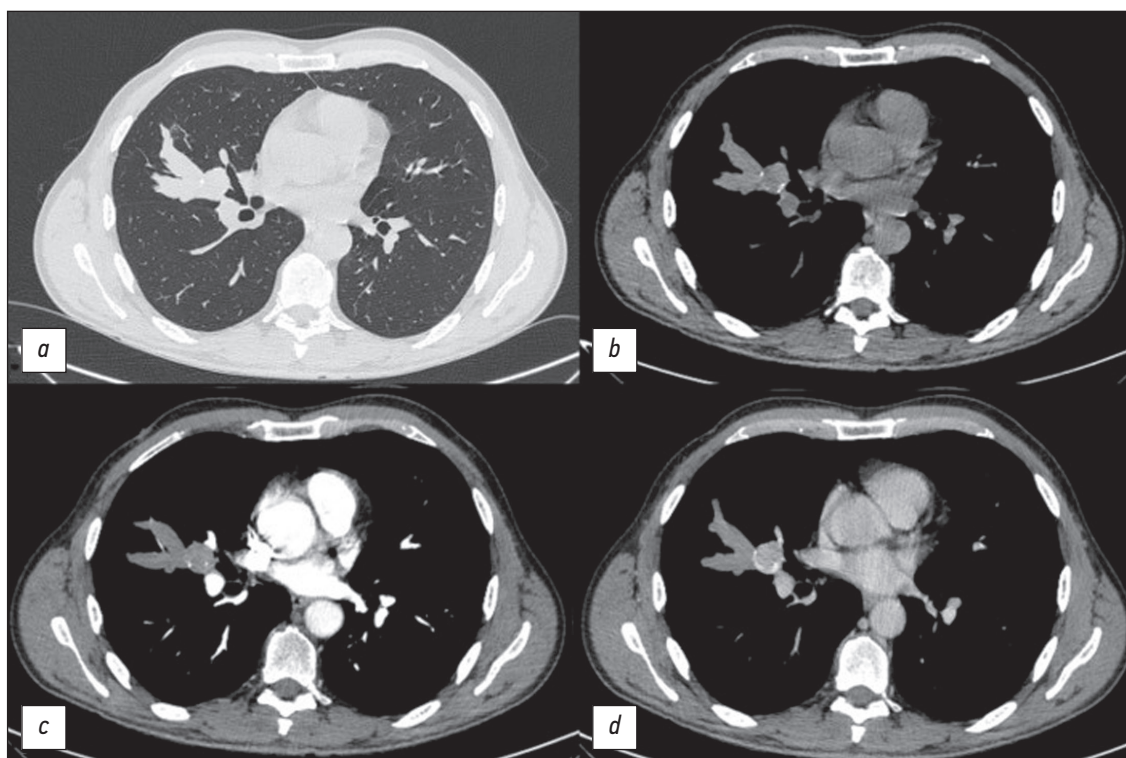
Fig. 3. Computed tomography scan of the chest cavity organs in the axial plane in the same patient: *a,* lung window; round lesion at the base of the bronchocele was detected during the native phase; *b,* mediastinum window; single calcifications along the periphery of the lesion were noted; *c,* mediastinum window; arterial phase; *d,* mediastinum window; signs of contrast accumulation by the lesion were detected in the venous phase.
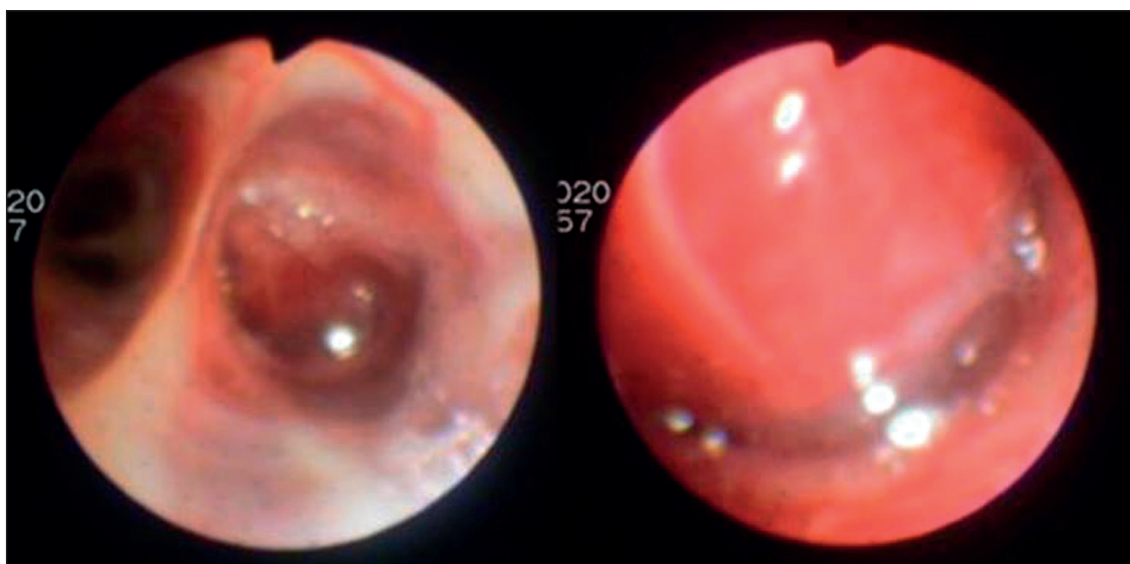
Fig. 4. Fibrobronchoscopy in the same patient. The lesion of the B4 ostium on the right completely blocked the bronchus lumen.

aspergillosis, and tuberculosis. Solitary local retention cysts are more often caused by the obstruction of the bronchus by a neoplasm (benign or malignant) [2, 6].

A typical carcinoid accounts for 1%–2% of lung neoplasms [7]. In 70% of the cases, the tumor is localized in the main bronchi, more often in the right lung, primarily in the middle lobe [8]. Typical carcinoid is commonly observed in people aged 40–50 years. With this form of lung neoplasm, studies have not established a reliable relationship between carcinogens and smoking [9, 10].

In most cases, bronchial carcinoid is asymptomatic and is detected as an accidental finding during a routine examination; however, in 2%–5% of the cases, bronchial carcinoids can produce neuroamines and peptide hormones, such as serotonin, adrenocorticotropic hormone, somatostatin, and bradykinin [11]. Clinical manifestations of carcinoid syndrome include periodic hot flashes or a sensation of blood rushing to the head, neck, and arms, bronchospasm, diarrhea, and mental disorders [11–13].

On X-ray imaging, a typical carcinoid is seen as a round or oval lesion with clear and even (sometimes lobular) contours. In up to 30% of the cases, eccentrically located or diffuse calcifications are observed [2, 3].

On computed tomography, a typical carcinoid is revealed as a rounded lesion with clear, even, or lobed contours. With intravenous contrast enhancement, there is an accumulation of a contrast agent, and in some cases, it is possible to trace the feeding artery entering the lesion from the bronchial arteries [6]. In relation to the bronchus, the carcinoid was located intrabronchially, extrabronchially, or mixed iceberg type, causing partial or total obstruction of the bronchial lumen [2, 3].

In the present case, although the cause of the bronchocele development was not established in the initial comprehensive examination, retrospective assessment of computed tomography data presented on a film carrier revealed the presence of a lesion at the base of the bronchocele (Fig. 2). With its extrabronchial location, changes during fibrobronchoscopy may not be detected.

The densitometric parameters of the lesion located at the base of the retention cyst may not be substantially different from the mucus, and small ones can be difficult to visualize. Central carcinoid may be suspected when signs of obstruction (atelectasis, "air traps," or bronchocele) are detected.

Differentiation of a typical carcinoid should be performed with type II neuroendocrine lesions of the lungs (atypical carcinoid), bronchogenic cyst, and bronchocele.

The typical carcinoid is extremely slow growing. According to Raz et al. [14], the average doubling time of typical carcinoid tumors is 7 years; therefore, it is difficult to judge the dynamics based on the annual prophylactic radiography of the lungs, since it is difficult to detect visually a minor increase in tumor size. Thus, in the presence of a localized bronchocele of an unknown nature, despite the apparent lack of dynamics according to X-ray data, control studies by contrast-enhanced computed tomography of the chest cavity organs should be conducted at regular intervals to assess reliably the dynamics of changes and exclude bronchial obstruction by a neoplasm.

Computed tomography is a preferred diagnostic method; however, given the peculiarities of the location of typical carcinoids, many authors have recommended fibrobronchoscopy with transbronchial biopsy as complementary imaging methods [4, 5, 15].

Surgical resection is the gold standard for the treatment of typical carcinoids, as this pathology has a low sensitivity to chemotherapy and radiation therapy. In the case of complete endobronchial location of the carcinoid in the central regions, resection can be performed using the transbronchial approach [6, 8, 13].

CONCLUSION

Bronchocele is a benign finding in most cases, but in localized bronchocele, the oncological nature of bronchial obstruction should be ruled out. For this purpose, computed tomography of the chest cavity organs with intravenous contrast enhancement and fibrobronchoscopy with biopsy are recommended.

Some types of neoplasms, such as a typical carcinoid, are characterized by extremely slow growth. Even with negative results on the initial examination of a local bronchocele, these changes require oncological alertness and periodic examinations over time.

REFERENCES

1. Hansell DM, Bankier AA, MacMahon H, et al. Fleischner Society: glossary of terms for thoracic imaging. *Radiology*. 2008;246(3):697–722. doi: 10.1148/radiol.2462070712

2. Martinez S, Heyneman LE, McAdams HP, et al. Mucoid impactions: finger-in-glove sign and other CT and radiographic features. *Radiographics*. 2008;28(5):1369–1382. doi: 0.1148/rg.285075212

3. Nguyen ET. The gloved finger sign. *Radiology*. 2003;227(2):453–454. doi: 10.1148/radiol.2272011548

4. Farrell C, Goggins M, Casserly M. Unexpected diagnosis resulting from presentation with chronic obstructive pulmonary disease (COPD) exacerbation. *International Journal of Case Reports and Images*. 2019;43–47. doi: 10.36811/jcri.2019.110007

5. Kulkarni GS, Gawande SC, Chaudhari DV, Bhoyar AP. Bronchial carcinoid: case report and review of literature. *MVP J Med Sci*. 2016;3(1):71–78. doi: 10.18311/mvpjms/2016/v3/i1/740

6. Yadav V, Rathi V. Bronchial carcinoid with bronchocele masquerading as Scimitar syndrome on chest radiograph. *Radiol Case Rep*. 2021;16(3):710–713. doi: 10.1016/j.radcr.2021.01.013

7. Jeung MY, Gasser B, Gangi A, et al. Bronchial carcinoid tumors of the thorax: spectrum of radiologic findings. *Radiographics*. 2002;22(2):351–365. doi: 10.1148/radiographics.22.2. g02mr01351

8. Paladugu RR, Benfield JR, Pak HY, et al. Bronchopulmonary Kulchitzky cell carcinomas. A new classification scheme for typi-

cal and atypical carcinoids. *Cancer*. 1985;55(6):1303–1311. doi: 10.1002/1097-0142(19850315)55:6<1303::aid-cncr2820550625>3.0.co;2-a

9. Grote TH, Macon WR, Davis B, et al. Atypical carcinoid of the lung. A distinct clinicopathologic entity. *Chest*. 1988;93(2):370–375. doi: 10.1378/chest.93.2.370. PMID: 2827965

10. Harpole DH, Feldman JM, Buchanan S, et al. Bronchial carcinoid tumors: a retrospective analysis of 126 patients. *Ann Thorac Surg*. 1992;54(1):50–54; discussion 54-5. doi: 10.1016/0003-4975(92)91139-z

11. Kuznetsov NS, Latkina NV, Dobreva EA. ACTH-ectopic syndrome: clinic, diagnosis, treatment. *Endocrine surgery*. 2012;6(1):24–36. (In Russ).

12. Buryakina SA, Karmazanovsky GG, Volevodz NN, et al. CT-signs of neuroendocrine lung tumors and their relationship with ACTH-ectopic syndrome. *REJR*. 2018;8(4):56–72. (In Russ). doi: 10.21569/2222–7415-2018-8-4-56-72

13. Trachtenberg AH, Kolbanov KI, Frank GA, et al. Features of diagnosis and treatment of lung carcinoid tumors. *Atmosphere. Pulmonology and allergology*. 2009;(1):2–6. (In Russ).

14. Raz DJ, Nelson RA, Grannis FW, Kim JY. Natural history of typical pulmonary carcinoid tumors: a comparison of nonsurgical and surgical treatment. *Chest*. 2015;147(4):1111–1117. doi: 10.1378/chest.14-1960

15. Kaifi JT, Kayser G, Ruf J, Passlick B. The diagnosis and treatment of bronchopulmonary carcinoid. *Dtsch Arztebl Int*. 2015;112(27-28):479–485. doi: 10.3238/arztebl.2015.0479

СПИСОК ЛИТЕРАТУРЫ

1. Hansell D.M., Bankier A.A., MacMahon H., et al. Fleischner Society: glossary of terms for thoracic imaging // Radiology. 2008. Vol. 246, N 3. P. 697–722. doi: 10.1148/radiol.2462070712

2. Martinez S., Heyneman L.E., McAdams H.P., et al. Mucoid impactions: finger-in-glove sign and other CT and radiographic features // Radiographics. 2008. Vol. 28, N 5. P. 1369–1382. doi: 10.1148/rg.285075212

3. Nguyen E.T. The gloved finger sign // Radiology. 2003. Vol. 227, N 2. P. 453–454. doi: 10.1148/radiol.2272011548

4. Farrell C., Goggins M., Casserly M. Unexpected diagnosis resulting from presentation with chronic obstructive pulmonary disease

(COPD) exacerbation // International Journal of Case Reports and Images. 2019;43–47. doi: 10.36811/jcri.2019.110007

5. Kulkarni G.S., Gawande S.C., Chaudhari D.V., Bhoyar A.P. Bronchial carcinoid: case report and review of literature // MVP J Med Sci. 2016. Vol. 3, N 1. P. 71–78. doi: 10.18311/mvpjms/2016/v3/i1/740

6. Yadav V., Rathi V. Bronchial carcinoid with bronchocele masquerading as Scimitar syndrome on chest radiograph // Radiol Case Rep. 2021. Vol. 16, N 3. P. 710–713. doi: 10.1016/j.radcr.2021.01.013

7. Jeung M.Y., Gasser B., Gangi A., et al. Bronchial carcinoid tumors of the thorax: spectrum of radiologic find-

ings // Radiographics. 2002. Vol. 22, N 2. P. 351–365. doi: 10.1148/radiographics.22.2. g02mr01351

8. Paladugu R.R., Benfield J.R., Pak H.Y., et al. Bronchopulmonary Kulchitzky cell carcinomas. A new classification scheme for typical and atypical carcinoids // Cancer. 1985. Vol. 55, N 6. P. 1303–1311. doi: 10.1002/1097-0142(19850315)55:6<1303::aid-cncr2820550625>3.0.co;2-a

9. Grote T.H., Macon W.R., Davis B., et al. Atypical carcinoid of the lung. A distinct clinicopathologic entity // Chest. 1988. Vol. 93, N 2. P. 370–375. doi: 10.1378/chest.93.2.370

10. Harpole D.H., Feldman J.M., Buchanan S., et al. Bronchial carcinoid tumors: a retrospective analysis of 126 patients // Ann Thorac Surg. 1992. Vol. 54, N 1. P. 50–54; discussion 54-5. doi: 10.1016/0003-4975(92)91139-z

11. Кузнецов Н.С., Латкина Н.В., Добрева Е.А. АКТГ — эктопиро-ванный синдром: клиника, диагностика, лечение // Эндокрин-ная хирургия. 2012. Т. 6, № 1. С. 24–36.

12. Бурякина С.А., Кармазановский Г.Г., Волеводз Н.Н., и др. КТ-признаки нейроэндокринных опухолей легких и их взаимосвязь с АКТГ-эктопическим синдромом // REJR. 2018. Т. 8, № 4. С. 56–72. doi: 10.21569/2222–7415-2018-8-4-56-72

13. Трахтенберг А.Х., Колбанов К.И., Франк Г.А., и др. Особен-ности диагностики и лечения карциноидных опухолей лег-ких // Атмосфера. Пульмонология и аллергология. 2009. № 1. С. 2–6.

14. Raz D.J., Nelson R.A., Grannis F.W., Kim J.Y. Natural history of typical pulmonary carcinoid tumors: a comparison of nonsurgical and surgical treatment // Chest. 2015. Vol. 147, N 4. P. 1111–1117. doi: 10.1378/chest.14-1960

15. Kaifi J.T., Kayser G., Ruf J., Passlick B. The diagno-sis and treatment of bronchopulmonary carcinoid // Dtsch Arztebl Int. 2015. Vol. 112, N 27-28. P. 479–485. doi: 10.3238/arztebl.2015.0479

AUTHORS' INFO

* Pavel V. Gavrilov, MD, Cand. Sci. (Med.);
address: 2-4, Ligovskiy pr., Saint-Petersburg, 191036, Russia;
e-mail: spbniifrentgen@mail.ru;
ORCID: https://orcid.com/0000-0003-3251-4084

Kseniya V. Prusakova, MD;
e-mail: ksenya.rush@mail.ru;
ORCID: https://orcid.com/0000-0002-3934-6290

ОБ АВТОРАХ

* Гаврилов Павел Владимирович, к.м.н.;
адрес: Россия, 191036, Санкт-Петербург, Лиговский пр., д. 2-4;
e-mail: spbniifrentgen@mail.ru;
ORCID: https://orcid.com/0000-0003-3251-4084

Прусакова Ксения Владимировна;
e-mail: ksenya.rush@mail.ru;
ORCID: https://orcid.com/0000-0002-3934-6290

* Corresponding author / Автор, ответственный за переписку